

Proposed Turkey Point Units 6 and 7  
Docket Nos. 52-040 and 52-041  
FPL Revised Response to NRC RAI No. 02.05.02-3 (eRAI 5896)  
L-2014-282 Attachment 2 Enclosure A Page 1 of 3

## **Enclosure A**

### **SSHAC Caribbean Questionnaire**

**PREAMBLE:**

As a preliminary "straw man" model, we have identified the following six seismic sources in the northern Caribbean region as relevant to seismic hazard in southern Florida (see attached figure):

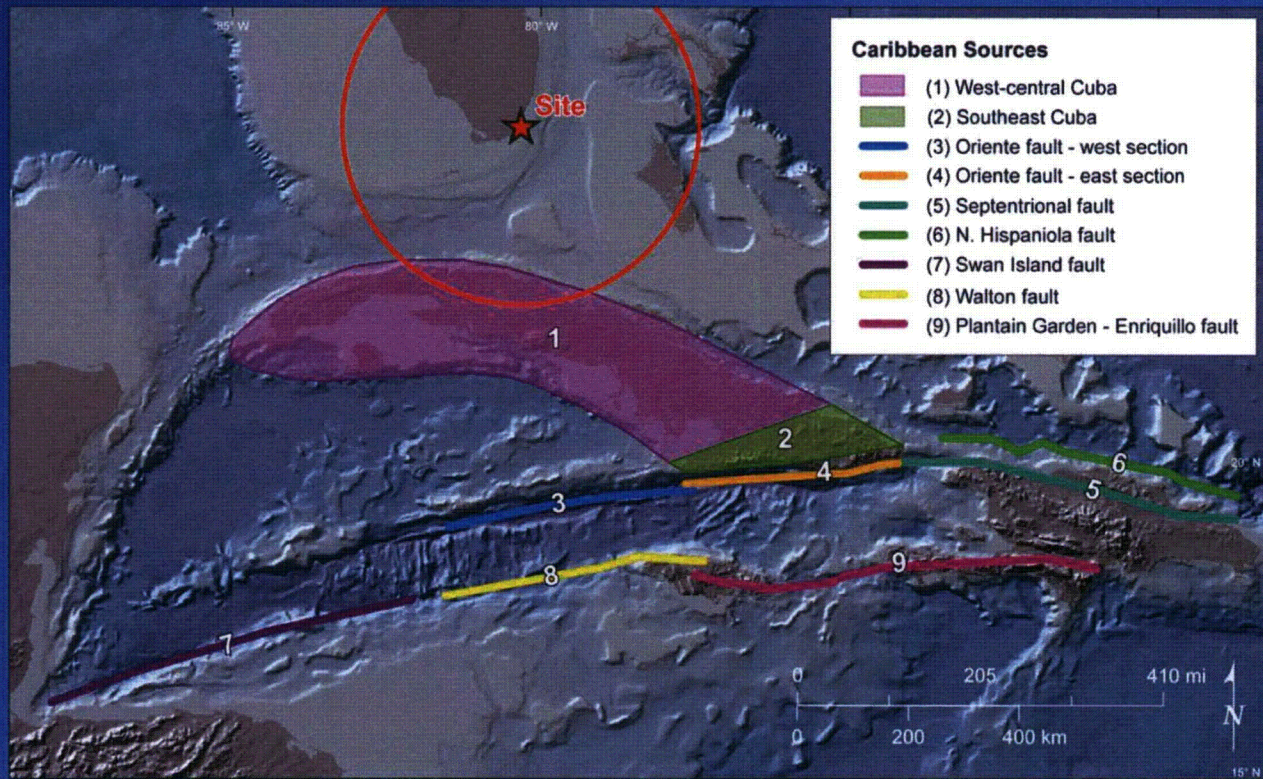
- (1) West-central Cuba (area source)
- (2) Southeastern Cuba (area source)
- (3) Oriente fault zone west, between Cuba and the Cayman spreading center
- (4) Oriente fault zone east, directly south of Cuba
- (5) Septentrional fault, between the northern Dominican Republic and eastern Cuba
- (6) North Hispaniola thrust fault, north of the Dominican Republic
- (7) Swan Island fault zone, west of the Cayman spreading center
- (8) Walton fault zone, between Jamaica and the Cayman spreading center
- (9) Plantain Garden-Enriquillo fault zone, between southern Dominican Republic and Jamaica

It is our assessment that faults in Cuba are not sufficiently characterized to warrant fault (line) sources. The source zone boundaries for Cuba are defined by tectonic landforms, geology, and seismicity (see figure).

**QUESTIONS:**

- 1) Are all possible sources of magnitude 7 or greater events within ~1,000 km of south Florida included? If not, what are other potential sources?
  
- 2) For each fault source, in your opinion:
  - a) What is the maximum magnitude the fault is capable of generating?
  - b) What is the maximum seismogenic depth of each fault?
  - c) Do you have or know of any estimates of recurrence times for large ( $M \geq 7$ ) events on any or all of these faults?
  - d) What is the magnitude distribution of large events on any or all of these faults?
  - e) What is the best estimate of slip rate and seismic coupling on these faults?
  
- 3) In regards to seismic hazards on the island of Cuba:
  - a) Do you know of any individuals or groups that are studying and/or have published reports on active faulting on the island of Cuba? If so please provide names and references.
  - b) Do you have any knowledge or opinions regarding seismic hazards on Cuba?

# New Caribbean Model Geometry



**NRC RAI Letter No. PTN-RAI-LTR-037**

**SRP Section: 02.05.02 - Vibratory Ground Motion**

Question for Geosciences and Geotechnical Engineering Branch 1 (RGS1)

**NRC RAI Number: 02.05.02-4 (eRAI 5896)**

FSAR Subsection 2.5.1.1.1.3.2.4 describes that due to lack of knowledge about individual faults' characteristics, the applicant used an areal source zone to model the seismic hazard from the Cuban seismic sources. In accordance with NUREG-0800, Standard Review Plan, Chapter 2.5.2, "Vibratory Ground Motion," and Regulatory Guide (RG) 1.208, "A Performance-Based Approach to Define the Site-Specific Earthquake Ground Motion," please provide the following:

- a. Rationale for the exclusive use of an areal source rather than multiple areal sources or a combination of fault sources and areal sources. Given the uncertainties, does the use of a single areal source result in a more conservative representation of the hazard from the Cuba seismic sources?
- b. Details of the PSHA implementation for the Cuba areal source zone. Specifically, is Cuba seismicity modeled using the EPRI approach, using a uniform source zone, or using some other methodology?
- c. A description of how well the seismic source model parameters represent the observed spatial patterns and concentrations of seismicity. Is a uniform seismic source zone justified considering FSAR Figure 2.5.1-267, which shows prominent clusters of seismicity? Discuss evidence, if any, that frequency-magnitude behavior is different for the subset of earthquakes concentrated in western and northern Cuba than for the entire zone.
- d. Details on the earthquake catalog completeness, methodology used to compute the  $a$  and  $b$  values, the computed  $a$  and  $b$  values and rates of earthquakes equal to or greater than moment magnitude 5. If used, please also discuss smoothing operators applied to the  $a$  and  $b$  values.
- e. A detailed description of the PSHA implementation for the Cuba seismicity model. Are large earthquakes modeled as finite faults? If so, can they extend outside the zone boundary, and is there a preferred azimuth? If so, what is their closest distance of approach to the TPNPP site?

**FPL RESPONSE:**

This response provides additional information pertaining to the areal seismic source for Cuba used in the probabilistic seismic hazard analysis (PSHA) for the Turkey Point Units 6 & 7 site. This single areal source approach for Cuba was developed following Senior Seismic Hazard Analysis Committee (SSHAC) Level 2 guidelines (SSHAC 1997) (FSAR 2.5.2 Reference 318), as described in FSAR Subsection 2.5.2.4.4.3.

This response also investigates the potential impacts on the PSHA from alternative modeling approaches for Cuba through the use of hazard sensitivity calculations. The input parameters for these alternative modeling approaches were developed through a separate SSHAC Level 2 study that post-dates the SSHAC Level 2 study described in FSAR

Subsection 2.5.2.4.4.3. The SSHAC Level 2 study that supports the current hazard sensitivity calculations is described primarily in the response to RAI 02.05.01-21, but input from that study also pertains to this (current) response. Specifically, the hazard sensitivity calculations include alternative scenarios for: (1) areal seismic sources in Cuba (Figure 1); and (2) fault sources for intraplate Cuba (Figure 2).

Three scenarios by which areal source zones are implemented in the hazard sensitivity calculations are summarized below and in Table 1. The results of the areal source sensitivity hazard calculations are discussed in more detail in part (a) of this response.

- Single areal source zone scenario (Z1): In the single areal source zone model, a single areal source for Cuba is used, with a uniform seismicity rate throughout the zone that is based on observed seismicity from the Phase 2 earthquake catalog (Figure 1). This is the base case for the hazard sensitivity calculations and is the seismic source characterization for intraplate Cuba used in the PSHA (FSAR Section 2.5.2). The Z1 model results in a contribution to hazard that is intermediate between the Z6 and Z11% zone scenarios (Table 1).
- Elevated rate areal source zone scenario (Z11%): In the elevated rate zone scenario, a single areal source for Cuba is used, with a uniform seismicity rate throughout the zone that is based on observed seismicity from the Phase 2 earthquake catalog. The geometry of this zone is equivalent to that in the Z1 scenario. Unlike the Z1 scenario, however, the uniform rate for the Z11% scenario is based on a small subzone in northern Cuba (the “northern Cuba subzone” shown in Figure 1) that is located partially within the site region and that exhibits a higher rate of seismicity than surrounding regions. The seismicity rate from the northern subzone is approximately 11% higher than that for the entire Cuba areal source zone, and this higher rate is applied to the Z1 scenario. The Z11% scenario results in the highest contribution to hazard from the three zone scenarios (Table 1).
- Six areal source zones scenario (Z6): In the six areal source zones scenario, Cuba is divided into six zones largely on the basis of observed patterns in seismicity (Figure 1). The seismicity *b*-value is constant across all six zones and equivalent to that used in the Z1 scenario; the seismicity *a*-values vary from zone to zone, are uniform within each zone, and are based on the observed seismicity within each zone. The Z6 scenario results in the lowest contribution to hazard from the three zone scenarios (Table 1).

The detailed characterization of sensitivity fault sources in Cuba is described in the response to RAI 02.05.01-21 and the sensitivity of hazard results is provided in part (a) of this (current) response. For the hazard sensitivity calculations, there are three scenarios for fault sources, as shown in Table 1 and summarized below.

- No fault sources scenario: This scenario excludes fault sources from the hazard sensitivity calculations. This is consistent with the seismic source characterization used for the PSHA and presented in FSAR Section 2.5.2.
- Full fault model scenario (FF): In the full fault model scenario, the 15 fault sources summarized in response to RAI 02.05.01-21 (see especially Table 3 from that response) are included in the hazard sensitivity calculations.

- Scaled fault model scenario (SF): The SF scenario is derived from the FF scenario such that the total seismic moment rate from the fault sources is equivalent to the seismic moment rate from the observed seismicity (Z1 scenario). The SF scenario results in a contribution to hazard that is lower than that from the FF fault source scenario (Table 1).

A total of eleven possible combinations of areal and fault scenarios are shown in Table 1. Among the various ways to model the distribution of seismic activity and seismic moment release rate of Cuba, shown in Table 1 and discussed in part (a) of this response, five of these scenarios are evaluated quantitatively. Of these, four scenarios are judged by the TI team as the most likely to encompass the center, body, and range of the views of the informed technical community and to be useful for the sensitivity analysis comparisons. Based on the results of these comparisons, it is concluded that the use of a single areal source zone and the parameters used to characterize it as presented in the FSAR gives a reasonably conservative estimate of the contribution to site hazard from intraplate Cuba.

**a) Rationale for the exclusive use of an areal source rather than multiple areal sources or a combination of fault sources and areal sources. Given the uncertainties, does the use of a single areal source result in a more conservative representation of the hazard from the Cuba seismic sources?**

As described above, hazard sensitivity calculations are used to assess the impact of several alternative modeling approaches for intraplate Cuba. The preferred seismic source model for Cuba is presented in FSAR Subsection 2.5.2.4.4.3. As described in that subsection, this model was developed following SSHAC Level 2 guidelines (SSHAC 1997) (FSAR 2.5.2 Reference 318). This preferred model comprises a single areal source zone with a large  $M_{max}$  and no fault sources (scenario Z1 in Table 1). This is an appropriate representation of Cuba seismic hazard in comparison to other scenarios. This model derives rate information from observed seismicity, extrapolated to earthquake magnitudes that envelop published  $M_{max}$  estimates for faults in Cuba, and extends one magnitude unit larger than the largest event observed in the approximately 500-yr record of observed seismicity for intraplate Cuba.

*Zone Models*

The influence of variations in seismicity rate within the single areal zone (Z1) are investigated through hazard sensitivity calculations in two scenarios: (1) the Z11% scenario, in which the rate for the entire single areal source zone is increased by 11%, corresponding to the average rate within a small portion of that zone nearest the site (i.e., the "northern Cuba subzone") (Figure 1); and (2) the Z6 scenario, in which the single areal zone is divided into six subzones defined by variations in seismicity patterns and rates (Figure 1). Part (c) of this response includes additional details on recurrence parameters for the Z11% scenario. The Z11% scenario provides a conservative representation of the effect of potentially diluting the effects of apparent higher seismicity rates in northern Cuba through use of a single large areal zone that includes areas of relatively lower seismicity activity rate.

For the six-zone scenario (Z6), each of the six zones is given equally weighted maximum moment magnitudes of 7.0 and 7.3 with uniformly distributed seismicity parameters (complete smoothing) determined from the earthquakes within each zone. The completeness table for Cuba from Garcia et al. (2008) (FSAR 2.5.2 Reference 255) is also

used here. The  $a$ -values were determined by counting the number of events in each subzone greater than or equal to  $M_w$  3. The  $b$ -value calculated in the FSAR for Z1 is used for all six subzones. Focal depth for the six subzones is the same as was implemented in the FSAR, which uses a three-point distribution to represent the 0 - 15 km seismogenic thickness: 2.5, 7.5, and 12.5 km, equally weighted.

The SSHAC Level 2 inputs from experts described in the response to RAI 02.05.01-21 (see especially Tables 2A through 2G from that response) include suggestions that the variations in seismicity patterns and rates within Cuba could be modeled as well with some form of spatial smoothing, although one expert (Wong) suggested that the six zone model (Z6) would likely approximate spatial smoothing. A complete smoothing model, in which all parts of each seismic source have the same seismicity recurrence parameters, was implemented for sensitivity hazard calculations of Cuba sources for several reasons:

- This smoothing model approach (constant seismicity rate throughout the zone) was used in the original FSAR source model.
- A strongly defined source zone boundary between Cuba and the Straits of Florida is indicated by the dramatic differences in geologic evolution and structure between northern Cuba and the Straits of Florida, so that implementation of a less complete smoothing seismicity model for Cuba that did not recognize this boundary would result in migration northward of seismic activity into areas previously characterized with much lower rates.
- Seismic hazard in the Straits of Florida has already been accounted for in the seismic source model by extending existing EPRI-SOG areal zones south from Florida to northern Cuba (see FSAR Figures 2.5.2-204 through 2.5.2-209).
- In the characterization adopted for the FSAR, seismicity in Cuba appears to be dramatically higher than in the Straits of Florida (Figure 1) and this difference is not easily attributable to differences in detection capability. For example, the June 2, 1990  $M_w$  3.3 (from the Phase 2 catalog) or Emb 4.09 (from the Phase 1 catalog) earthquake lies just north of the island of Cuba and southwest of the Bahamas, and originated from the Cuba source catalog (Alvarez et al. 1999) (FSAR 2.5.2 Reference 205), which is one of the source catalogs used to develop the Phase 1 and Phase 2 earthquake catalogs (FSAR Subsections 2.5.2.1.2 and 2.5.2.1.3). This implies some detection capability to this magnitude level and distance north of the island, from the Cuba source catalog at least, for the past 20 years. This is in agreement with estimates of detection capability as a function of magnitude for the "Near Florida" area (including the Straits of Florida between southern Florida and the Cuba area) as tabulated in Table 2.5.2-206 of the FSAR.
- The CEUS-SSC catalog (EPRI et al. 2012) includes the Straits of Florida, which is judged to be complete to magnitude 3.5 for the past 20 years (Table 3.5-3 in EPRI et al. 2012). No earthquakes exist in this catalog in the Straits of Florida (Figure 3.2-7 in EPRI et al. 2012).
- The six zone model (Z6) already represents a "coarse" smoothing approach by isolating or segregating areas of high and low rates, while not smoothing rates northward beyond Cuba.

### *Fault Models*

The lack of available data to characterize slip rates and faults in Cuba indicates that estimation of the relative contribution from faults and background earthquake sources is a significant source of uncertainty in the source model as described in the response to RAI 02.05.01-21. The preferred seismic source model accounts for this uncertainty by the use of a large Mmax on the Z1 areal source zone, without inclusion of specific fault sources. Adding regional fault sources (FF or SF) on top of this model creates additional seismic moment in the seismic source model and results in additional conservatism through possible double-counting the inferred contributions from the largest earthquakes.

To evaluate the potential influence on seismic hazard from the poorly known faults in Cuba, a SSHAC Level 2 study was used to develop a fault characterization model, as described in the response to RAI 02.05.01-21. From this process, 15 fault sources (Figure 2) and a weighted range of fault characterization parameters (Table 3 in response to RAI 02.05.01-21) were developed for the FF scenario in hazard sensitivity calculations. This characterization includes for each fault source three slip rate options, in which the high, middle, and low values on slip rate correspond to three orders of magnitude, reflecting the considerable uncertainty in the available data.

The SF scenario is derived from the FF scenario such that the total seismic moment rate from the fault sources is equivalent to the seismic moment rate from the observed seismicity (Z1 scenario). The scaling factor for the SF scenario is 0.2728, the inverse of the seismic moment ratio of 3.6657 shown in Table 2.

Maximum moment magnitudes of 7.0 and 7.3 are equally weighted as for the areal source(s). A weighted set of slip rates was developed after evaluation of inputs through a SSHAC Level 2 process. All faults are vertical, except for the Nortecubana West, Nortecubana Central, and Nortecubana East fault sources, which dip 30° to the south. All faults extend from 0 to 15 km depth. Magnitude recurrence for the faults is implemented using a model in which the maximum magnitudes are treated as characteristic magnitudes.

The hazard sensitivity calculations for both the zone model scenarios and the fault model scenarios use ground motion attenuation relationships developed for Caribbean crustal seismic sources described in FSAR Subsection 2.5.2.4.5.2.

### *Results*

This section describes the results of hazard sensitivity calculations for individual areal and fault source scenarios, as well as scenarios that combine areal and fault sources. A total of eleven possible combinations of areal and fault scenarios are shown in Table 1. One of these (Z1) is the base case presented in the FSAR. In addition to Z1, five of these scenarios are evaluated quantitatively in this response (Z6, Z11%, SF, Z1+SF, and FF) and are described below. Figures 3 and 4 present 1 Hz and 10 Hz hazard curves for these five scenarios. These figures also present the corresponding total hazard curves that include each of these Cuba scenarios.

- The Z6 scenario results in a decrease in hazard relative to the Z1 base case from the FSAR.
- The Z11% scenario results in an increase in hazard relative to the Z1 base case.

- The SF scenario results in a lower hazard relative to the Z1 base case.
- The Z1+SF scenario results in a higher hazard relative to the Z1 base case.
- The FF scenario results in a higher hazard relative to the Z1 base case.

Of these five scenarios, four are judged by the TI team to be most likely to encompass the center, body, and range of the views of the informed technical community (Z6, Z11%, SF, and Z1+SF). In contrast, the FF scenario is judged as overly conservative and therefore technically indefensible. The rationale for this assessment is based on the discrepancy between the observed historical rate of large earthquakes in Cuba and that predicted by the moment rate for the FF scenario. The moment rate for the FF scenario is derived from the weighted mean of slip rate distributions for the 15 Cuba fault sources. The bottom row of Table 2 illustrates that the moment rate for the weighted mean slip rate (FF model) yields a return period of 124 years for  $M_w$  7 events. The completeness period for earthquakes in Cuba in the  $M_w$  6.0 to 7.0 range is given as about 500 years according to Garcia et al. (2008) (FSAR 2.5.2 Reference 255) (Table 3). In the approximately 500-yr record of observed seismicity in Cuba, there are no magnitude 7 events and the largest earthquake in that time in the Phase 2 earthquake catalog from intraplate Cuba is approximately  $M_w$  6.3 (see FSAR Subsection 2.5.2.4.4.3.3.1). Another way to examine the overly conservative rate derived from the FF scenario is to compare the ratio of moment rate derived from seismicity to moment rate derived from the assumed fault slip rates in the middle column of Table 2. That comparison shows that the FF scenario moment rate is 367% greater (3.6657 ratio in Table 2) than the moment rate derived from historical seismicity. While the individual FF scenario is presented in Figures 3 and 4, it is not considered further. Likewise, combinations involving the FF scenario are also eliminated and not presented, as they would be overly conservative and technically indefensible.

The remaining five combination scenarios (Z6+FF, Z1+FF, Z11%+FF, Z6+SF, and Z11%+SF) are discarded from further consideration based on the rationale provided below:

- Three combination scenarios, Z6+FF, Z1+FF, and Z11%+FF, are discarded due to the inclusion of the FF scenario as described above.
- The Z6+SF combination scenario is judged to lie within the likely center, body, and range of the views of the informed technical community, but would result in an intermediate hazard not useful for this sensitivity analyses because SF is also combined with the Z1 scenario. The Z1+SF scenario results in higher hazard (Figures 3 and 4).
- The Z11%+SF combination scenario includes an areal zone scenario that is based on an arbitrary activity rate increase applied to the entire zone.

In order to assess the impact of various Cuba sensitivity scenarios on the Turkey Point Units 6 & 7 site hazard, based on the evaluation of the hazard results presented in Figures 3 and 4, four sensitivity scenarios (Z6, Z11%, SF, and Z1+SF) were selected to represent the Cuba hazard in lieu of the Z1 base case scenario used for the original FSAR hazard total. Total hazard curves that include these four scenarios are presented in Figure 5, along with the original FSAR total hazard.

Detailed comparisons of the differences in total hazard for the four scenarios with respect to the FSAR total hazard are compiled in Tables 4 and 5. Two acceleration spectral response frequencies (1 and 10 Hz) and two MAFE levels ( $10^{-4}$  and  $10^{-5}$ ) are considered.

Table 4 shows the percent differences in MAFE for each scenario at the respective FSAR amplitudes. Negative values indicate lower hazard levels than the FSAR levels, positive values are higher. The FSAR values are shown in the first pair of columns, and the subsequent four scenarios increase in hazard level from left to right. Differences for the Z6 scenario range from -8.8% to -1.1% of the FSAR total. Differences for the SF scenario range from -12% to +1.0%. For the Z11% scenario, differences range from -0.1% to +2.5%. For the Z1+SF scenario, differences are the greatest, ranging from +1.4% to +13.1%. Note that the apparent decrease (-0.1%) in 10 Hz MAFE at the  $10^{-5}$  MAFE amplitudes for scenario Z11% is due to the limited number of significant digits presented in the FSAR for total mean hazard, the process of interpolation, and rounding. That this is only an apparent decrease is supported by the fact that the  $10^{-5}$  MAFE amplitudes for scenario Z11% match the FSAR amplitudes exactly to three significant figures (Table 5).

Table 5 shows the changes in rock motion amplitude for the four scenarios. The largest of these changes are negative relative to the FSAR amplitudes. These are shown as absolute and percent differences in amplitudes. The largest percent increase is +4.4% and results from the Z1+SF scenario and the greatest decrease is -6.9% from the SF scenario. Of greater importance than the percentages is the maximum increase in rock motion amplitude from the different scenarios. None of the increases in rock motions from all scenarios exceeds 0.004 g.

Bommer (2012, p. 1724) emphasizes the importance of capturing epistemic uncertainty in logic trees for the input to PSHA and states, "for those conducted for nuclear power plant sites it becomes imperative to make concerted efforts to identify and quantify epistemic uncertainties, and to demonstrate that they have been captured in the logic tree." One approach to incorporating this range of epistemic uncertainty into the PSHA results would be to weight the different scenarios, and recalculate the probabilistic ground motions. This approach is not included as part of the hazard sensitivity calculations described in this response because, as Bommer (2012, p. 1727) states, "in the context of considering available models that might be included, it is perfectly feasible that several models ... will be effectively assigned weights of zero not because of a belief that they should not be used but simply because they are not needed in order to construct the distribution of uncertainty." The question addressed here asks whether the addition of fault sources results in a more conservative assessment of the ground motion hazard. The results of the hazard sensitivity calculations show that the maximum increase in rock motions at MAFE levels of  $10^{-4}$  and  $10^{-5}$  is insignificant ( $\ll 0.004$  g). Therefore, further consideration of fault scenarios for the Cuba seismic source is unnecessary.

The scenarios presented in Figure 5 are derived from a reasonable range of technically defensible seismic source characterizations for intraplate Cuba. As shown in Table 5, this range of seismic source characterizations results in only small changes in hazard at the Turkey Point Units 6 & 7 site. Based on the results of these hazard sensitivity calculations, it is concluded that the use of a single areal source zone and the parameters used to characterize it as presented in the FSAR gives a reasonably conservative estimate of the contribution to site hazard from intraplate Cuba seismic sources.

**b) Details of the PSHA implementation for the Cuba areal source zone. Specifically, is Cuba seismicity modeled using the EPRI approach, using a uniform source zone, or using some other methodology?**

The PSHA implementation for the Cuba areal source zone differs from the EPRI-SOG approach. In the PSHA presented in FSAR Section 2.5.2, intraplate Cuba was modeled as a single areal source zone with spatially uniform (complete smoothing) seismicity (total annual rate ( $M_w \geq 5.0$ ) = 0.0592,  $\beta = 1.932$  ( $b = 0.839$ )). An exponential magnitude model was assumed with an  $M_{max}$  distribution [and weights] of  $M_w$  7 [0.5] and  $7\frac{1}{4}$  [0.5]. For the purposes of the PSHA presented in FSAR Section 2.5.2 and the current sensitivity calculations, the upper limit of this distribution is rounded up to  $M_w$  7.3.

**c) A description of how well the seismic source model parameters represent the observed spatial patterns and concentrations of seismicity. Is a uniform seismic source zone justified considering FSAR Figure 2.5.1-267, which shows prominent clusters of seismicity? Discuss evidence, if any, that frequency-magnitude behavior is different for the subset of earthquakes concentrated in western and northern Cuba than for the entire zone.**

The single Cuba areal seismic source (Z1) is modeled by assuming a uniform rate for the entire source zone. An exponential frequency-magnitude distribution of the Gutenberg-Richter form  $\text{Log}(N) = a - b(M)$ , where  $N$  is the number of events greater than or equal to magnitude  $M$ , was fit to the observed seismicity using the maximum likelihood technique. The  $a$ -value reflects the seismicity rate, and the  $b$ -value indicates relative number of small to large magnitudes. This approach produces a uniform rate of seismicity within the areal source zone and does not account for local, above-average rates associated with areas of more concentrated or "prominent clusters" of seismicity, nor areas of less than average seismicity rate. Figure 1 depicts seismicity in Cuba in greater detail than shown on FSAR Figure 2.5.1-267. Figure 1 also shows the areal zonation scenarios used in the hazard sensitivity calculations described in this response.

If the Cuba areal source zone were to be subdivided in an attempt to model areas with higher rates of earthquake occurrence (Z6), this would result in areas of lower rates than the average uniform rate applied to the Cuba areal source zone. In particular, the offshore region of the Cuba areal source nearest the Turkey Point Units 6 & 7, which is nearly devoid of seismicity (Figure 1), likely would generate little or no hazard. Therefore, this modification may result in a less conservative characterization if the reduction in hazard from the nearest portion of the zone is greater than any increases in hazard from more distant areas of higher seismicity in Cuba. This point is illustrated by inspection of FSAR Figure 2.5.2-227, which shows the  $M$  and  $R$  deaggregation for 5 and 10 Hz for the  $10^{-4}$  uniform hazard response spectrum (UHRS). The Cuba areal source contribution to the site hazard appears in the  $M_w$  6.5 to 7.5 range and abruptly begins appearing in the 210 to 240 kilometer (130 to 150 mile) distance bin and beyond. The closest distance from the site to the Cuba areal source is approximately 220 kilometers (140 miles).

In order to address the question of how modeling of Cuba areal source zones would impact the hazard at the Turkey Point Units 6 & 7 site, two alternate zonation models (Z11% and Z6) were developed. The Z6 (six-zone model) is discussed in part (a) of this response. Details of how the Z11% model was developed are discussed below.

*Elevated Rate Areal Source Zone Scenario (Z11%)*

Seismicity in Cuba is not perfectly uniform, in that the density appears to be greatest in the southeast, west, and north-central portions of the island. In recognition of this, a “northern Cuba subzone” was defined that encompasses apparently higher than average seismicity in the north of Cuba (Figure 1). The northern Cuba subzone rate is found to be approximately 11% higher than the single-zone (Z1) rate, on a per-area basis. This 11% increase is then conservatively applied to the entire single areal zone rate to develop the Z11% scenario. The only difference between the Z1 and Z11% model is a +11% difference in rate in the latter. The effect of this rate increase on the PSHA results is discussed in part (a) of the current response. The following discussion provides details on the development of the Z11% model.

The northern Cuba subzone envelops the seismicity in north-central and western Cuba (Figure 4). Recurrence statistics were computed for this subzone by calculating the annual rate of  $M_w \geq 3$  earthquakes in the subzone, and assuming that the previously calculated  $b$ -value for the Cuba areal source zone represents the most stable estimate. The annual rates of  $M_w$  5 to 7.3 earthquakes from the two zones were then compared.

Before computing recurrence for the Cuba areal source zone, the earthquakes in Figure 1 were filtered to account for the completeness periods published in Garcia et al. (2008) (FSAR 2.5.2 Reference 255). The number of earthquakes decreases, but the general pattern of concentrated or “spatially clustered” seismicity remains.

Maximum likelihood recurrence parameters were computed for the Cuba areal source zone, using the Weichert (1980) formulation. The  $a$ -value is computed from the annual rate of  $M_w \geq 3$  events in the subzone. The  $a$ -value, or rate parameter, is normalized to events per square kilometer per year, to permit a comparison normalized to a common area.

Table 6 lists the recurrence statistics for the Z1 and Z11% zonation scenarios. The last column provides the computed rate of  $M_w$  5 to 7.3 earthquakes on a square kilometer per year basis, which allows for direct comparisons of the rates of earthquakes producing ground motions at the site. A comparison of the northern Cuba subzone rate to the rate for the Cuba areal source indicates that the northern Cuba subzone rate is 11% higher than the single zone model (Z1) on a rate per square kilometer per year basis (Table 6).

**d) Details on the earthquake catalog completeness, methodology used to compute the  $a$  and  $b$  values, the computed  $a$  and  $b$  values and rates of earthquakes equal to or greater than moment magnitude 5. If used, please also discuss smoothing operators applied to the  $a$  and  $b$  values.**

For use in the PSHA presented in FSAR Section 2.5.2, completeness periods as a function of magnitude for Cuba were taken directly from Garcia et al. (2008) (FSAR 2.5.2 Reference 255). These completeness periods are shown in the first three columns of Table 3. The number of earthquakes in each magnitude bin, taken from the Phase 2 earthquake catalog and filtered for these completeness periods, is shown in the last column of Table 3.

The objective is to solve for  $a$  and  $b$  in the Gutenberg-Richter equation for earthquake recurrence equation,

$$\text{Log}(N) = a - b(M) \quad (1)$$

where  $N$  is the cumulative annual number of earthquakes greater than or equal to magnitude  $M$ .

As presented in McGuire (2004, p. 190, Eq. A5), the maximum likelihood estimate for  $b$  is

$$Mbar = \frac{\sum_i t_i m_i e^{-\beta m_i}}{\sum_i t_i e^{-\beta m_i}} \quad (2)$$

where  $Mbar$  is the average magnitude of the data,  $t$  is the completeness duration in years,  $i$  corresponds to the magnitude bin, and  $\beta = b \times \ln(10)$ .  $m$  refers to the midpoint of the magnitude range. This is also the formulation presented in Weichert (1980).  $\beta$  in equation (2) is solved for using Newton's method, as suggested in Weichert (1980). The convergence criterion for  $\beta$  is when the difference in  $\beta$  between successive iterations falls below 0.0001.

Weichert (1980) defines  $N_a$  as the cumulative number of events at and above the minimum magnitude. His equation (10) (also McGuire 2004, p. 191, Eq. A9), states:

$$N_a = Z \frac{\sum_i e^{-\beta m_i}}{\sum_i t_i e^{-\beta m_i}} \quad (3)$$

where  $Z$  is the total number of events in the data set,  $N_a$  is the number of events above the minimum magnitude ( $M_w$  3.0) per annum. Once  $N_a$  is determined,  $a$  can be solved via Equation (1).

The results are:

$$b = 0.839$$

$$N_a = 2.821$$

$$a = 2.967$$

From Equation (1), the number of events greater than or equal to  $M_w$  5 per year is 0.0592. This equates to an average return period of about 17 years for earthquakes in this magnitude range for source zone Z1. No smoothing operators were applied to the  $a$ - and  $b$ -values. That is, recurrence parameters were assumed to be uniform throughout the source zone. Note that in Table 6 the  $a$  value has been normalized to  $\text{km}^{2/\text{yr}}$ , while in the list above it is for the entire zone.

**e) A detailed description of the PSHA implementation for the Cuba seismicity model. Are large earthquakes modeled as finite faults? If so, can they extend outside the zone boundary, and is there a preferred azimuth? If so, what is their closest distance of approach to the TPNPP site?**

For use in the PSHA presented in FSAR Section 2.5.2, earthquakes are modeled as point sources in the Cuba areal source zone, not as faults. Therefore, without finite faults, ruptures cannot extend outside the zone boundary and there is no preferred azimuth. Hypocentral depths are modeled as an equally weighted distribution of 2.5, 7.5, and 12.5

Proposed Turkey Point Units 6 and 7  
Docket Nos. 52-040 and 52-041  
FPL Revised Response to NRC RAI No. 02.05.02-4 (eRAI 5896)  
L-2014-282 Attachment 3 Page 11 of 40

km, representing depth ranges of 0 - 5, 5 - 10, and 10 - 15 km, respectively. The closest distance from the Turkey Point Units 6 & 7 site to the Cuba areal source is approximately 220 kilometers (140 miles).

**Table 1.** Cuba seismic source scenarios for sensitivity calculations

|   |                            | Source Zone Scenarios |                         |                           |   |
|---|----------------------------|-----------------------|-------------------------|---------------------------|---|
|   |                            | Increasing hazard →   |                         |                           |   |
|   |                            | No areal sources      | Z6<br>Six areal sources | Z1<br>Single areal source | Z11%<br>Elevated rate areal source<br>(+11% increase in rate) |
| Fault Source Scenarios<br>← Increasing hazard | No fault sources           | N/A                   | Z6                      | Z1<br>(FSAR)              | Z11%  |
|   | SF<br>Scaled fault sources | SF                    | Z6+SF*                  | Z1+SF*                    | Z11%+SF**   |
|   | FF<br>Full fault sources   | FF***                 | Z6+FF***                | Z1+FF***                  | Z11%+FF***  |

Shaded source scenarios are not quantitatively evaluated:

\* Z1+SF was evaluated as a reasonable combination scenario in the hazard sensitivity calculations. As discussed in the text, area source scenario Z6 was found to result in lower hazard than area source scenario Z1. Thus, it is unnecessary to further investigate the combination scenario Z6+SF.

\*\* As discussed in the text, source area scenario Z11% is considered a conservative assessment of the seismic hazard derived from the cataloged seismicity, therefore the combination scenario Z11%+SF is considered overly conservative for consideration in the hazard sensitivity calculations.

\*\*\* As discussed in the text, fault source scenario FF was determined to be technically indefensible compared to the cataloged seismicity. Therefore, any combination scenarios with FF were similarly eliminated as technically indefensible.

**Table 2.** Moment rates, ratio of seismicity-based moment rate to fault-based moment rates, and return periods for  $M_w$  6.5 and 7.0 from Cuba sensitivity options

| Moment Rate Option          | Moment Rate (dyne-cm/yr) | Ratio, Seismicity/Fault-based | Return Period for $M_w$ 6.5 (years) | Return Period for $M_w$ 7 (years) |
|-----------------------------|--------------------------|-------------------------------|-------------------------------------|-----------------------------------|
| Historical Seismicity*      | 7.7844E+23               | Not applicable                | 81                                  | 456                               |
| Low Slip Rate Option**      | 6.6686E+22               | 0.0857                        | 946                                 | 5321                              |
| Middle Slip Rate Option**   | 6.6686E+23               | 0.8567                        | 95                                  | 532                               |
| High Slip Rate Option**     | 6.6686E+24               | 8.5666                        | 9.5                                 | 53                                |
| Weighted Mean Slip Rate *** | 2.8535E+24               | 3.6657                        | 22                                  | 124                               |

\* Moment rate obtained from seismicity catalog and used for Cuba areal source (Z1) and for scaled fault scenario (SF).

\*\* Moment rates obtained from low, middle, and high slip rate values presented in RAI 02.05.01-21.

\*\*\* Moment rate obtained from weighted mean of slip rate values presented in RAI 02.05.01-21 and used for full fault scenario (FF).

**Table 3.** Completeness periods from Garcia et al. (2008) (FSAR 2.5.2 Reference 255) and earthquake counts in each bin from the Phase 2 earthquake catalog

| Magnitude Range ( $M_w$ ) | Start Date | End Date | Number of Earthquakes from Phase 2 Earthquake Catalog |
|---------------------------|------------|----------|---|
| 3.0 – 4.0                 | 1/1960     | 3/2008   | 119   |
| 4.0 – 5.0                 | 1/1940     | 3/2008   | 17  |
| 5.0 – 6.0                 | 1/1850     | 3/2008   | 14  |
| 6.0 – 7.0                 | 1/1500     | 3/2008   | 2   |

**Table 4.** Summary of hazard sensitivity study results: comparison of MAFE

|   | FSAR Z1  |        | Scenario Z6 |        | Scenario SF |        | Scenario Z11% |        | Scenario Z1+SF |        |
|---|----------|--------|-------------|--------|-------------|--------|---------------|--------|----------------|--------|
| <b>10<sup>-4</sup> mean annual frequency of exceedance (MAFE)</b> |          |        |             |        |             |        |               |        |                |        |
| Freq  | MAFE     | Amp*   | MAFE        | % Diff | MAFE        | % Diff | MAFE          | % Diff | MAFE           | % Diff |
| 1 Hz  | 1.00E-04 | 0.0343 | 9.499E-05   | -5.0%  | 9.6764E-05  | -3.2%  | 1.018E-04     | 1.8%   | 1.114E-04      | 11.4%  |
| 10 Hz   | 1.00E-04 | 0.0822 | 9.122E-05   | -8.8%  | 8.797E-05   | -12.0% | 1.025E-04     | 2.5%   | 1.094E-04      | 9.4%   |
| <b>10<sup>-5</sup> mean annual frequency of exceedance (MAFE)</b> |          |        |             |        |             |        |               |        |                |        |
| Freq  | MAFE     | Amp*   | MAFE        | % Diff | MAFE        | % Diff | MAFE          | % Diff | MAFE           | % Diff |
| 1 Hz  | 1.00E-05 | 0.0663 | 9.539E-06   | -4.6%  | 1.010E-05   | 1.0%   | 1.013E-05     | 1.3%   | 1.131E-05      | 13.1%  |
| 10 Hz   | 1.00E-05 | 0.278  | 9.891E-06   | -1.1%  | 9.969E-06   | -0.3%  | 9.992E-06     | -0.1%  | 1.014E-05      | 1.4%   |

\*Rock motion (g)

**Table 5.** Summary of hazard sensitivity results: comparison of rock motion amplitudes

|   | FSAR Z1 |        | Scenario Z6 |        | Scenario SF |          | Scenario Z11% |        | Scenario Z1+SF |        |        |          |        |
|---|---------|--------|-------------|--------|-------------|----------|---------------|--------|----------------|--------|--------|----------|--------|
| <b>Rock motions (g) at 10<sup>-4</sup> mean annual frequency of exceedance (MAFE)</b> |         |        |             |        |             |          |               |        |                |        |        |          |        |
| Freq  | Amp     | Amp    | Amp Diff    | % Diff | Amp         | Amp Diff | % Diff        | Amp    | Amp Diff       | % Diff | Amp    | Amp Diff | % Diff |
| 1 Hz  | 0.0343  | 0.0338 | -0.0005     | -1.5%  | 0.0340      | -0.0003  | -0.9%         | 0.0345 | 0.0002         | 0.6%   | 0.0354 | 0.0011   | 3.2%   |
| 10 Hz   | 0.0822  | 0.0784 | -0.0038     | -4.6%  | 0.0765      | -0.0057  | -6.9%         | 0.0832 | 0.0010         | 1.2%   | 0.0858 | 0.0036   | 4.4%   |
| <b>Rock motions (g) at 10<sup>-5</sup> mean annual frequency of exceedance (MAFE)</b> |         |        |             |        |             |          |               |        |                |        |        |          |        |
| Freq  | Amp     | Amp    | Amp Diff    | % Diff | Amp         | Amp Diff | % Diff        | Amp    | Amp Diff       | % Diff | Amp    | Amp Diff | % Diff |
| 1 Hz  | 0.0663  | 0.0654 | -0.0009     | -1.4%  | 0.0665      | 0.0002   | 0.3%          | 0.0665 | 0.0002         | 0.3%   | 0.0686 | 0.0023   | 3.5%   |
| 10 Hz   | 0.278   | 0.276  | -0.0020     | -0.7%  | 0.278       | 0.0000   | 0.0%          | 0.278  | 0.0000         | 0.0%   | 0.280  | 0.0020   | 0.7%   |

**Table 6.** Cuba areal source zone and northern Cuba subzone recurrence parameters

| Zone                   | Zone area (km <sup>2</sup> ) | # Events <sup>(a)</sup> | a-value <sup>(b)</sup> | b-value              | Rate of M <sub>w</sub> 5 to 7.3 events per year/km <sup>2</sup> |
|------------------------|------------------------------|-------------------------|------------------------|----------------------|---|
| Cuba areal source zone | 250,286                      | 152                     | -2.430                 | 0.839                | 2.341E-7  |
| Northern Cuba subzone  | 80,770                       | 46                      | -2.383 <sup>(d)</sup>  | 0.839 <sup>(c)</sup> | 2.609E-7  |

(a) Events  $\geq M_w$  3.0, filtered for completeness periods

(b) Normalized to events per year/km<sup>2</sup>

(c) Fixed to Cuba areal source zone b-value

(d) Value represents the 11% increase discussed in text

**Figure 1.** Map showing Cuba single areal source zone (Z1) (solid black line), six areal source zones (Z6) (dashed black lines), and northern Cuba subzone (green shading). Seismicity (blue circles) is from the Phase 2 earthquake catalog. Thick red lines show plate boundary fault sources included in FSAR PSHA.

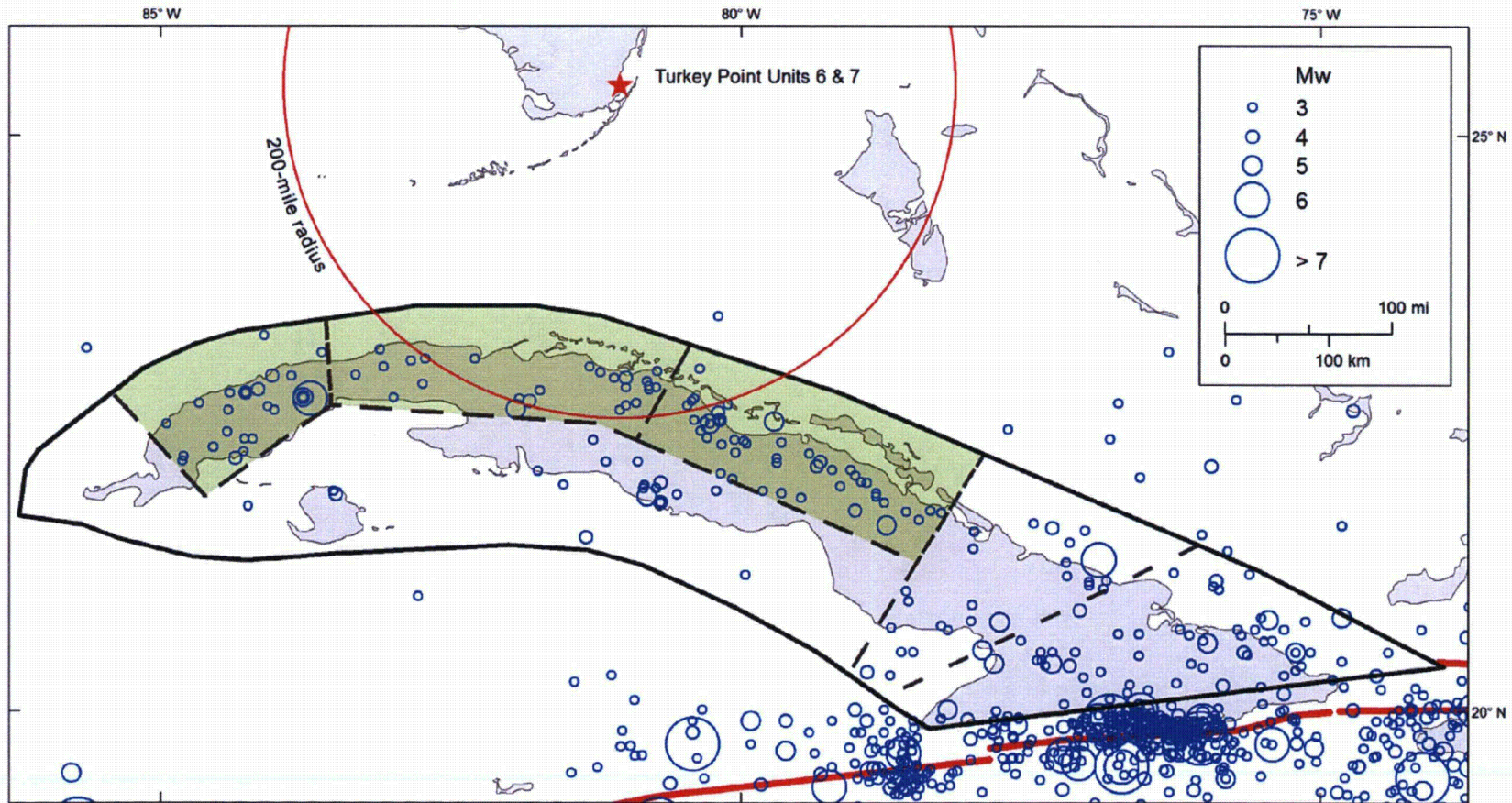
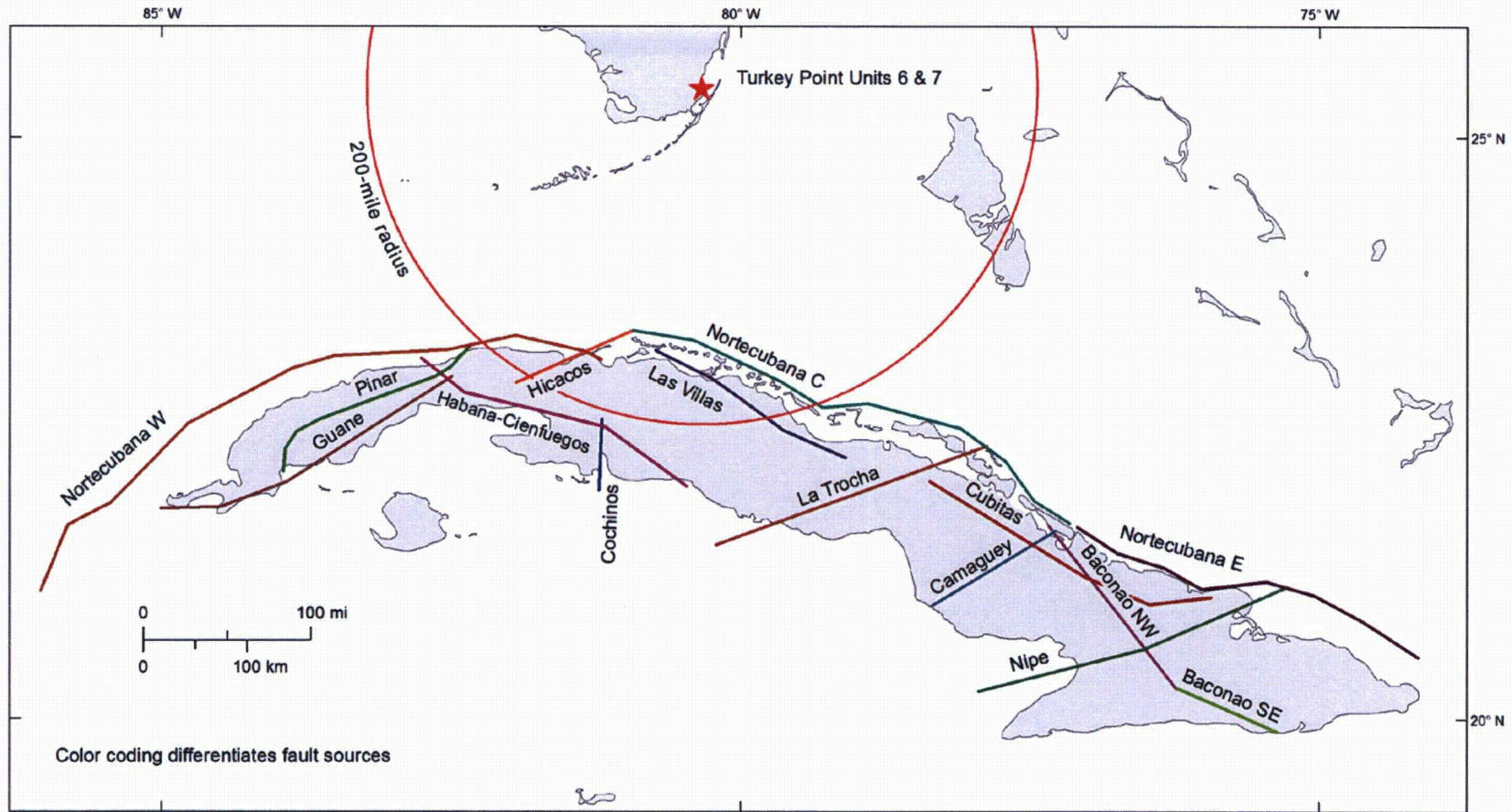
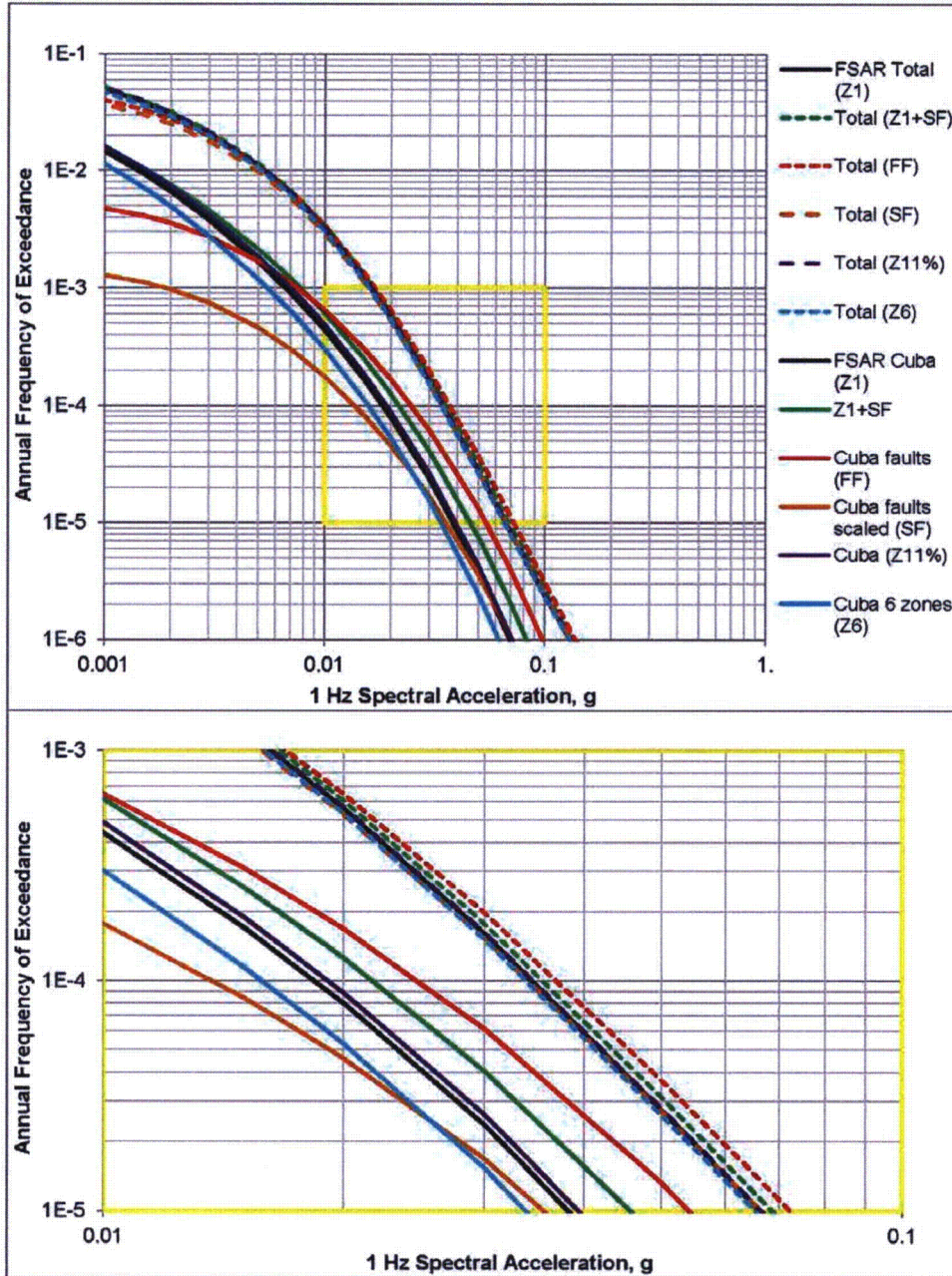


Figure 2. Map of intraplate Cuba fault sources as modeled for hazard sensitivity calculations.



**Figure 3.** 1 Hz mean hazard curves showing sensitivity to Cuba source scenarios. Lower panel is expanded view of yellow box in upper panel.



**Figure 4.** 10 Hz mean hazard curves showing sensitivity to Cuba source scenarios. Lower panel is expanded view of yellow box in upper panel.

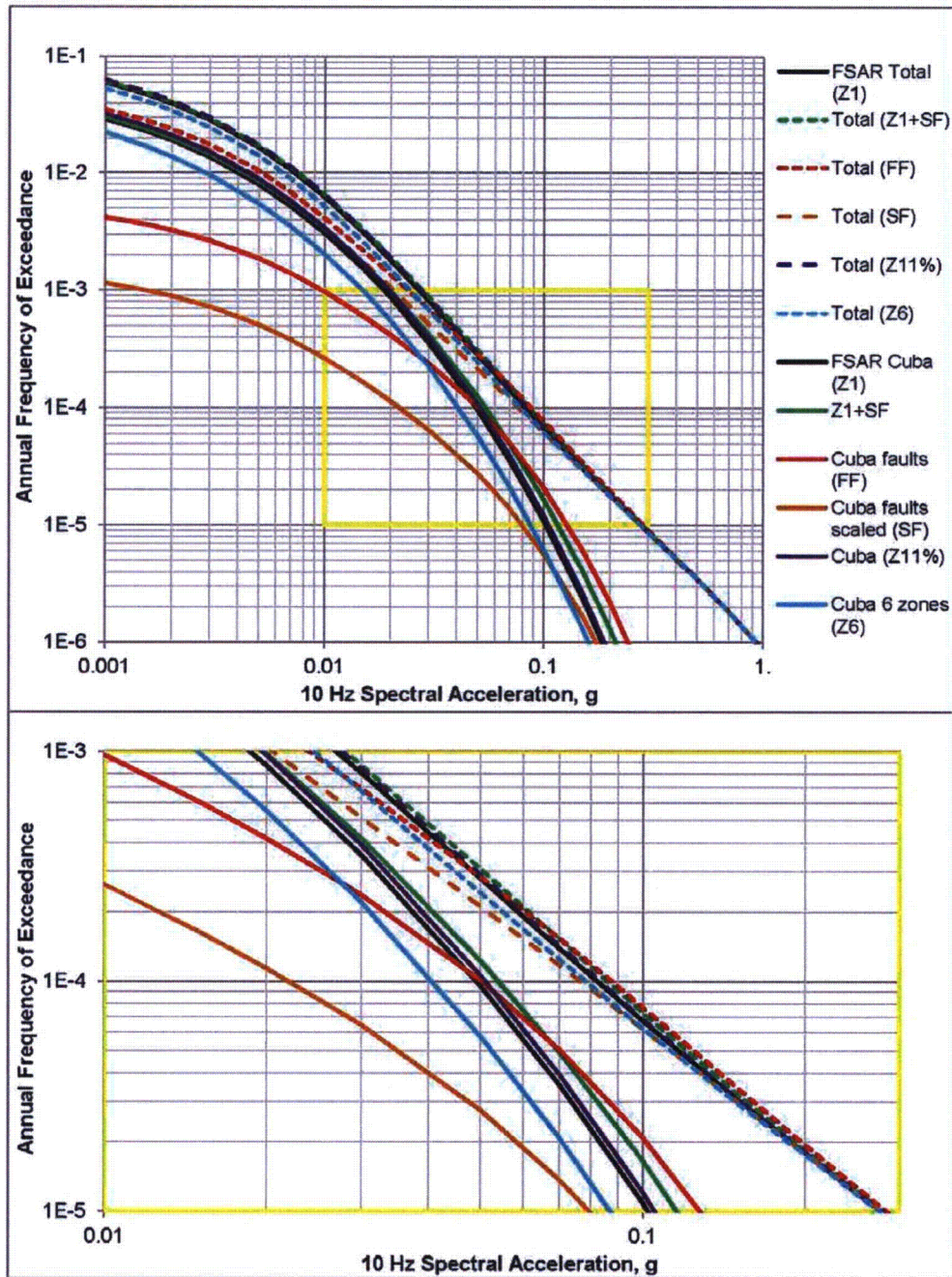
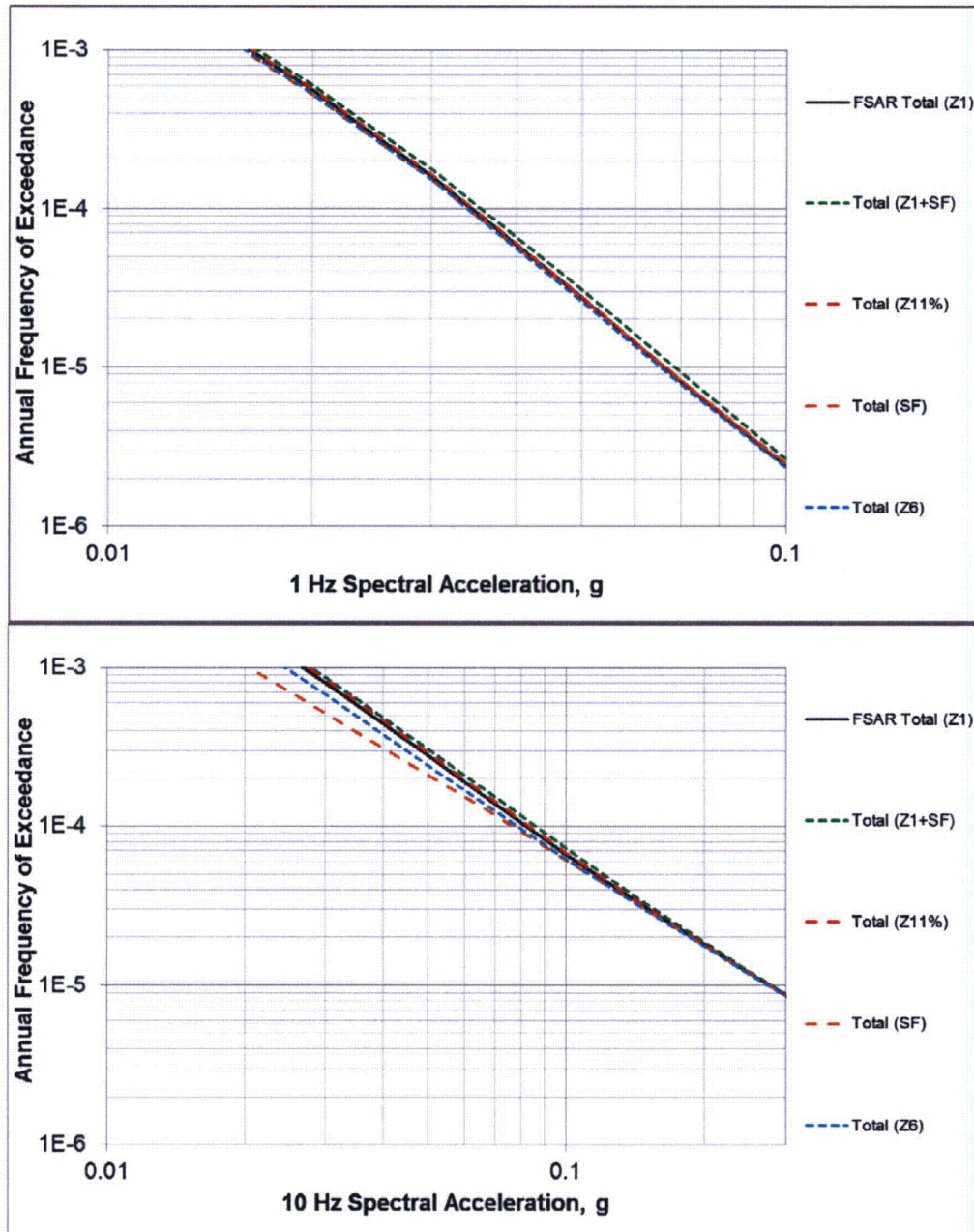


**Figure 5.** Total mean hazard curves for 1 Hz (upper) and 10 Hz (lower) showing sensitivity to four Cuba source scenarios.



This response is PLANT SPECIFIC.

**References:**

Bommer, J.J., 2012, Challenges of Building Logic Trees for Probabilistic Seismic Hazard Analysis (Opinion Paper), *Earthquake Spectra*, v. 28, no. 4, pp. 1723-1735.

EPRI, U.S. DOE, and U.S. NRC, 2012, *Technical Report: Central and Eastern United States Seismic Source Characterization for Nuclear Facilities*, EPRI, Palo Alto, CA, U.S. DOE, and U.S. NRC.

McGuire, R.K., 2004, *Seismic Hazard Analysis*, Earthquake Engineering Research Institute Monograph MNO-10, 221 p.

Weichert, D., 1980, Estimation of the earthquake recurrence parameters for unequal observation periods for different magnitudes, *Bulletin of the Seismological Society of America*, 70, pp. 1337-1347.

**ASSOCIATED COLA REVISIONS:**

Several new paragraphs will be inserted into a new FSAR Subsection 2.5.2.4.4.3.4.2 to describe the hazard sensitivity studies for the Cuba faults and alternative Cuba areal source zones. The text below will be added in a future FSAR revision:

**2.5.2.4.4.3.4.2 Cuba Hazard Sensitivity Calculations**

**This subsection describes the characterization and results of intraplate Cuba seismic sources for use in a hazard sensitivity calculation performed to assess the potential impact on the Turkey Point Units 6 & 7 PSHA. As described in Subsection 2.5.1.1.1.3.2.4, it is unclear which, if any, of the faults in intraplate Cuba are capable tectonic sources. For this reason, hazard sensitivity calculations were performed to assess the potential impact of intraplate Cuba seismic sources. The seismic source parameters for both areal and fault sources used in these hazard sensitivity calculations were developed through the use of SSHAC Level 2 methodology (Reference 318). Subsection 2.5.2.4.4.3.1 describes the SSHAC Level 2 methodology.**

**For the SSHAC Level 2 study of Cuba seismic sources, the TI team comprised Dean Ostenaar, Roland LaForge, Scott Lindvall, and Ross Hartleb. Participatory peer review was provided by Robert Creed. A total of eleven experts were contacted by the TI team with questions regarding the sensitivity calculations. These experts include geologists, seismologists, and hazard analysts from Cuba, the U.S., and elsewhere (Table 2.5.2-232). The level of detail provided to the TI team by the experts varies (Table 2.5.2-232). Some experts provided detailed responses and interacted with the TI team, whereas other experts provided only terse responses. Four experts either declined to participate or did not respond at all.**

**2.5.2.4.4.3.4.2.1 Cuba Seismic Sources for Hazard Sensitivity Calculation**

**Based on review of published literature and interaction with experts, the TI team developed a seismic source characterization for intraplate Cuba seismic sources for use in a hazard sensitivity calculation to assess the impact on hazard at the Turkey Point Units 6 & 7 site. This subsection describes the characterization of both areal**

**sources and fault sources for the hazard sensitivity calculations.**

**Three scenarios by which areal source zones are implemented in the hazard sensitivity calculations are summarized below and in Table 2.5.2-233.**

- **Single areal source zone scenario (Z1):** In the single areal source zone model, a single areal source for Cuba is used, with a uniform seismicity rate throughout the zone that is based on observed seismicity from the Phase 2 earthquake catalog (Figure 2.5.2-271). This is the base case for the hazard sensitivity calculations and is the seismic source characterization for intraplate Cuba used in the PSHA (Subsection 2.5.2.4.6). The Z1 model results in a contribution to hazard that is intermediate between the Z6 and Z11% zone scenarios (Table 2.5.2- 233).
- **Elevated rate areal source zone scenario (Z11%):** In the elevated rate zone scenario, a single areal source for Cuba is used, with a uniform seismicity rate throughout the zone that is based on observed seismicity from the Phase 2 earthquake catalog. The geometry of this zone is equivalent to that in the Z1 scenario. Unlike the Z1 scenario, however, the uniform rate for the Z11% scenario is based on a small subzone in northern Cuba (the “northern Cuba subzone” shown in Figure 2.5.2-271) that is located partially within the site region and that exhibits a higher rate of seismicity than surrounding regions. The seismicity rate from the northern subzone is approximately 11 percent higher than that for the entire Cuba areal source zone, and this higher rate is applied to the Z1 scenario. The Z11% scenario results in the highest contribution to hazard from the three zone scenarios (Table 2.5.2-233).
- **Six areal source zones scenario (Z6):** In the six areal source zones scenario, Cuba is divided into six zones largely on the basis of observed patterns in seismicity (Figure 2.5.2-271). The seismicity *b*-value is constant across all six zones and equivalent to that used in the Z1 scenario; the seismicity *a*-values vary from zone to zone, are uniform within each zone, and are based on the observed seismicity within each zone. For the six-zone scenario (Z6), the *a*-values were determined by counting the number of events in each subzone greater than or equal to  $M_w$  3.0. The *b*-value in base case Z1 is used for all six subzones. The Z6 scenario results in the lowest contribution to hazard from the three zone scenarios (Table 2.5.2-233).

All areal source scenarios are given equally weighted maximum moment magnitudes  $M_w$  of 7.0 and 7.3 with uniformly distributed seismicity parameters (complete smoothing) determined from the earthquakes within each zone. Values for Z1 and Z11% are shown in Table 2.5.2-234, using the completeness table for Cuba from Garcia et al. (Reference 255) (Table 2.5.2-235). Focal depth for all areal sources is the same as was implemented in Subsection 2.5.2.4.6, which uses a three-point distribution to represent the 0-15 kilometer (0-9 miles) seismogenic thickness: 2.5, 7.5, and 12.5 kilometers (1.6, 4.7, and 7.8 miles), equally weighted.

The input parameters for the Cuba sensitivity fault sources are described below and are summarized in Table 2.5.2-236 and Figure 2.5.2-272:

- **Fault sources and geometries:** Intraplate Cuba fault sources include Cotilla-

Rodriguez et al.'s (Reference 321) seismoactive faults in Cuba plus the Pinar fault (Figure 2.5.2-272). For the purpose of the hazard sensitivity calculation, it is assumed that all of these faults are capable tectonic sources. The Nortecubana fault is divided into three sensitivity fault sources, the Nortecubana West, Nortecubana Central, and Nortecubana East fault sources. The Baconao fault is divided into two sensitivity fault sources, the Baconao Northwest and the Baconao Southeast fault sources. Seismogenic depth for all fault sources in the hazard sensitivity calculation extends from 0-15 kilometers (0-9 miles). All fault sources are modeled with vertical dip angle, except the three Nortecubana fault sources, all of which are modeled as dipping 30 degrees to the south.

- **Probability of activity:** For the purpose of the hazard sensitivity calculation, it is assumed that each of the Cuba faults listed in Table 2.5.2-236 is a capable tectonic source with a probability of activity of 1.0. This is a conservative decision given the available geologic data.
- **Maximum magnitude assessment:** Modeled magnitude distribution [and weight] for all of the Cuba sensitivity fault sources is  $M_w$  7.0 [0.5], 7.3 [0.5]. These values and weights are the same as those used in the Cuba areal source zone (Subsection 2.5.2.4.4.3.2.1). The maximum magnitude ( $M_{max}$ ) values for the sensitivity fault sources are higher than those presented in published literature. For example, Garcia et al.'s (Reference 254) Table 4 shows the range of  $M_{max}$  values for fault sources in intraplate Cuba (their sources 1 through 24) from their study and previous studies, which range from  $M_w$  5.0 to 7.0, with many at the middle to low end of this range.
- **Slip rate assessment:** There are no data to directly determine late Quaternary slip rates for potential Cuba sensitivity fault sources. For most sensitivity fault sources, slip rates in millimeters/year [and weights] are assigned as 0.001 [0.33], 0.01 [0.34], 0.1 [0.33]. For the three sensitivity fault sources most proximal to the modern plate boundary, higher slip rates are assigned as 0.01 [0.1], 0.1 [0.5], 1.0 [0.4]. These slip rate distributions span orders of magnitude, reflecting the lack of data and considerable uncertainty. It is assumed that all slip is seismogenic (i.e., fully coupled).
- **Recurrence model:** For the purpose of the hazard sensitivity calculation, a characteristic earthquake recurrence model is assumed for the Cuba sensitivity fault sources, but with no contribution from the exponential portion of the recurrence curve at lower magnitudes.

For the hazard sensitivity calculations, there are three scenarios for fault sources, as shown in Table 2.5.2-233 and summarized below:

- **No fault sources scenario:** This scenario excludes fault sources from the hazard sensitivity calculations. This is consistent with the seismic source characterization used for the PSHA presented in Subsection 2.5.2.4.6.
- **Full fault model scenario (FF):** The full fault model scenario includes 15 fault sources, as summarized in Table 2.5.2-236.
- **Scaled fault model scenario (SF):** The SF scenario is derived from the FF scenario

such that the total seismic moment rate from the fault sources is equivalent to the seismic moment rate from the observed seismicity (Z1 scenario). The SF scenario results in a contribution to hazard that is lower than that from the FF fault source scenario (Table 2.5.2-233).

A total of eleven possible combinations of areal and fault scenarios are shown in Table 2.5.2-233. The results of hazard sensitivity calculations using these scenarios is presented in Subsection 2.5.2.4.4.3.4.2.2. The hazard sensitivity calculations for both the areal and fault source scenarios use ground motion attenuation relationships developed for Caribbean crustal seismic sources described in Subsection 2.5.2.4.5.2.

#### 2.5.2.4.4.3.4.2.2 Results of Cuba Hazard Sensitivity Calculations

This section describes the results of hazard sensitivity calculations for individual areal and fault source scenarios as well as scenarios that combine areal and fault sources. A total of eleven possible combinations of areal and fault scenarios are shown in Table 2.5.2-233. One of these (Z1) is the base case used in the PSHA (Subsection 2.5.2.4.6). In addition to Z1, five of these scenarios are evaluated quantitatively (Z6, Z11%, SF, Z1+SF, and FF) and are described below in this subsection. Figures 2.5.2-273 and 2.5.2-274 present 1 Hz and 10 Hz hazard curves for these five scenarios. These figures also present the corresponding total hazard curves that include each of these Cuba scenarios.

- The Z6 scenario results in a decrease in hazard relative to the Z1 base case.
- The Z11% scenario results in an increase in hazard relative to the Z1 base case.
- The SF scenario results in a lower hazard relative to the Z1 base case.
- The Z1+SF scenario results in a higher hazard relative to the Z1 base case.
- The FF scenario results in a higher hazard relative to the Z1 base case.

Of these five scenarios, four are judged by the TI team to be most likely to encompass the center, body, and range of the views of the informed technical community (Z6, Z11%, SF, and Z1+SF). In contrast, the FF scenario is judged as overly conservative and therefore technically indefensible. The rationale for this assessment is based on the discrepancy between the observed historical rate of large earthquakes in Cuba and that predicted by the moment rate for the FF scenario. The moment rate for the FF scenario is derived from the weighted mean of slip rate distributions for the 15 Cuba fault sources. The bottom row of Table 2.5.2-237 illustrates that the moment rate for the weighted mean slip rate (FF model) yields a return period of 124 years for  $M_w$  7.0 events. The completeness period for earthquakes in Cuba in the  $M_w$  6.0 to 7.0 range is given as about 500 years according to Garcia et al. (Reference 255) (Table 2.5.2-234). In the approximately 500-year record of observed seismicity in Cuba, there are no magnitude 7 events, and the largest earthquake in that time in the Phase 2 earthquake catalog from intraplate Cuba is approximately  $M_w$  6.3 (Subsection 2.5.2.4.4.3.3.1). Another way to examine the overly conservative rate derived from the FF scenario is to compare the ratio of moment rate

derived from seismicity to moment rate derived from the assumed fault slip rates in the middle column of Table 2.5.2-237. That comparison shows that the FF scenario moment rate is 367 percent greater (3.67 factor in Table 2.5.2-237) than the moment rate derived from historical seismicity. While the individual FF scenario is presented in Figures 2.5.2-273 and 2.5.2-274, it is not considered further. Likewise, combinations involving the FF scenario are also eliminated and not presented, as they would be overly conservative and technically indefensible.

The remaining five combination scenarios (Z6+FF, Z1+FF, Z11%+FF, Z6+SF, and Z11%+SF) are discarded from further consideration based on the rationale provided below:

- Three combination scenarios, Z6+FF, Z1+FF, and Z11%+FF, are discarded due to the inclusion of the FF scenario as described above.
- The Z6+SF combination scenario is judged to lie within the likely center, body, and range of the views of the informed technical community, but would result in an intermediate hazard not useful for this sensitivity analyses because SF is also combined with the Z1 scenario. The Z1+SF scenario results in higher hazard (Figures 2.5.2-273 and 2.5.2-274).
- The Z11%+SF combination scenario includes an areal zone scenario that is based on an arbitrary activity rate increase applied to the entire zone.

To assess the impact of various Cuba sensitivity scenarios on the Turkey Point Units 6 & 7 site hazard, based on the evaluation of the hazard results presented in Figures 2.5.2-273 and 2.5.2-274, four sensitivity scenarios (Z6, Z11%, SF, and Z1+SF) were selected to represent the Cuba hazard in lieu of the Z1 base case scenario used for the original base case hazard total. Total hazard curves that include these four scenarios are presented in Figure 2.5.2-275, along with the original total hazard.

Detailed comparisons of the differences in total hazard for the four scenarios with respect to the base case total hazard are compiled in Tables 2.5.2-238 and 2.5.2-239. Two acceleration spectral response frequencies (1 Hz and 10 Hz) and two MAFE levels ( $10^{-4}$  and  $10^{-5}$ ) are considered. Table 2.5.2-238 shows the percent differences in MAFE for each scenario at the respective base case amplitudes. Negative values indicate lower hazard levels than the base case levels, positive values are higher. The base case values are shown in the first pair of columns, and the subsequent four scenarios increase in hazard level from left to right. Differences for the Z6 scenario range from -8.8 percent to -1.1 percent of the base case total. Differences for the SF scenario range from -12 percent to 1.0 percent. The Z11% scenario is based on an increased seismicity rate for the entire areal zone compared to the base case and results in differences which range from -0.1 percent to 2.5 percent. For the Z1+SF scenario, differences are the greatest, ranging from 1.4 percent to 13.1 percent. Note that the apparent decrease (0.1 percent) in 10 Hz MAFE at the  $10^{-5}$  MAFE amplitudes for scenario Z11% is due to the limited number of significant digits presented in the base case for total mean hazard, the process of interpolation, and rounding. That this is only an apparent decrease is supported by the fact that the  $10^{-5}$  MAFE amplitudes for scenario Z11% match the base case amplitudes exactly to three significant figures

**(Table 2.5.2-239).**

**Table 2.5.2-239 shows the changes in rock motion amplitude for the four scenarios. The largest of these changes is negative relative to the base case amplitudes. These are shown as absolute and percent differences in amplitudes. The largest percent increase is 4.4 percent and results from the Z1+SF scenario and the greatest decrease is -6.9 percent from the SF scenario. Of greater importance than the percentages is the maximum increase in rock motion amplitude from the different scenarios. None of the increases in rock motions from all scenarios exceeds 0.004 g.**

**The scenarios presented in Figure 2.5.2-275 are derived from a reasonable range of technically defensible seismic source characterizations for intraplate Cuba. As shown in Table 2.5.2-239, this range of seismic source characterizations results in only small changes in hazard at the Turkey Point Units 6 & 7 site. Based on the results of these hazard sensitivity calculations, it is concluded that the use of a single areal source zone and the parameters used to characterize it as presented in Subsection 2.5.2.4.6 gives a reasonably conservative estimate of the contribution to site hazard from intraplate Cuba seismic sources.**

The following table will be revised in a future revision of the FSAR:

**Table 2.5.2-217  
Summary of Cuba and Northern Caribbean Seismic Source Parameters**

| Area Source               | Closest Distance to Units 6 & 7 (mi) | Annual Number of Earthquakes of $M_w$ 5.0 and Greater | $b$ -value | $M_{max}$ ( $M_w$ )                    |
|---------------------------|--------------------------------------|---|------------|--|
| 1. Cuba areal source zone | 140                                  | 0.0592  | 0.839      | 7.0 [0.5]<br>7.25 [0.5] <sup>(a)</sup> |

(a) For the PSHA calculation, this value was rounded up to  $M_w$  7.3.

| Fault Source                         | Closest Distance to Units 6 & 7 (mi) | Fault Type/<br>Dip         | Slip Rate (mm/yr)                | Seismic Coupling                    | $M_{max}$ ( $M_w$ )                 |
|--------------------------------------|--------------------------------------|----------------------------|----------------------------------|-------------------------------------|-------------------------------------|
| 2. Oriente – Western                 | 420                                  | Strike-slip/<br>90°        | 8 [0.1]<br>11 [0.7]<br>13 [0.2]  | 0.6 [0.2]<br>0.8 [0.2]<br>1.0 [0.6] | 7.5 [0.3]<br>7.7 [0.4]<br>8.0 [0.3] |
| 3. Oriente – Eastern                 | 445                                  | Strike-slip/<br>90°        | 8 [0.1]<br>11 [0.7]<br>13 [0.2]  | 1.0 [1.0]                           | 7.5 [0.2]<br>7.7 [0.6]<br>7.9 [0.2] |
| 4. Septentrional                     | 545                                  | Strike-slip/<br>90°        | 6 [0.2]<br>9 [0.6]<br>12 [0.2]   | 1.0 [1.0]                           | 8.0 [0.5]<br>8.25 [0.5]             |
| 5. Northern Hispaniola – Western     | 550                                  | Thrust/<br>20-25°<br>south | 4 [0.2]<br>6 [0.7]<br>8 [0.1]    | 1.0 [1.0]                           | 7.8 [0.2]<br>8.0 [0.6]<br>8.3 [0.2] |
| 6. Northern Hispaniola – Eastern     | 760                                  | Thrust/<br>20-25°<br>south | 4 [0.2]<br>6 [0.7]<br>8 [0.1]    | 1.0 [1.0]                           | 8.6 [0.2]<br>8.3 [0.6]<br>8.6 [0.2] |
| 7. Swan Islands – Western            | 620                                  | Strike-slip/<br>90°        | 18 [0.2]<br>19 [0.6]<br>20 [0.2] | 1.0 [1.0]                           | 7.8 [0.2]<br>8.0 [0.7]<br>8.3 [0.1] |
| 8. Swan Islands – Eastern            | 540                                  | Strike-slip/<br>90°        | 18 [0.2]<br>19 [0.6]<br>20 [0.2] | 0.6 [0.2]<br>0.8 [0.2]<br>1.0 [0.6] | 7.2 [0.4]<br>7.5 [0.5]<br>7.7 [0.1] |
| 9. Walton – Duanvale                 | 490                                  | Strike-slip/<br>90°        | 6 [0.2]<br>8 [0.6]<br>10 [0.2]   | 0.8 [0.3]<br>1.0 [0.7]              | 7.3 [0.3]<br>7.6 [0.6]<br>7.8 [0.1] |
| 10. Enriquillo-Plantain Garden fault | 560                                  | Strike-slip/<br>90°        | 6 [0.2]<br>8 [0.6]<br>10 [0.2]   | 1.0 [1.0]                           | 7.5 [0.2]<br>7.7 [0.6]<br>7.9 [0.2] |

The following will be added as a new FSAR table in a future revision of the FSAR:

**Table 2.5.2-232  
Experts Contacted for the SSHAC Level 2 Study in Support of Cuba  
Hazard Sensitivity Calculations**

| <b>Expert</b>                           | <b>Affiliation</b>  | <b>Expertise</b>  | <b>Response</b>   |
|---|---|---|---|
| <b>Coppersmith, Kevin</b>               | <b>Coppersmith Consulting</b>   | <b>Seismic hazard modeling, seismic source characterization</b> | <b>Email response.</b>  |
| <b>Cotilla Rodriguez, Mario Octavio</b> | <b>Departamento de Física de la Tierra y Astrofísica, Facultad de Ciencias Físicas, Universidad Complutense de Madrid (Madrid, Spain)</b>                 | <b>Cuba faults and neotectonics</b>                             | <b>Detailed email response.</b>                                   |
| <b>Garcia, Julio</b>                    | <b>Centro Nacional de Investigaciones Sismológicas (CENAIIS) (Havana, Cuba)</b>   | <b>Seismic hazard modeling in Cuba</b>                          | <b>No response.</b>   |
| <b>Hanson, Kathryn</b>                  | <b>AMEC</b>   | <b>Seismic hazard modeling, seismic source characterization</b> | <b>Declined to participate.</b>                                   |
| <b>Ituralde-Vinent, Manuel</b>          | <b>Museo Nacional de Historia Natural (Havana, Cuba) and Departamento de Geociencias, Instituto Superior Politécnico J. A. Echeverría (Havana, Cuba)</b>  | <b>Geology of Cuba</b>  | <b>No response.</b>   |
| <b>Moreno Toiran, Bladimir</b>          | <b>Inst. Of Solid Earth Physics, University of Bergen (Norway) and Centro Nacional de Investigaciones Sismológicas (CENAIIS) (Santiago de Cuba, Cuba)</b> | <b>Seismology and geophysics of Cuba</b>                        | <b>Email response.</b>  |
| <b>Slejko, Dario</b>                    | <b>Istituto Nazionale di Oceanografia e di Geofisica Sperimentale (OGS) (Trieste, Italy)</b>  | <b>Seismic hazard modeling in Cuba</b>                          | <b>Detailed email response.</b>                                   |
| <b>Toscano, Marguerite</b>              | <b>Department of Paleobiology, Smithsonian Institute</b>  | <b>Marine terrace mapping and dating in northern Cuba</b>       | <b>Email response and telephone conversation regarding marine</b> |
| <b>Wong, Ivan</b>                       | <b>URS Corporation</b>  | <b>Seismic hazard modeling, seismic source characterization</b> | <b>Detailed email responses.</b>                                  |
| <b>Youngs, Robert</b>                   | <b>AMEC</b>   | <b>Seismic hazard modeling</b>                                  | <b>Declined to participate.</b>                                   |
| <b>Zapata Balanque, Jose Alejandro</b>  | <b>Universidad de Oriente (Santiago de Cuba, Cuba)</b>  | <b>Cuba faults and neotectonics</b>                             | <b>Email response regarding plans for future paleoseismic</b>     |

The following will be added as a new FSAR table in a future revision of the FSAR:

**Table 2.5.2-233  
Cuba Seismic Source Alternatives for Hazard Sensitivity Calculations**

|   |                            | Source Zone Scenarios |                         |                           |   |
|---|----------------------------|-----------------------|-------------------------|---------------------------|---|
|   |                            | Increasing hazard →   |                         |                           |   |
|   |                            | No areal sources      | Z6<br>Six areal sources | Z1<br>Single areal source | Z11%<br>Elevated rate areal source<br>(+11% increase in rate) |
| Fault Source Scenarios<br>← Increasing hazard | No fault sources           | N/A                   | Z6                      | Z1                        | Z11%  |
|   | SF<br>Scaled fault sources | SF                    | Z6+SF <sup>(a)</sup>    | Z1+SF <sup>(a)</sup>      | Z11%+SF <sup>(b)</sup>  |
|   | FF<br>Full fault sources   | FF <sup>(c)</sup>     | Z6+FF <sup>(c)</sup>    | Z1+FF <sup>(c)</sup>      | Z11%+FF <sup>(c)</sup>  |

- (a) Z1+SF was evaluated as a reasonable combination scenario in the hazard sensitivity calculations. As discussed in the text, area source scenario Z6 was found to result in lower hazard than area source scenario Z1. Thus, it is unnecessary to further investigate the combination scenario Z6+SF.
- (b) As discussed in the text, source area scenario Z11% is considered a conservative assessment of the seismic hazard derived from the cataloged seismicity. Therefore the combination scenario Z11%+SF is considered overly conservative for consideration in the hazard sensitivity calculations.
- (c) As discussed in the text, fault source scenario FF was determined to be technically indefensible compared to the cataloged seismicity. Therefore, any combination scenarios with FF were similarly eliminated as technically indefensible.

Shaded source scenarios not quantitatively evaluated.

The following will be added as a new FSAR table in a future revision of the FSAR:

**Table 2.5.2-234**  
**Cuba Areal Source Zone and Northern Cuba Subzone Recurrence Parameters**

| Zone                   | Zone area (km <sup>2</sup> ) | # Events <sup>(a)</sup> | a-value <sup>(b)</sup> | b-value              | Rate of M <sub>w</sub> 5 to 7.3 events per year/km <sup>2</sup> |
|------------------------|------------------------------|-------------------------|------------------------|----------------------|---|
| Cuba areal source zone | 250,286                      | 152                     | -2.430                 | 0.839                | 2.341E-7  |
| Northern Cuba subzone  | 80,770                       | 46                      | -2.383 <sup>(c)</sup>  | 0.839 <sup>(d)</sup> | 2.609E-7  |

(a) Events ≥ M<sub>w</sub> 3.0, filtered for completeness periods.

(b) Normalized to events per year/kmm<sup>2</sup>.

(c) Value represents the 11 percent increase discussed in text.

(d) Fixed to Cuba areal source zone b-value.

The following will be added as a new FSAR table in a future revision of the FSAR:

**Table 2.5.2-235**  
**Completeness Periods and Earthquake Counts in Each Bin from the Phase 2 Earthquake Catalog**

| Magnitude Range (M <sub>w</sub> ) | Start Date | End Date | Number of Earthquakes from Phase 2 Earthquake Catalog |
|-----------------------------------|------------|----------|---|
| 3.0 – 4.0                         | 1/1960     | 3/2008   | 119   |
| 4.0 – 5.0                         | 1/1940     | 3/2008   | 17  |
| 5.0 – 6.0                         | 1/1850     | 3/2008   | 14  |
| 6.0 – 7.0                         | 1/1500     | 3/2008   | 2   |

Source: Reference 255

The following will be added as a new FSAR table in a future revision of the FSAR:

**Table 2.5.2-236**  
**Summary of Seismic Source Parameters for Intraplate Cuba Fault Sources for Hazard Sensitivity Calculation**

| Sensitivity Fault Source | Dip   | Rupture Depth Range (km) | Length (km) | Magnitude ( $M_w$ ) [and weight] | Slip Rate (mm/yr) [and weight]            |
|--------------------------|-------|--------------------------|-------------|----------------------------------|---|
| Baconao SE               | 90°   | 0-15                     | 101         | 7.0 [0.5]<br>7.3 [0.5]           | 0.01 [0.1]<br>0.1 [0.5]<br>1.0 [0.4]      |
| Baconao NW               | 90°   | 0-15                     | 191         | 7.0 [0.5]<br>7.3 [0.5]           | 0.001 [0.33]<br>0.01 [0.34]<br>0.1 [0.33] |
| Camaguey                 | 90°   | 0-15                     | 131         | 7.0 [0.5]<br>7.3 [0.5]           | 0.001 [0.33]<br>0.01 [0.34]<br>0.1 [0.33] |
| Cochinos                 | 90°   | 0-15                     | 68          | 7.0 [0.5]<br>7.3 [0.5]           | 0.001 [0.33]<br>0.01 [0.34]<br>0.1 [0.33] |
| Cubitas                  | 90°   | 0-15                     | 283         | 7.0 [0.5]<br>7.3 [0.5]           | 0.001 [0.33]<br>0.01 [0.34]<br>0.1 [0.33] |
| Guane                    | 90°   | 0-15                     | 292         | 7.0 [0.5]<br>7.3 [0.5]           | 0.001 [0.33]<br>0.01 [0.34]<br>0.1 [0.33] |
| Habana-Cienfuegos        | 90°   | 0-15                     | 269         | 7.0 [0.5]<br>7.3 [0.5]           | 0.001 [0.33]<br>0.01 [0.34]<br>0.1 [0.33] |
| Hicacos                  | 90°   | 0-15                     | 114         | 7.0 [0.5]<br>7.3 [0.5]           | 0.001 [0.33]<br>0.01 [0.34]<br>0.1 [0.33] |
| La Trocha                | 90°   | 0-15                     | 257         | 7.0 [0.5]<br>7.3 [0.5]           | 0.001 [0.33]<br>0.01 [0.34]<br>0.1 [0.33] |
| Las Villas               | 90°   | 0-15                     | 197         | 7.0 [0.5]<br>7.3 [0.5]           | 0.001 [0.33]<br>0.01 [0.34]<br>0.1 [0.33] |
| Nipe                     | 90°   | 0-15                     | 292         | 7.0 [0.5]<br>7.3 [0.5]           | 0.01 [0.1]<br>0.1 [0.5]<br>1.0 [0.4]      |
| Nortecubana West         | 30° S | 0-15                     | 595         | 7.0 [0.5]<br>7.3 [0.5]           | 0.001 [0.33]<br>0.01 [0.34]<br>0.1 [0.33] |
| Nortecubana Central      | 30° S | 0-15                     | 441         | 7.0 [0.5]<br>7.3 [0.5]           | 0.001 [0.33]<br>0.01 [0.34]<br>0.1 [0.33] |
| Nortecubana East         | 30° S | 0-15                     | 340         | 7.0 [0.5]<br>7.3 [0.5]           | 0.01 [0.1]<br>0.1 [0.5]<br>1.0 [0.4]      |
| Pinar                    | 90°   | 0-15                     | 215         | 7.0 [0.5]<br>7.3 [0.5]           | 0.001 [0.33]<br>0.01 [0.34]<br>0.1 [0.33] |

The following will be added as a new FSAR table in a future revision of the FSAR:

**Table 2.5.2-237**  
**Moment Rates, Ratio of Seismicity-Based Moment Rate to Fault-Based Moment Rates, and Return Periods for  $M_w$  6.5 and 7.0 from Cuba Sensitivity Options**

| <b>Moment Rate Options</b>                   | <b>Moment Rate (dyne-cm/yr)</b> | <b>Ratio, Seismicity/Fault - based</b> | <b>Return Period for <math>M_w</math> 6.5 (years)</b> | <b>Return Period for <math>M_w</math> 7 (years)</b> |
|--|---------------------------------|--|---|---|
| <b>Historical Seismicity<sup>(a)</sup></b>   | <b>7.7844E+23</b>               | <b>Not applicable</b>                  | <b>81</b>   | <b>456</b>  |
| <b>Low Slip Rate Option<sup>(b)</sup></b>    | <b>6.6686E+22</b>               | <b>0.0857</b>                          | <b>946</b>  | <b>5321</b>   |
| <b>Middle Slip Rate Option<sup>(b)</sup></b> | <b>6.6686E+23</b>               | <b>0.8567</b>                          | <b>95</b>   | <b>532</b>  |
| <b>High Slip Rate Option<sup>(b)</sup></b>   | <b>6.6686E+24</b>               | <b>8.5666</b>                          | <b>9.5</b>  | <b>53</b>   |
| <b>Weighted Mean Slip Rate<sup>(c)</sup></b> | <b>2.8535E+24</b>               | <b>3.6657</b>                          | <b>22</b>   | <b>124</b>  |

- (a) Moment rate obtained from seismicity catalog and used for Cuba areal source (Z1) and for scaled fault scenario (SF).
- (b) Moment rates obtained from low, middle, and high slip rate values presented in Table 2.5.2-236.
- (c) Moment rate obtained from weighted mean of slip rate values presented in Table 2.5.2-236 and used for full fault scenario (FF).

The following will be added as a new FSAR table in a future revision of the FSAR:

**Table 2.5.2-238**  
**Summary of Hazard Sensitivity Study Results: Comparison of MAFE**

|   | Base caseZ1 |                    | ScenarioZ6 |        | ScenarioSF |        | ScenarioZ11% |        | ScenarioZ1+SF |        |
|---|-------------|--------------------|------------|--------|------------|--------|--------------|--------|---------------|--------|
| <b>10<sup>-4</sup> mean annual frequency of exceedance (MAFE)</b> |             |                    |            |        |            |        |              |        |               |        |
| Freq  | MAFE        | Amp <sup>(a)</sup> | MAFE       | % Diff | MAFE       | % Diff | MAFE         | % Diff | MAFE          | % Diff |
| 1 Hz  | 1.00E-04    | 0.0343             | 9.499E-05  | -5.0%  | 9.676E-05  | -3.2%  | 1.018E-04    | 1.8%   | 1.114E-04     | 11.4%  |
| 10 Hz   | 1.00E-04    | 0.0822             | 9.122E-05  | -8.8%  | 8.798E-05  | -12.0% | 1.025E-04    | 2.5%   | 1.094E-04     | 9.4%   |
| <b>10<sup>-5</sup> mean annual frequency of exceedance (MAFE)</b> |             |                    |            |        |            |        |              |        |               |        |
| Freq  | MAFE        | Amp <sup>(a)</sup> | MAFE       | % Diff | MAFE       | % Diff | MAFE         | % Diff | MAFE          | % Diff |
| 1 Hz  | 1.00E-05    | 0.0663             | 9.539E-06  | -4.6%  | 1.010E-05  | 1.0%   | 1.013E-05    | 1.3%   | 1.131E-05     | 13.1%  |
| 10 Hz   | 1.00E-05    | 0.278              | 9.891E-06  | -1.1%  | 9.969E-06  | -0.3%  | 9.992E-06    | -0.1%  | 1.014E-05     | 1.4%   |

(a) Rock motion (g)

The following will be added as a new FSAR table in a future revision of the FSAR:

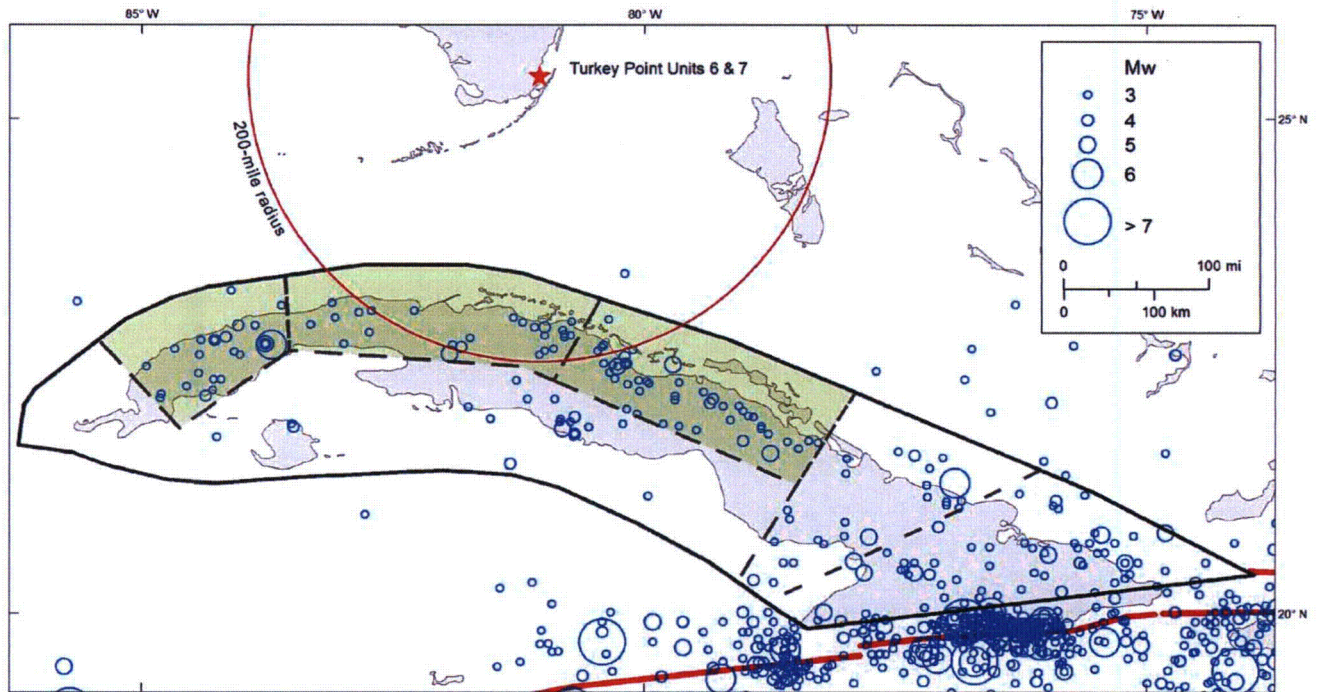
**Table 2.5.2-239**

**Summary of Hazard Sensitivity Results: Comparison of Rock Motion Amplitudes**

| Base case Z1  |        | ScenarioZ6 |          |        | ScenarioSF |          |        | ScenarioZ11% |          |        | ScenarioZ1+SF |          |        |
|---|--------|------------|----------|--------|------------|----------|--------|--------------|----------|--------|---------------|----------|--------|
| <b>Rock motions (g) at 10<sup>-4</sup> mean annual frequency of exceedance (MAFE)</b> |        |            |          |        |            |          |        |              |          |        |               |          |        |
| Freq  | Amp    | Amp        | Amp Diff | % Dif  | Amp        | Amp Diff | % Diff | Amp          | Amp Diff | % Diff | Amp           | Amp Diff | % Diff |
| 1 Hz  | 0.0343 | 0.0338     | -0.0005  | -1.5%  | 0.0340     | -0.0003  | -0.9%  | 0.0345       | 0.0002   | 0.6%   | 0.0354        | 0.0011   | 3.2%   |
| 10 Hz   | 0.0822 | 0.0784     | -0.0038  | -4.6%  | 0.0765     | -0.0057  | -6.9%  | 0.0832       | 0.0010   | 1.2%   | 0.0858        | 0.0036   | 4.4%   |
| <b>Rock motions (g) at 10<sup>-5</sup> mean annual frequency of exceedance (MAFE)</b> |        |            |          |        |            |          |        |              |          |        |               |          |        |
| Freq  | Amp    | Amp        | Amp Diff | % Diff | Amp        | Amp Diff | % Diff | Amp          | Amp Diff | % Diff | Amp           | Amp Diff | % Diff |
| 1 Hz  | 0.0663 | 0.0654     | -0.0009  | -1.4%  | 0.0665     | 0.0002   | 0.3%   | 0.0665       | 0.0002   | 0.3%   | 0.0686        | 0.0023   | 3.5%   |
| 10 Hz   | 0.278  | 0.276      | -0.0020  | -0.7%  | 0.278      | 0.0000   | 0.0%   | 0.278        | 0.0000   | 0.0%   | 0.280         | 0.0020   | 0.7%   |

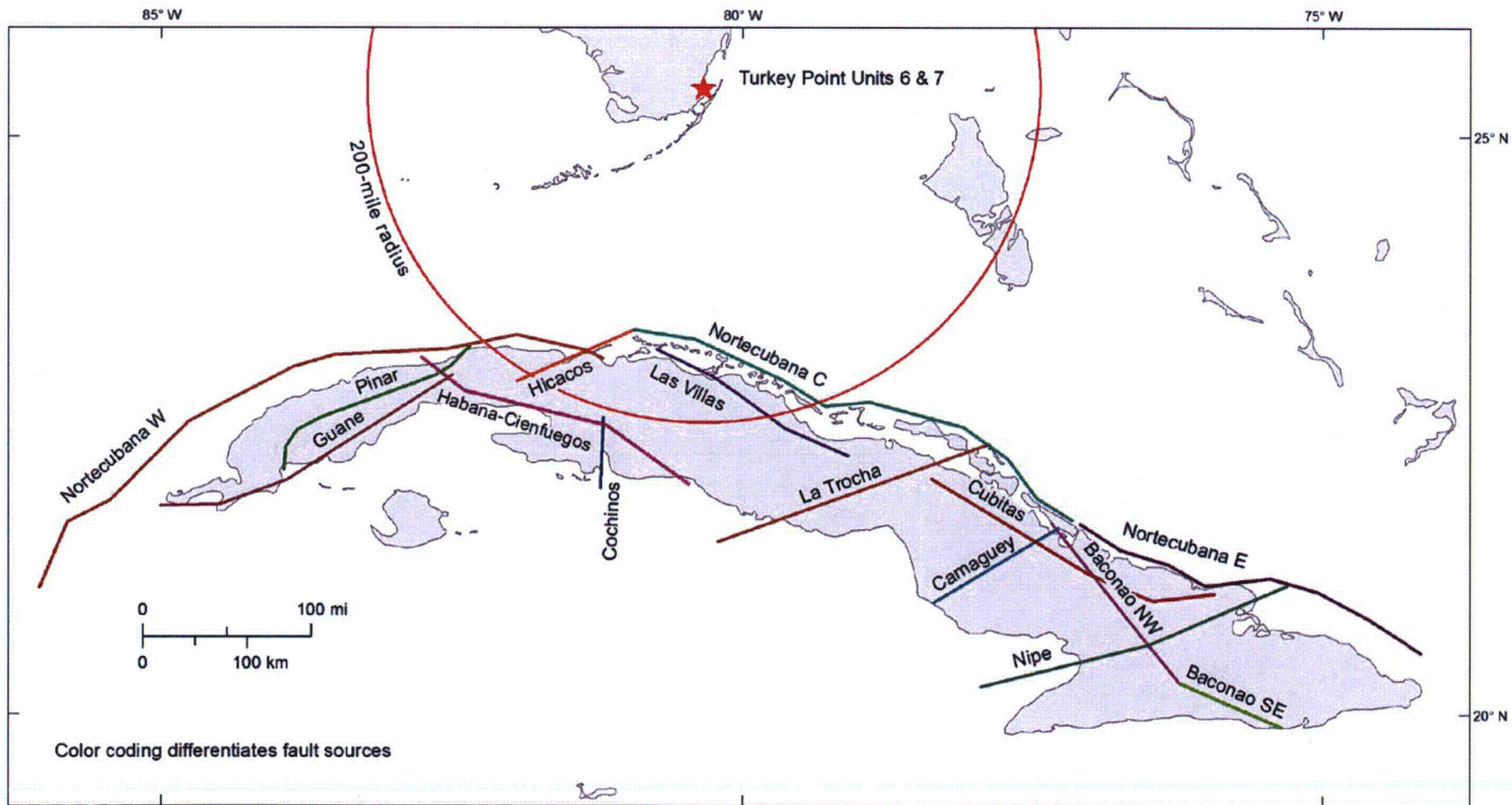
The following will be added as a new FSAR figure in a future revision of the FSAR

**Figure 2.5.2-271 Map Showing Cuba Single Areal Source Zone (solid black line), Six Sensitivity Areal Source Zones (dashed black lines), and Northern Cuba Subzone Used in Hazard Sensitivity Calculation (green shading). Seismicity (blue circles) is from the Phase 2 Earthquake Catalog. Thick Red Lines Show Plate Boundary Fault Sources Included in PSHA.**



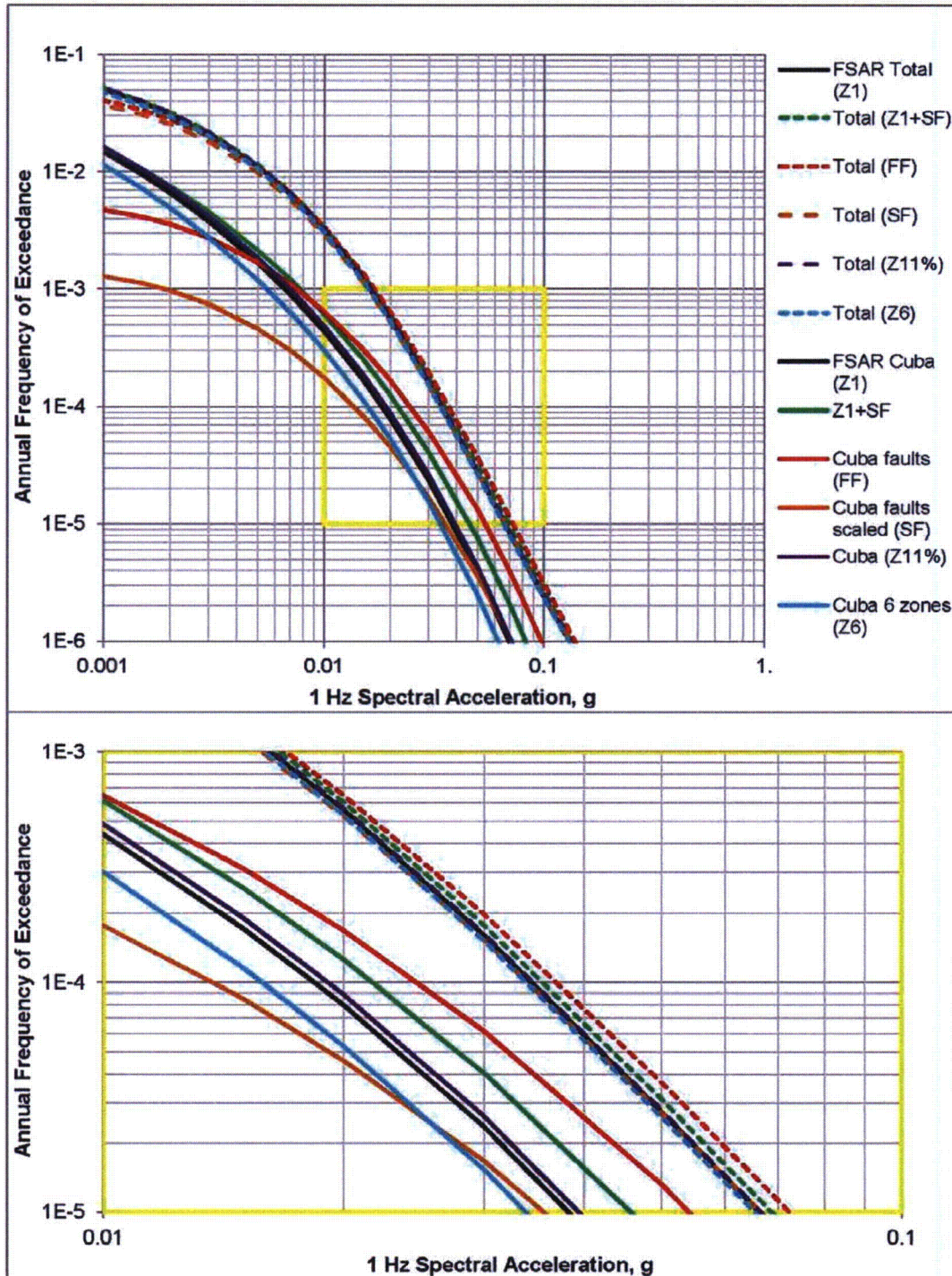
The following will be added as a new FSAR figure in a future revision of the FSAR

**Figure 2.5.2-272 Map of Intraplate Cuba Fault Sources for Hazard Sensitivity Calculation**



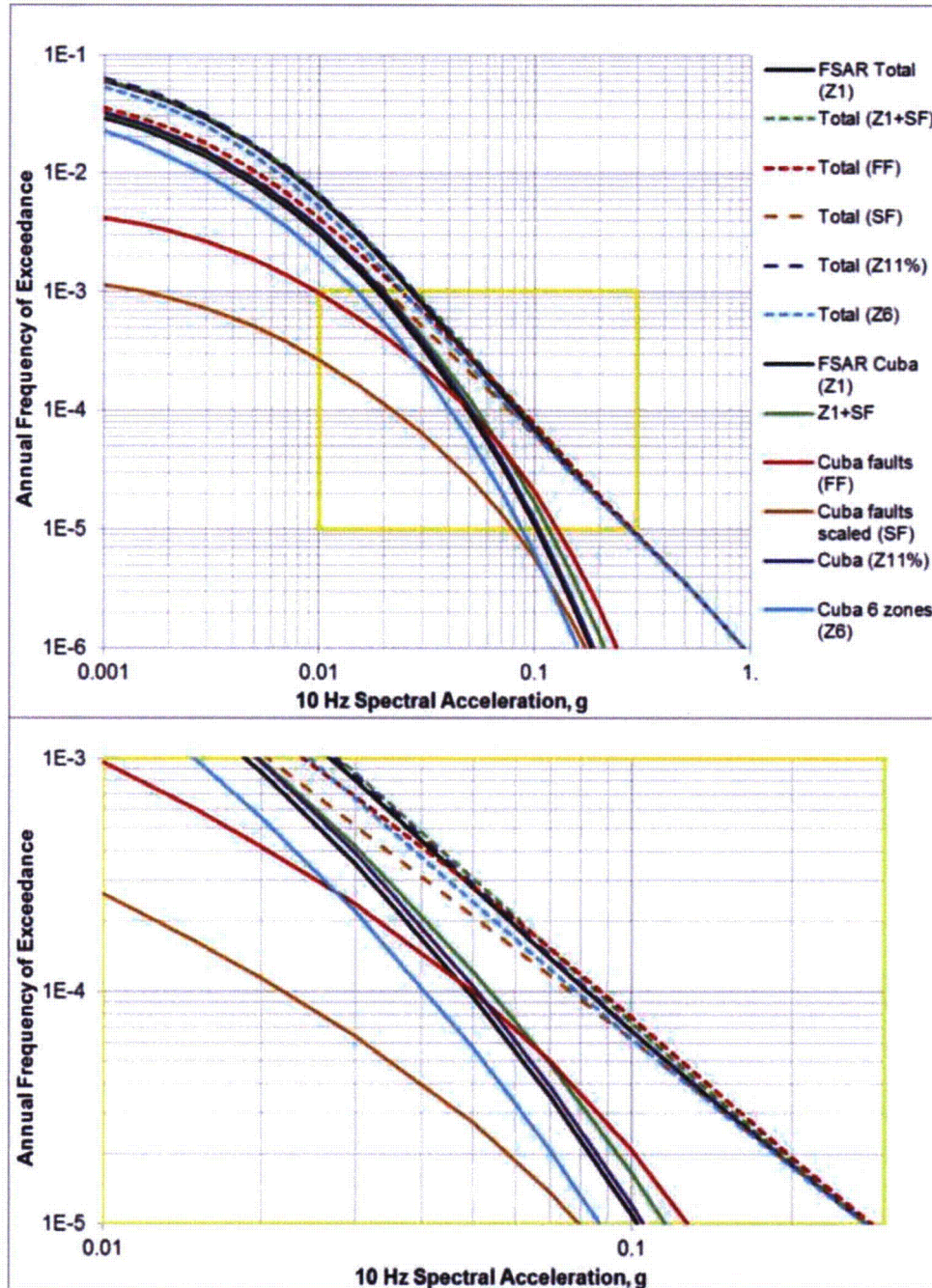
The following will be added as a new FSAR figure in a future revision of the FSAR:

**Figure 2.5.2-273 1 Hz Mean Hazard Curves Showing Sensitivity to Cuba Source Scenarios. Lower Panel is Expanded View of Yellow Box in Upper Panel**



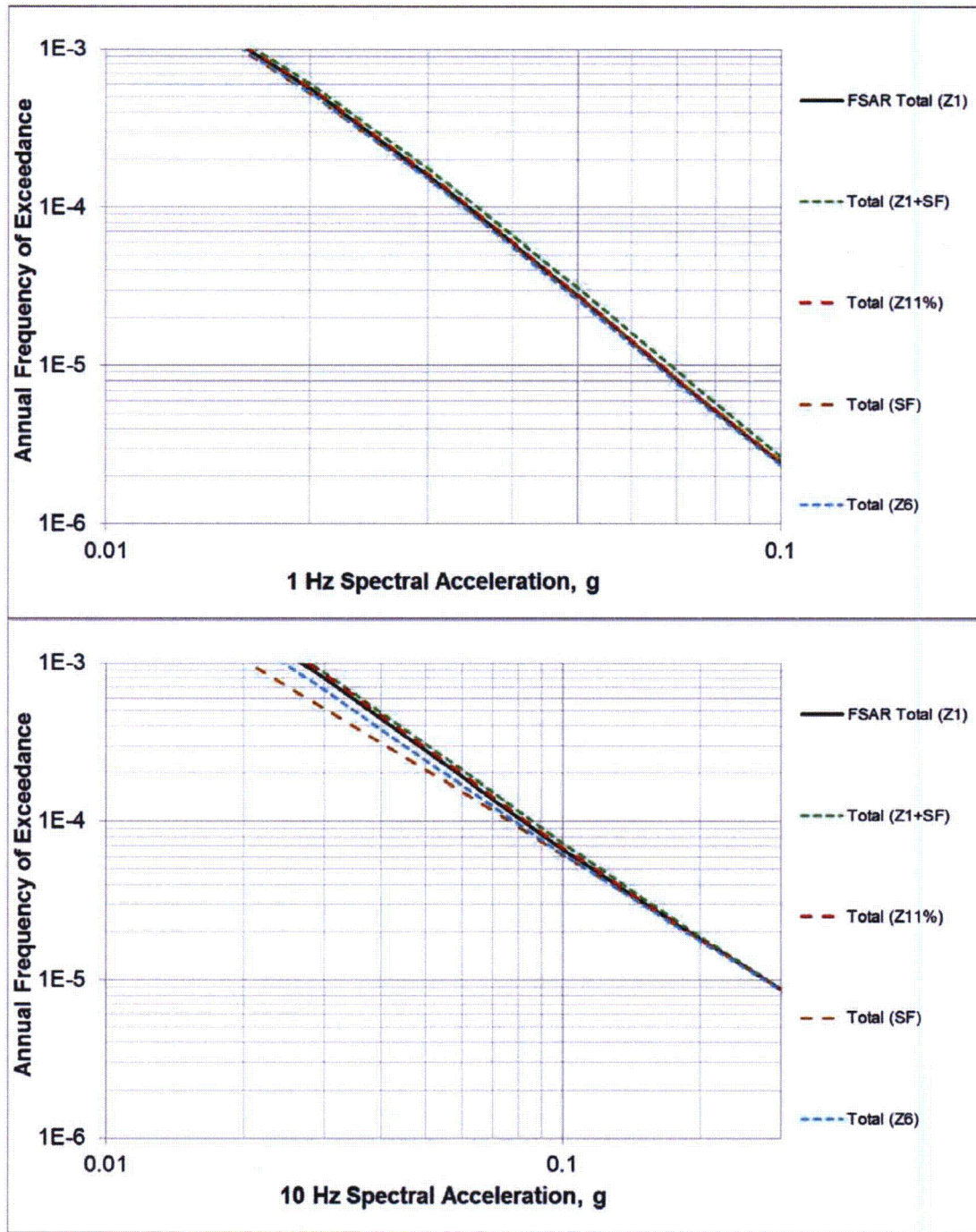
The following will be added as a new FSAR figure in a future revision of the FSAR:

**Figure 2.5.2-274 10Hz Mean Hazard Curves Showing Sensitivity to Cuba Source Scenarios. Lower Panel is Expanded View of Yellow Box in Upper Panel**



The following will be added as a new FSAR figure in a future revision of the FSAR:

**Figure 2.5.2-275 Total Mean Hazard Curves for 1 Hz (Upper) and 10Hz (Lower) Showing Sensitivity to Four Cuba Source Scenarios**



Source: Reference 242

Proposed Turkey Point Units 6 and 7  
Docket Nos. 52-040 and 52-041  
FPL Revised Response to NRC RAI No. 02.05.02-4 (eRAI 5896)  
L-2014-282 Attachment 3 Page 40 of 40

**ASSOCIATED ENCLOSURES:**

None

**NRC RAI Letter No. PTN-RAI-LTR-037**

**SRP Section: 02.05.02 - Vibratory Ground Motion**

Question for Geosciences and Geotechnical Engineering Branch 1 (RGS1)

**NRC RAI Number: 02.05.02-5 (eRAI 5896)**

FSAR Subsection 2.5.2.1.3.1 states that  $M_w$  was used as the uniform magnitude measure in Phase II (Caribbean region) earthquake catalog development efforts. Phase I earthquake catalog (EPRI updates), on the other hand, uses  $m_b$  as the uniform magnitude measure. In accordance with NUREG-0800, Standard Review Plan, Chapter 2.5.2, "Vibratory Ground Motion," and Regulatory Guide (RG)1.208, "A Performance-Based Approach to Define the Site-Specific Earthquake Ground Motion", please explain the rationale for selecting  $M_w$  as the uniform magnitude measure for the Caribbean earthquake catalog rather than  $m_b$ . Discuss what impact, if any, this choice had on the number of earthquakes listed in the Caribbean earthquake catalog. Were there any earthquakes with  $m_b$  of 3.0 (or perhaps larger) that did not make the  $M_w \geq 3.0$  cut used in Phase II catalog development?

**FPL RESPONSE:**

**Introduction**

The rationale for selecting moment magnitude ( $M_w$ ) as the uniform magnitude scale for the Phase 2 earthquake catalog, as is discussed below, is because  $M_w$  gives a better measure of the energy released for a greater range of magnitudes, including the very large earthquakes occurring in the Caribbean. The total number of earthquakes of body-wave magnitude ( $m_b$ ) greater than or equal to 3.0 or of  $M_w$  greater than or equal to 3.0 in the Caribbean earthquake catalog depends on details of magnitude conversion among many different magnitude scales given in many different parent catalogs. Using the FSAR magnitude conversion process for earthquakes in the Caribbean region, no earthquakes of  $m_b$  3.0 or larger were excluded by adopting  $M_w$  to characterize the size of Caribbean earthquakes. Alternative magnitude conversion schemes could lead to more or fewer earthquakes of magnitude 3.0 or greater for either choice of magnitude,  $m_b$  or  $M_w$ . As an example of this, magnitude scale conversion relations used for the recently published central and eastern United States seismic source characterization (CEUS SSC) model (EPRI et al., 2012) are found to lead to more earthquakes of  $M_w$  greater than or equal to 3.0 for the Caribbean catalog but fewer earthquakes of  $M_w$  5.0 and greater. The CEUS SSC magnitude conversion scheme, although specific to the CEUS and not presented here as applicable to the Caribbean, is investigated following a request from the NRC staff. The  $M_w$  scale that was used for the FSAR remains the preferred uniform magnitude scale.

**Rationale for Selecting  $M_w$  as the Uniform Magnitude Scale for the Phase 2 Catalog**

Seismologists performing current conventional probabilistic seismic hazard analyses, as well as development of ground motion prediction equations [e.g., the 2008 USGS seismic hazard maps (FSAR Reference 300) and the 2008 Next Generation of Ground-Motion Attenuation models (Chiou et al., 2008)], prefer the use of  $M_w$  over other magnitude scales, including  $m_b$  scale, because it is a more direct indication of the seismic energy associated with an earthquake, particularly for both shallow and deep focus earthquakes with large fault dimensions and/or complex rupture mechanisms that occur in the Caribbean. The  $m_b$

magnitude scale saturates, or is progressively insensitive to energy release beginning with magnitudes greater than about 5.0 due to the difference in the period and the seismic-wave type used to determine the magnitude size. While the magnitudes of earthquakes within the CEUS region have generally and traditionally been adequately represented by the  $m_b$  scale, the largest events in the Caribbean are not. This rationale for selecting moment magnitude was the basis for its use in developing the Phase 2 earthquake catalog.

Also, the update of the Phase 1 earthquake catalog was constrained to maintain the magnitude scale in  $m_b$  because both the EPRI-SOG seismicity catalog and recurrence characterization of the EPRI-SOG seismic sources already used the  $m_b$  scale.

NUREG-0800 Section 2.5.2 and RG 1.206 specify that the earthquake catalog should include all earthquakes having Modified Mercalli Intensity (MMI) greater than or equal to IV or magnitude greater than or equal to 3.0 that have been reported within 320 km (200 miles) of the site. Large earthquakes outside of this area that would impact the SSE (in NUREG-0800) or the GMRS (in RG 1.206) should be reported. The Phase 1 and Phase 2 catalogs were developed to meet these requirements. The magnitude scale is not explicitly specified in these requirements, although, both documents later state that "magnitude designations such as  $m_b$ ,  $M_L$ ,  $M_s$ ,  $M_w$  should be identified." There is no specification of the magnitude scale for the earthquake catalog given in RG 1.208.

The magnitude conversion relations between the moment magnitude scale and many other scales, such as  $m_b$  scale, show that the magnitudes less than about 4.5 (very short fault lengths) are assumed to be numerically equivalent to  $M_w$  and that the conversion relations are nonlinear at large magnitude values to reflect the saturation of some magnitude scales, specifically,  $m_b$  scale (Heaton et al., 1986). Therefore, in the development of the Phase 2 catalog, all small earthquakes of any magnitude scale less than 4.5 were assumed to be numerically equivalent to  $M_w$ . As a result of this assumption for small events, the selected threshold magnitude scale  $M_w \geq 3.0$  for the Phase 2 earthquake catalog and  $m_b$  (or (E) $m_b$ )  $\geq 3.0$  for the Phase 1 earthquake catalog presents no inconsistency in terms of minimum size or minimum seismic energy of a given earthquake considered in the two catalogs. Therefore, under the process used to develop moment magnitudes for the Phase 2 catalog, all earthquakes of magnitude 3.0 and larger, regardless of characterization as moment magnitude or body-wave magnitude, are included in both Phase 1 and Phase 2 earthquake catalogs, and there is no impact on the number of earthquakes in the two earthquake catalogs associated with the different magnitude scales used in the two earthquake catalogs.

During a public meeting conference call with the NRC, there was a brief discussion on the matter of characterization of magnitudes for the Phase 2 catalog of earthquakes and the question of the correlation between  $m_b$ , and  $M_w$  was again raised with specific reference to new work on correlating these two scales as part of the recently completed study on seismic sources in the CEUS region. Both topics are discussed below.

### **Details of the FSAR Magnitude Conversion Process for Earthquakes in the Caribbean Region**

The differences that exist among published seismotectonic region-specific magnitude conversion relations make the selection of appropriate relations for a given region important and, if such relations are not available, difficult. Seismic network operational histories are such that catalogs of events in a given region contain earthquakes located with different location programs. These programs use different station configurations and different crustal-velocity models with magnitudes calculated using different calibration. Therefore, conversions of diverse best estimates of magnitudes determined in different regions to a given uniform magnitude scale may show notable differences, dependent on tectonic setting (FSAR Reference 240).

In contrast to the CEUS tectonic environment considered for the Phase 1 earthquake catalog, the Caribbean region with its 1) different tectonic environments (e.g., plate boundary and near plate boundary shallow crustal faults and subduction zones), 2) different magnitude scales, and 3) different seismic network instrumentation and operational histories, required consideration of different global or regional magnitude conversion relationships for the Phase 2 earthquake catalog development.

In order to contrast the nature of earthquakes from the Caribbean region to the CEUS region, a magnitude conversion process was developed to consider the various magnitude scales used in the original source catalogs considered in the development of the Phase 2 earthquake catalog, and these various magnitude scales were converted to  $M_w$ .

Among the various earthquake source catalogs used for compiling the Phase 2 catalog, there were 19 different magnitude types that needed to be converted to moment magnitude. These different magnitude scale conversions are discussed further below, but as discussed in the FSAR, the process was based on the following simplified process. First, magnitudes of any type less than 4.5, with reference to the Heaton et al. (1986) correlation plot described below, were assumed to be equivalent to  $M_w$  directly. For magnitudes of any type of 4.5 and larger, the following simplified process was followed:

- Moment magnitudes were already moment magnitudes, so no conversion was necessary.
- Surface-wave magnitudes  $M_s$  were converted to  $M_w$  considering the Ekstrom and Dziewonski (1988) relations (FSAR Reference 240) and the Kanamori (1977) relation (FSAR Reference 269).
- Body-wave magnitudes  $m_b$  were converted to  $M_s$  using the Garcia et al. (2003) relation (FSAR Reference 254), and then the above process of conversion from  $M_s$  to  $M_w$  was followed.
- Intensity-based magnitudes in the Cuba catalog were considered equivalent to  $M_s$  magnitudes (FSAR Reference 254) and then the above process of conversion from  $M_s$  to  $M_w$  was followed.
- All other magnitude types were considered equivalent to  $m_b$  and then the above process to convert from  $m_b$  to  $M_s$  to  $M_w$  was followed.

The Heaton et al. (1986) magnitude correlations, following similar work by Kanamori (1983), plot various magnitude scales relative to  $M_w$  for a seismotectonic setting region (e.g., western US region or other active plate boundary) more similar to the Caribbean than the CEUS region, allowing conversion of Caribbean earthquake magnitudes in other scales into moment magnitude. These magnitude-scale plots graphically show relationships between the moment magnitude scale and several other magnitude scales, applicable magnitude ranges, and how they are nonlinear to reflect the saturation of some of the magnitude scales.

Following is a detailed summary of the approach that was used to provide specific magnitude scale conversions in order to estimate  $M_w$  for the Phase 2 earthquake catalog.

*Specific Magnitude Scales Used in the Phase 2 Earthquake Catalog*

The Phase 2 earthquake catalog developed for the Caribbean region contains 19 different measures of size for earthquakes that have occurred in notably different tectonic regions as compared to the CEUS region.

- Moment magnitudes ( $M_w$ )

The moment magnitude scale, which provides an estimation of total energy released in an earthquake, was the preferred magnitude scale in the Caribbean Phase 2 catalog under the rationale given above. Therefore, for all earthquakes in Phase 2 earthquake catalog that were originally reported in the  $M_w$  magnitude scale, these  $M_w$  values were directly included in the catalog.

- Surface-wave magnitudes ( $M_s$ )

The surface-wave magnitude ( $M_s$ ) scale is commonly used for shallow events larger than  $M_s$  5.0 (Kanamori, 1983; Mueller et al., 1997) which, by definition, are earthquakes where surface waves may have been generated. Since the surface-wave magnitude gives the poorest results for small earthquakes or those deep or at intermediate depth, there are relatively few earthquakes of this type of magnitude scale in the Phase 2 catalog. For those reported earthquakes with  $M_s$  less than 4.5, these  $M_s$  magnitude scales were considered to be numerically equivalent to  $M_w$ . For  $M_s$  values equal to or greater than 4.5, the 1988 global surface-wave magnitude to average seismic moment ( $M_o$ ) conversion relation of Ekstrom and Dziewonski (FSAR Reference 240) and then the seismic moment to moment magnitude conversion relation of Kanamori (1977) (FSAR Reference 269) was used to convert surface-wave magnitudes to  $M_w$  in the Phase 2 earthquake catalog development.

- Body-wave magnitudes ( $m_b$ )

The Heaton et al. (1986)  $m_b$ - $M_w$  magnitude correlation plot suggests that body-wave magnitude ( $m_b$ ) less than about 4.5 are consistent with  $M_w$ , and thus, they were assumed to be numerically equivalent to  $M_w$  for the Caribbean region. This consideration is also consistent with USGS Open File Report 97-464 (Mueller et al., 1997) for body-wave magnitudes in the western US region.

As may also be seen in the Heaton et al. (1986) magnitude correlation plot, there is an issue of saturation of the  $m_b$  scale beginning with magnitudes larger than about 5.0. The  $m_b$  scale stops increasing with increasing earthquake size at about magnitude 6.4 corresponding to a moment magnitude of about 7.5. Therefore, for  $m_b$  magnitudes of 4.5 and larger the magnitude conversion relation for  $m_b$  to  $M_s$  from the Garcia et al. study (FSAR

Reference 254) was used, and then the  $M_s$  to  $M_w$  scaling, discussed above, was applied for these larger  $m_b$  values in the Caribbean Phase 2 catalog.

- Intensity-based magnitudes ( $M_I$  and  $M_K$ ) in the Cuba catalog

The majority of earthquakes in the Cuba catalog have an estimate of intensity-based magnitude,  $M_I$  and  $M_K$ , as discussed in the Garcia et al. study (FSAR Reference 254). Both of these magnitude types are considered to be correlated to coda or duration magnitudes [see below]. For the FSAR, where there were no region-specific magnitude conversion relations for intensity-based magnitudes, as well as none for coda- or duration-magnitudes, to  $M_w$ , these  $M_I$  and  $M_K$  magnitudes were taken as equivalent to  $M_w$  for magnitudes less than 4.5, following Heaton et al. (1986), and equivalent to  $M_s$  for magnitudes 4.5 and larger, following the Garcia et al. study (FSAR Reference 254). The  $M_s$  magnitude scale values were then converted to  $M_w$ , as described above.

- Local, Duration, and Coda magnitudes ( $M_L$ ,  $M_d$ , DR and  $M_c$ )

The local magnitude ( $M_L$ ), duration magnitude ( $M_d$ ) [sometimes designated “DR” or “ $M_D$ ” in the National Geophysical Data Center database (NGDC), see FSAR 2.5.2] and coda magnitude ( $M_c$ ) are three types of measurements for earthquakes that are used to determine the local magnitudes and are conventionally considered equivalent. The instrumental  $M_c$  and  $M_d$  are typically reported for small and moderate magnitude earthquakes less than about 6.0, while it is found that  $M_L$  is also reported for larger earthquakes up to about 7.0. These three magnitude scales in the Phase 2 earthquake catalog, which are provided by different seismic networks with varying operational histories and different station calibrations, are comparable on average to  $M_w$  for magnitudes less than 4.5 in the Phase 2 earthquake catalog (Mueller et al., 1997, Heaton et al., 1986).

Nuttli and Herrmann (1982) report that  $M_L$  and  $m_b$  values are nearly equal in the western United States. Given the common equivalence of  $M_L$ ,  $M_d$ , and  $M_c$  magnitudes, and the Nuttli and Herrmann observation, these magnitudes when larger than 4.5 are considered equivalent to  $m_b$  and converted to  $M_w$ , as detailed above.

- Broad-band body-wave magnitudes ( $m_B$ ).

There are also some earthquakes larger than 6.0 in the Phase 2 catalog that are designated broad-band body-wave magnitude ( $m_B$ ). The main advantage of  $m_B$  magnitude scale rather than  $M_s$  is its applicability to both shallow and deep earthquakes. These  $m_B$  magnitude-scale events in the Phase 2 catalog are considered to be equivalent to  $M_s$  over the applicable magnitude range of events between about 6.0 and 8.0 (Heaton et al., 1986; Kanamori, 1983), and then converted to  $M_w$ , as described above.

- Intensity-based magnitudes ( $M(I_o)$ ), not in the Cuba catalog

These magnitudes are estimated from maximum intensity ( $I_o$ ) using the Gutenberg-Richter (1956) relationship, which correlates to local magnitude  $M_L$ . Therefore, these earthquakes are converted from  $M_L$  to  $M_w$ , as described above.

- Equivalent local and coda-duration magnitudes ( $m_1$ ,  $m_2$ ,  $f_m$ ,  $x_m$ , MA, and  $m_t$ )

The Puerto Rico Seismic Network [PRSN] earthquake catalog, which locally collects the events in the Caribbean region, has recorded earthquakes whose magnitudes are

determined using different local magnitude relations ( $m_1$  and  $x_m$ ), as well as different magnitude-coda duration relations ( $m_2$  and  $f_m$ ) – the  $x_m$  and  $f_m$  magnitudes are determined using the earthquake location program Hypoellipse (Lahr, 1999). An event less than magnitude 3.0, excluded from the Phase 2 catalog, is reported as a type MA magnitude, attributed to PRSN – it may be expected that this small magnitude is one of or an average of the other PRSN magnitudes. Also reported in the PRSN catalog are earthquakes from the Jamaica Seismic Network [JSN], which determines average coda magnitudes ( $m_t$ ) based on the regression between standard  $m_b$  and log of the signal duration (Wiggins-Grandison, 2001).

As for local, duration, and coda magnitudes described above when greater than 4.5 these magnitudes are considered equivalent to  $m_b$  and are converted to  $M_w$ .

- Unspecified magnitudes (nk and MG)

Finally, there are some earthquakes in the Phase 2 catalog with unknown magnitude scale labeled “nk” or “ ” (e.g., the computational method was unknown and could not be determined from published sources), as well as an unspecified magnitude scale labeled “MG” (e.g., magnitudes either have been reported by the contributor without listing the type [e.g., “MG 3.5”] or have been computed using procedures, which are not defined by the magnitude types routinely reported). These types of earthquakes were considered to be equivalent to  $m_b$  for small ( $3 \leq M_w < 4.5$ ) and moderate ( $4.5 \leq M_w < 6$ ) earthquake magnitudes in the Phase 2 catalog. Lamarre and Shah (1988) have plotted the unspecified magnitude scales versus  $M_L$  for the NGDC database used in the Phase 2 earthquake catalog, and have indicated that it is very closely approximated by the  $M_L$  and  $m_b$  for earthquakes in magnitude range less than about 5.0. Taken as equivalent to  $m_b$ , these magnitudes were converted to  $M_w$ , as described above.

Since the types of data used in determination of these magnitude scales are very different from region to region (e.g., observational errors and intrinsic variations in source properties), it is important to establish tectonically-similar regional magnitude scale correlations (Kanamori, 1983). Therefore, it should be emphasized that this magnitude conversion process was not incorporated into Phase 1 earthquake catalog that includes all events in the CEUS region with a notably different tectonic environment as compared to the Caribbean region (FSAR 2.5.1).

### **Application of CEUS-SSC Magnitude Conversion Relationships to the Phase 2 Catalog**

While recognizing that, according to the findings of the CEUS SSC study (EPRI et al., 2012), the correlation between  $m_b$  and  $M_w$  is region-dependent, and that nothing in the CEUS SSC study addresses earthquakes in the Cuba and Caribbean region, an analysis was performed to investigate the hypothetical effect of the use of CEUS-SSC magnitude conversions (EPRI et al., 2012) on the number of earthquakes listed in the Phase 2 earthquake catalog.

In this section, an alternative methodology of magnitude conversion is considered using the magnitude conversion relations from the CEUS SSC report (EPRI et al., 2012), as proposed by the NRC staff.

### Magnitude Conversion Using CEUS SSC Relations

In order to consider the impact on the Phase 2 earthquake catalog of using the CEUS SSC magnitude conversion relationships from CEUS SSC report (EPRI et al. 2012), there are two primary elements that need to be addressed. First, the 19 different magnitude types of the original earthquake catalogs have to be correlated to the magnitude conversion relationships available in the CEUS SSC report. Second, given the possibility that some of the CEUS SSC magnitude conversions could result in larger values of moment magnitude than obtained originally in the FSAR Phase 2 catalog, it is necessary to consider the smaller magnitude events that had been filtered in the development of the final Phase 2 earthquake catalog. This addresses the fundamental issue raised originally in RAI 02.05.02-5.

Given that the final Phase 2 earthquake catalog has been developed to include only independent events, it is necessary to perform cluster analysis on any additional smaller events that may arise for use of the CEUS SSC correlations. Therefore, the steps required for consideration of the CEUS SSC magnitude conversion relations are the following:

- Bring the smaller magnitude events back into the Phase 2 earthquake catalog that had been previously filtered out to obtain the final FSAR catalog of  $M_w$  3.0 and greater.
- Perform de-clustering analysis to identify and remove dependent events among the added-in smaller magnitude events.
- Convert all magnitudes to moment magnitudes using the CEUS SSC relations.

These steps result in a **modified** Phase 2 earthquake catalog, where the CEUS SSC-derived moment magnitudes can be compared to those of the FSAR Phase 2 catalog.

#### *Smaller Magnitude Events*

As will be shown below, in order to capture any earthquake of moment magnitude 3 or greater converted using the CEUS SSC magnitude conversion equations, it is necessary to consider magnitudes of any type greater than 2.0. One exception could have been for earthquakes whose  $M_w$  would be developed from a very small  $M_s$  value. However, the smallest  $M_s$  magnitude in the preferred source catalogs from which a modified Phase 2 catalog  $M_w$  would be developed, is  $M_s$  2.1, corresponding to a CEUS SSC  $M_w$  3.5 (see below). Therefore, in practice the smallest  $M_s$  magnitude has been considered in this response.

#### *De-clustering Analysis of the Smaller Magnitude Events*

In order to consistently add any additional small earthquakes [ $2.0 \leq \text{magnitude} < 3.0$ ] to the FSAR Phase 2 catalog, dependent events (foreshocks and aftershocks) must be identified within this magnitude range and excluded from the modified Phase 2 earthquake catalog. For the purpose of de-clustering, the magnitudes of any type of the additional small events were considered equivalent to  $M_w$ , similar to the methodology considered in the FSAR. As described in the FSAR, the Gardner and Knopoff (1974) de-clustering method (FSAR Reference 256) was used to identify dependent events among the added-in small magnitude events, which were then removed from the originally modified catalog.

*Magnitude Conversion Using CEUS SSC Relations*

In order to apply the limited number of types of CEUS SSC magnitude conversion relations, it is necessary to defensibly correlate the 19 magnitude types of the original Phase 2 catalog with the six magnitude types considered in the CEUS SSC report. Given the descriptions of the original 19 magnitude types above, Table 1 indicates the correlation of magnitude types used in this analysis.

Table 1. Correlation of the Original Magnitude Types to those in the CEUS SSC Report (EPRI et al., 2012)

| Original Magnitude Types                      | Corresponding CEUS SSC Magnitude Type |
|---|---------------------------------------|
| $m_b$ , MG, nk or {blank}                     | $m_b$                                 |
| $M_c$ , fm, MA, $M_l$ , $M_k$ , $m_t$ , $m_2$ | $M_c$                                 |
| $M_d$ , DR                                    | $M_d$                                 |
| $M_L$ , xm, $m_1$ , lo                        | $M_L$                                 |
| $M_s$ , $m_B$                                 | $M_s$                                 |
| $M_w$   | $M_w$                                 |

1)  $m_b$ - $M_w$  magnitude conversion

Using the  $m_b$ - $M_w$  magnitude conversion from CEUS SSC report (EPRI et al., 2012, Table 3.3-1 in Chapter 3) – as specified for midcontinent, exclusive of the northeast region and Canada, and exclusive of recordings from the Geological Survey of Canada – to convert body-wave magnitudes in the Phase 2 earthquake catalog to moment magnitudes:

$$M_w = m_b - 0.316 \quad (1)$$

leads to a smaller estimate of moment magnitude than considered in the FSAR – see Figure 1. For example, if the CEUS-SSC magnitude conversion relations had been considered for the Phase 2 catalog, the moment magnitude equivalent to  $m_b$  3.0 would be about  $M_w$  2.7, instead of the  $M_w$  3.0 in the FSAR.

2)  $(M_c, M_d, M_L)$ - $M_w$  magnitude conversion

The CEUS SSC report (EPRI et al., 2012)  $(M_c, M_d, M_L)$ - $M_w$  magnitude conversion equation is:

$$M_w = 0.762 [M_c, M_d, M_L] + 0.869 \quad (2)$$

Figure 1 indicates that for about  $M_w$  3.5 and greater, the CEUS SSC leads to smaller converted  $M_w$  magnitudes, notably so for the largest magnitudes. For  $M_w$  less than about 3.5 the CEUS SSC magnitude conversions lead to slightly larger  $M_w$  magnitudes. Further, considering the intent of presenting the Phase 2 catalog as  $M_w$  3.0 and greater, the CEUS SSC magnitude conversions would add some additional events which the FSAR catalog would have considered  $M_w$  2.8 to 3.0.

3)  $M_s$ - $M_w$  magnitude conversion

Using the quadratic  $M_s$ - $M_w$  magnitude conversion from CEUS SSC report (EPRI et al., 2012),

$$M_w = 2.654 + 0.334 M_s + 0.04 M_s * M_s \quad (3)$$

leads to very similar estimates of moment magnitude for earthquakes larger than 4.5 as those that were considered in the FSAR (FSAR 2.5.2) – see Figure 1. For the relatively few events

with  $M_s$  less than 4.5 in the Phase 2 catalog, the CEUS SSC magnitude conversion leads to larger  $M_w$  magnitudes than the conversion assumption of equivalence in the FSAR.

### Conclusions

Using the FSAR magnitude conversion process for earthquakes in the Caribbean region, no earthquakes of  $m_b$  3.0 or larger were excluded.

The impact on the number of Phase 2 catalog earthquakes of  $M_w$  3.0 and greater, considering the CEUS SSC magnitude scale conversion relations in lieu of the relations used in the FSAR, is summarized in Table 2. The number of  $M_w$  3.0 and greater events would increase from 8747 to 9212 when using the CEUS SSC relations. The number of  $M_w$  5.0 and greater would decrease from 787 events to 552 events. Figure 1 graphically presents the related conclusion, that considering the CEUS SSC magnitude scale conversion relations, there would be an increase in the number of smallest magnitude events, while there would be an equivalence or decrease in magnitude for all events of FSAR  $M_w$  4.5 and greater.

Table 2. Comparison of the Binned Seismicity for the Phase 2 Catalog Considering Moment Magnitudes as Determined in the FSAR as Compared to Application of the CEUS SSC (EPRI et al., 2012) Magnitude Conversion Relations.

| Magnitude Range                  | Number of Events: FSAR | Number of Events: CEUS SSC |
|----------------------------------|------------------------|----------------------------|
| $3.0 \leq M_w < 4.0$             | 5815                   | 7150                       |
| $4.0 \leq M_w < 5.0$             | 2145                   | 1510                       |
| $5.0 \leq M_w < 6.0$             | 541                    | 333                        |
| $6.0 \leq M_w < 7.0$             | 167                    | 159                        |
| $7.0 \leq M_w < 8.0$             | 73                     | 56                         |
| $8.0 \leq M_w$                   | 6                      | 4                          |
| <b><math>5.0 \leq M_w</math></b> | <b>787</b>             | <b>552</b>                 |
| <b><math>3.0 \leq M_w</math></b> | <b>8747</b>            | <b>9212</b>                |

The CEUS SSC magnitude conversion scheme, although specific to the CEUS and not presented here as applicable to the Caribbean, is investigated following a suggestion from the NRC staff. The  $M_w$  scale that was used for the FSAR remains the preferred uniform magnitude scale.

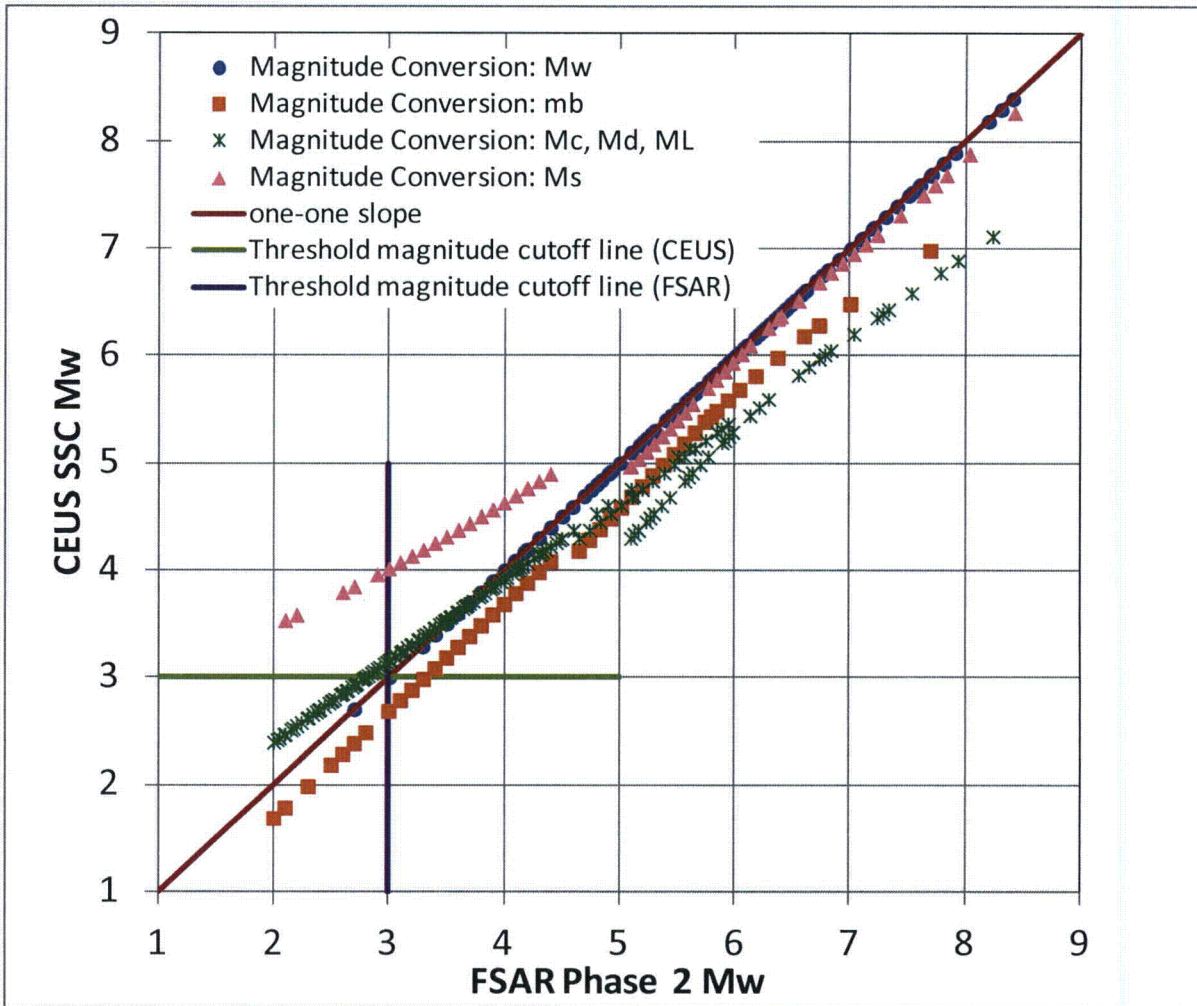


Figure 1. Comparison of converted magnitudes for the complete modified Phase 2 catalog: FSAR vs. CEUS SSC (EPRI et al., 2012). This figure represents the  $M_w$  correlation among 10,747 events.

This response is PLANT SPECIFIC.

**References:**

- Chiou, B., R. Darragh, N. Gregor, and W. Silva (2008). NGA Project Strong-Motion Database, Earthquake Spectra v.24, pp.23-44.
- Electric Power Research Institute [EPRI], U.S. Department of Energy [DOE], and U.S. Nuclear Regulatory Commission [NRC] (2012). "Technical Report: Central and Eastern United States Seismic Source Characterization for Nuclear Facilities". EPRI, Palo Alto, CA, U.S. DOE, and U.S. NRC.
- Gutenberg, B. and C. F. Richter (1956). Earthquake magnitude, intensity, energy and acceleration. Bulletin of the Seismology Society of America, v. 46, p 105-145.
- Heaton, T., F. Tajima and A. W. Mori (1986). Estimating ground motions using recorded accelerograms. Surveys in Geophysics, v.8, p 25-83.
- Kanamori, H. (1983). Magnitude scale and quantification of earthquakes. in Duda, S.J. and K. Aki (eds.), Quantification of Earthquakes. Tectonophysics, v. 93, p185-199.
- Lahr, J.C. (1999), HYPOELLIPSE: a computer program for determining local earthquake hypocentral parameters, magnitude, and first-motion pattern: U.S. Geological Survey Open-File Report 99-23, version 1, 119 p.
- Lamarre, M. and Shah, H. C. (1988). Seismic hazard evaluation for sites in California: Development of an expert system. Report No. 85. 180p.
- Mueller, C., M. Hopper, and A. Frankel (1997). Preparation of earthquake catalogs for the National Seismic Hazard Maps—Contiguous 48 States: U.S. Geological Survey Open-File Report 97-464, 36 p.
- Nuttli, O. W. and R. B. Herrmann (1982). Earthquake magnitude scales. J. Geotech. Eng. Div. ASCE, v.108, p 783-786.
- Wiggins-Grandison, M. D. (2001). Preliminary results from the new Jamaica Seismograph network. Seismological Research Letters, v.72, p525-537.

**ASSOCIATED COLA REVISIONS:**

The entire FSAR subsection 2.5.2.1.3.1 should be replaced with the following new text.

**2.5.2.1.3.1 Uniform Magnitude  $M_w$**

In the Phase 2 earthquake catalog,  $M_w$  was used as the unifying magnitude because it is the most commonly used magnitude in recent seismic hazard studies.

**~~Converting Various Magnitude Scales to  $M_w$~~**

~~Various magnitude scales may be available for a given event. Each available magnitude was considered in the evaluation of  $M_w$  for that event. If an  $M_w$  was available, it was adopted directly. Other magnitudes were converted to estimates of  $M_w$  using the Equation 2.5.2-8 (Reference 240).~~

Global average relationships between  $M_S$  and  $\log M_0$  (logarithm of the seismic moment) were used in which the independent variable is  $\log M_0$  based on the assumption that the slope of the regression is 1 for small and 2/3 for large values of  $M_0$  (Reference 240). The following global  $\log M_0$ - $M_S$  relation was used to convert surface-wave magnitude ( $M_S$ ) to seismic moment ( $M_0$ ) for all events:

$$\begin{aligned} \log M_0 &= 19.24 + M_S && M_S < 5.3 && \text{Equation 2.5.2-8} \\ \log M_0 &= 30.20 - \sqrt{92.45 - 11.4M_S} && 5.3 \leq M_S \leq 6.8 \\ \log M_0 &= 16.14 + 1.5M_S && M_S > 6.8 \end{aligned}$$

Moment magnitudes were estimated from seismic moment for all events as a linear transformation of the logarithm of the seismic moment,  $M_0$ , given by (Reference 269):

$$M_w = (2/3) \log M_0 - 10.7 \quad \text{Equation 2.5.2-9}$$

in which  $M_0$  is in dyne-cm units ( $10^{-7}$  Nm).

A new linear relationship to compute  $M_S$  from  $m_b$ , valid in the interval  $4.0 < m_b < 6.0$  and  $3.1 < M_S < 6.7$ , was applied by the following linear regression (Reference 254):

$$M_S = 1.37 m_b - 2.34 \quad \text{Equation 2.5.2-10}$$

**In this Subsection, the rationale for selecting moment magnitude ( $M_w$ ) as the uniform magnitude scale for the Phase 2 earthquake catalog is discussed and the magnitude conversion process adopted for all events in the Cuba and Caribbean Phase 2 earthquake catalog is described in detail.**

#### **Rationale for Selecting $M_w$ as the Uniform Magnitude Scale for the Phase 2 Catalog**

**Seismologists performing current conventional probabilistic seismic hazard analyses, as well as development of ground motion prediction equations (References 300 and 344), prefer the use of  $M_w$  over other magnitude scales, including  $m_b$  scale, because it is a more direct indication of the seismic energy associated with an earthquake, particularly for both shallow and deep focus earthquakes with large fault dimensions and/or complex rupture mechanisms that occur in the Caribbean. The  $m_b$  magnitude scale saturates, or is progressively insensitive to, energy release, beginning with magnitudes greater than approximately 5.0 due to the difference in the period and the seismic-wave type used to determine the magnitude size. While the magnitudes of earthquakes within the CEUS region have generally and traditionally been adequately represented by the  $m_b$  scale, the largest events in the Caribbean are not. This rationale for selecting moment magnitude was the basis for its use in developing the Phase 2 earthquake catalog.**

Also, the update of the Phase 1 earthquake catalog, as discussed in Subsection 2.5.2.1.2, was constrained to maintain the magnitude scale in  $m_b$  because both the EPRI-SOG seismicity catalog and recurrence characterization of the EPRI-SOG seismic sources use the  $m_b$  scale.

NUREG-0800 Section 2.5.2 and RG 1.206 specify that the earthquake catalog should include all earthquakes having Modified Mercalli Intensity (MMI) greater than or equal to IV, or magnitude greater than or equal to 3.0 that have been reported within 320 kilometers (200 miles) of the site. Large earthquakes outside of this area that would impact the SSE (in NUREG-0800) or the GMRS (in RG 1.206) should be reported. The Phase 1 and Phase 2 catalogs were developed to meet these requirements. The magnitude scale is not explicitly specified in these requirements, although both documents later state that "magnitude designations such as  $m_b$ ,  $M_L$ ,  $M_s$ ,  $M_w$  should be identified." There is no specification of the magnitude scale for the earthquake catalog given in RG 1.208.

The magnitude conversion relations between the moment magnitude scale and many other scales, such as  $m_b$  scale, show that the magnitudes less than about 4.5 (very short fault lengths) are assumed to be numerically equivalent to  $M_w$  and that the conversion relations are nonlinear at large magnitude values to reflect the saturation of some magnitude scales, specifically  $m_b$  scale (Reference 346). Therefore, in the development of the Phase 2 catalog, all small earthquakes of any magnitude scale less than 4.5 were assumed to be numerically equivalent to  $M_w$ . As a result of this assumption for small events, the selected threshold magnitude scale  $M_w \geq 3.0$  for the Phase 2 earthquake catalog and  $m_b$  (or  $(E)m_b$ )  $\geq 3.0$  for the Phase 1 earthquake catalog presents no inconsistency in terms of minimum size or minimum seismic energy of a given earthquake considered in the two catalogs. Therefore, under the process used to develop moment magnitudes for the Phase 2 catalog, all earthquakes of magnitude 3.0 and larger, regardless of characterization as moment magnitude or body-wave magnitude, are included in both Phase 1 and Phase 2 earthquake catalogs, and there is no impact on the number of earthquakes in the two earthquake catalogs associated with the different magnitude scales used in the two earthquake catalogs.

#### Magnitude Conversion Process for Earthquakes in the Caribbean Region

The differences that exist among published seismotectonic region-specific magnitude conversion relations make the selection of appropriate relations for a given region important and, if such relations are not available, difficult. Seismic network operational histories are such that catalogs of events in a given region contain earthquakes located with different location programs. These programs use different station configurations and different crustal-velocity models with magnitudes calculated using different calibration. Therefore, conversions of diverse best estimates of magnitudes determined in different regions to a given uniform magnitude scale may show notable differences, depending on tectonic setting (Reference 240).

In contrast to the CEUS tectonic environment considered for the Phase 1 earthquake catalog, the Caribbean region with its (1) different tectonic environments (e.g., plate

boundary and near plate boundary shallow crustal faults and subduction zones), (2) different magnitude scales, and (3) different seismic network instrumentation and operational histories, required consideration of different global or regional magnitude conversion relationships for the Phase 2 earthquake catalog development.

To contrast the nature of earthquakes from the Caribbean region to the CEUS region, a magnitude conversion process was developed to consider the various magnitude scales used in the original source catalogs considered in the development of the Phase 2 earthquake catalog, and these various magnitude scales were converted to  $M_w$ .

Among the various earthquake source catalogs used for compiling the Phase 2 catalog, there were 19 different magnitude types that needed to be converted to moment magnitude. These different magnitude scale conversions are discussed further below based on the following simplified process. First, magnitudes of any type less than 4.5, with reference to the Heaton et al. (Reference 346) correlation plot described below, were assumed to be equivalent to  $M_w$  directly. For magnitudes of any type of 4.5 and larger, the following simplified process was followed:

- Moment magnitudes were already moment magnitudes, so no conversion was necessary.
- Surface-wave magnitudes  $M_s$  were converted to  $M_w$  considering the Ekstrom and Dziewonski relations (Reference 240) and the Kanamori relation (Reference 269).
- Body-wave magnitudes  $m_b$  were converted to  $M_s$  considering the Garcia et al. relation (Reference 254), and then the above process of conversion from  $M_s$  to  $M_w$  was followed.
- Intensity-based magnitudes in the Cuba catalog were considered equivalent to  $M_s$  magnitudes (Reference 254) and then the above process of conversion from  $M_s$  to  $M_w$  was followed.
- All other magnitude types were considered equivalent to  $m_b$  and then the above process to convert from  $m_b$  to  $M_s$  to  $M_w$  was followed.

The Heaton et al. (Reference 346) magnitude correlations, following similar work by Kanamori (Reference 347), plot various magnitude scales relative to  $M_w$  for a seismotectonic setting more similar to the Caribbean than the CEUS region (e.g., western U.S. region or other active plate boundary regions), allowing conversion of Caribbean earthquake magnitudes in other scales into moment magnitude. These magnitude-scale plots graphically show relationships between the moment magnitude scale and several other magnitude scales, applicable magnitude ranges, and how they are nonlinear to reflect the saturation of some of the magnitude scales.

Following is a detailed summary of the approach that was used to provide specific magnitude scale conversions to estimate  $M_w$  for the Phase 2 earthquake catalog.

### Specific Magnitude Scales Used in the Phase 2 Earthquake Catalog

The Phase 2 earthquake catalog developed for the Caribbean region contains 19 different measures of size for earthquakes that have occurred in notably different tectonic regions as compared to the CEUS region.

- **Moment magnitudes ( $M_w$ )**

The moment magnitude scale, which provides an estimation of total energy released in an earthquake, was the preferred magnitude scale in the Caribbean Phase 2 catalog under the rationale given above. Therefore, for all earthquakes in Phase 2 earthquake catalog that were originally reported in the  $M_w$  magnitude scale, these  $M_w$  values were directly included in the catalog.

- **Surface-wave magnitudes ( $M_s$ )**

The surface-wave magnitude ( $M_s$ ) scale is commonly used for shallow events larger than  $M_s$  5.0 (References 347 and 350) which, by definition, are earthquakes where surface waves may have been generated. Since the surface-wave magnitude gives the poorest results for small earthquakes or those deep or at intermediate depth, there are relatively few earthquakes of this type of magnitude scale in the Phase 2 catalog. For those reported earthquakes with  $M_s$  less than 4.5, these  $M_s$  magnitude scales were considered to be numerically equivalent to  $M_w$ . For  $M_s$  values equal to or greater than 4.5, the 1988 global surface-wave magnitude to average seismic moment ( $M_o$ ) conversion relations of Ekstrom and Dziewonski (Reference 240) and then the seismic moment-to-moment magnitude conversion relation of Kanamori (Reference 269) was used to convert surface-wave magnitudes to  $M_w$  in the Phase 2 earthquake catalog development.

- **Body-wave magnitudes ( $m_b$ )**

The Heaton et al. (Reference 346)  $m_b$ - $M_w$  magnitude correlation plot suggests that body-wave magnitude ( $m_b$ ) less than about 4.5 are consistent with  $M_w$ , and thus, they were assumed to be numerically equivalent to  $M_w$  for the Caribbean region. This consideration is also consistent with USGS Open File Report 97-464 (Reference 350) for body-wave magnitudes in the western US region.

As may also be seen in the Heaton et al. (Reference 346) magnitude correlation plot, there is an issue of saturation of the  $m_b$  scale beginning with magnitudes larger than approximately 5.0. The  $m_b$  scale stops increasing with increasing earthquake size at about magnitude 6.4 corresponding to a moment magnitude of approximately 7.5. Therefore, for  $m_b$  magnitudes of 4.5 and larger the magnitude conversion relation for  $m_b$  to  $M_s$  from the Garcia et al. study (Reference 254) was used, and then the  $M_s$  to  $M_w$  scaling, discussed above, was applied for these larger  $m_b$  values in the Caribbean Phase 2 catalog.

- **Intensity-based magnitudes ( $M_I$  and  $M_k$ ) in the Cuba catalog**

The majority of earthquakes in the Cuba catalog have an estimate of intensity-based magnitude,  $M_I$  and  $M_k$ , as discussed in the Garcia et al. study (Reference 254). Both of these magnitude types are considered to be correlated to coda or duration magnitudes [see below]. For the magnitude conversion process, where there were no

region-specific magnitude conversion relations for intensity-based magnitudes, as well as none for coda- or duration-magnitudes, to  $M_w$ , these  $M_l$  and  $M_k$  magnitudes were taken as equivalent to  $M_w$  for magnitudes less than 4.5, following Heaton et al. (Reference 346), and equivalent to  $M_s$  for magnitudes 4.5 and larger, following the Garcia et al. study (Reference 254). The  $M_s$  magnitude scale values were then converted to  $M_w$  as described above.

- Local, Duration, and Coda magnitudes ( $M_L$ ,  $M_d$ , DR and  $M_c$ )

The local magnitude ( $M_L$ ), duration magnitude ( $M_d$ ) sometimes designated “DR” or “ $M_D$ ” in the National Geophysical Data Center database (NGDC) database, and coda magnitude ( $M_c$ ) are three types of measurements for earthquakes that are used to determine the local magnitudes and are conventionally considered equivalent. The instrumental  $M_c$  and  $M_d$  are typically reported for small and moderate magnitude earthquakes less than approximately 6.0, while it is found that  $M_L$  is also reported for larger earthquakes up to about 7.0. These three magnitude scales in the Phase 2 earthquake catalog, which are provided by different seismic networks with varying operational histories and different station calibrations, are comparable on average to  $M_w$  for magnitudes less than 4.5 in the Phase 2 earthquake catalog (References 346 and 350). Nuttli and Herrmann (Reference 351) report that  $M_L$  and  $m_b$  values are nearly equal in the western United States. Given the common equivalence of  $M_L$ ,  $M_d$ , and  $M_c$  magnitudes and the Nuttli and Herrmann observation, these magnitudes when larger than 4.5 are considered equivalent to  $m_b$  and converted to  $M_w$  as detailed above.

- Broadband body-wave magnitudes ( $m_B$ ).

There are also some earthquakes larger than 6.0 in the Phase 2 catalog that are designated broadband body-wave magnitude ( $m_B$ ). The main advantage of  $m_B$  magnitude scale rather than  $M_s$  is its applicability to both shallow and deep earthquakes. These  $m_B$  magnitude-scale events in the Phase 2 catalog are considered to be equivalent to  $M_s$  over the applicable magnitude range of events between about 6.0 and 8.0 (References 346 and 347), and then converted to  $M_w$ , as described above.

- Intensity-based magnitudes ( $M(I_o)$ ), not in the Cuba catalog

These magnitudes are estimated from maximum intensity ( $I_o$ ) using the Gutenberg-Richter (Reference 345) relationship, which correlates to local magnitude  $M_L$ . Therefore, these earthquakes are converted from  $M_L$  to  $M_w$  as described above.

- Equivalent local and coda-duration magnitudes ( $m_1$ ,  $m_2$ , fm, xm, MA, and  $m_t$ )

The PRSN earthquake catalog, which locally collects the events in the Caribbean region, has recorded earthquakes whose magnitudes are determined using different local magnitude relations ( $m_1$  and xm), as well as different magnitude-coda duration relations ( $m_2$  and fm) – the xm and fm magnitudes are determined using the earthquake location program Hypoellipse (Reference 348). An event less than magnitude 3.0, excluded from the Phase 2 catalog, is reported as a type MA magnitude, attributed to PRSN – it may be expected that this small magnitude is one of or an average of the other PRSN magnitudes. Also reported in the PRSN catalog

are earthquakes from the Jamaica Seismic Network (JSN), which determines average coda magnitudes ( $m_t$ ) based on the regression between standard  $m_b$  and log of the signal duration (Reference 352).

As for local, duration, and coda magnitudes described above when greater than 4.5 these magnitudes are considered equivalent to  $m_b$  and are converted to  $M_w$ .

- Unspecified magnitudes (nk and MG)

Finally, there are some earthquakes in the Phase 2 catalog with unknown magnitude scale labeled "nk" or " " (e.g., the computational method was unknown and could not be determined from published sources) as well as an unspecified magnitude scale labeled "MG" (e.g., magnitudes either have been reported by the contributor without listing the type [e.g., "MG 3.5"] or have been computed using procedures which are not defined by the magnitude types routinely reported). These types of earthquakes were considered to be equivalent to  $m_b$  for small ( $3 \leq M_w < 4.5$ ) and moderate ( $4.5 \leq M_w < 6$ ) earthquake magnitudes in the Phase 2 catalog. Lamarre and Shah (Reference 349) have plotted the unspecified magnitude scales versus  $M_L$  for the NGDC database used in the Phase 2 earthquake catalog, and have indicated that it is very closely approximated by the  $M_L$  and  $m_b$  for earthquakes in magnitude range less than about 5.0. Taken as equivalent to  $m_b$ , these magnitudes were converted to  $M_w$  as described above.

Since the types of data used in determination of these magnitude scales are very different from region to region (e.g., observational errors and intrinsic variations in source properties), it is important to establish tectonically-similar regional magnitude scale correlations (Reference 347). Therefore, it should be emphasized that this magnitude conversion process was not incorporated into Phase 1 earthquake catalog that includes all events in the CEUS region with a notably different tectonic environment as compared to the Caribbean region (Section 2.5.1).

The following references will be added to FSAR subsection 2.5.2.7 in a future COLA revision.

344. Chiou, B., R. Darragh, N. Gregor, and W. Silva, *NGA Project Strong-Motion Database, Earthquake Spectra Vol . 24*, pp. 23-44, 2008.
345. Gutenberg, B. and C. Richter (1956), *Earthquake Magnitude, Intensity, Energy and Acceleration*, Bulletin of the Seismology Society of America, Vol. 46, pp. 105-145, 1956.
346. Heaton, T., F. Tajima, and A. Mori, *Estimating Ground Motions Using Recorded Accelerograms*, Surveys in Geophysics, Vol. 8, pp. 25-83, 1986.
347. Kanamori, H., *Magnitude Scale and Quantification of Earthquakes*, S. Duda and K. Aki (eds.), Quantification of Earthquakes. Tectonophysics, Vol. 93, pp. 185-199, 1983.
348. Lahr, J., HYPOELLIPSE: a Computer Program for Determining Local Earthquake Hypocentral Parameters, Magnitude, and First-Motion Pattern: U.S. Geological Survey, Open-File Report 99-23, Ver. 1, 1999.
349. Lamarre, M. and H. Shah, *Seismic Hazard Evaluation For Sites in California: Development of an Expert System*, Report No. 85, 1988.
350. Mueller, C., M. Hopper, and A. Frankel, Preparation of Earthquake Catalogs for the National Seismic Hazard Maps-Contiguous 48 States: U.S. Geological Survey, Open-File Report 97-464, 1997.
351. Nuttli, I. and R. Herrmann, *Earthquake Magnitude Scales*, J. Geotech, Eng. Div. ASCE, Vol. 108, pp. 783-786, 1982.
352. Wiggins-Grandison, M., *Preliminary Results from the New Jamaica Seismograph Network*. Seismological Research Letters, Vol. 72, pp. 525-537, 2001.

**ASSOCIATED ENCLOSURES:**

None

**NRC RAI Letter No. PTN-RAI-LTR-037**

**SRP Section: 02.05.02 - Vibratory Ground Motion**

Question for Geosciences and Geotechnical Engineering Branch 1 (RGS1)

**NRC RAI Number: 02.05.02-6 (eRAI 5896)**

FSAR Subsection 2.5.2.2.1 describes that among the six EPRI-SOG earth science teams only one team identified more than one seismic source within the site region. In accordance with NUREG-0800, Standard Review Plan, Chapter 2.5.2, "Vibratory Ground Motion," and Regulatory Guide (RG) 1.208, "A Performance-Based Approach to Define the Site-Specific Earthquake Ground Motion", please explain:

- a. Whether any attempt has been made to identify potential EPRI seismic sources that are outside the site region, but might contribute to the site hazard above the 1% of the total hazard.
  
- b. Whether the use of the updated EPRI (2004, 2006) GMPEs significantly increases the hazard contributions of any of the EPRI seismic sources that are outside the site region to justify their use in the TPNPP PSHA calculations?

**FPL RESPONSE:**

- a. All EPRI-SOG seismic sources within the site region (200 miles) were identified. In addition, sources beyond the site region that might contribute to hazard (including Charleston and New Madrid seismic sources) were identified. A seismic hazard sensitivity study was performed to determine if the sources beyond the site region contributed to the hazard. Those sources that were found to have a low contribution to hazard (denoted by a single asterisk in Table 1) were excluded from the rock seismic hazard base calculation. For these sources, the sum of hazard is less than 1% of the total rock hazard from all sources, at 10 Hz and 1 Hz spectral accelerations corresponding to about 10-4 annual frequency of exceedance. Table 1 shows the results of the evaluation of the seismic sources.
  
- b. The EPRI (2004, 2006) ground motion prediction equations were used in the sensitivity calculations to evaluate significant contributions to seismic hazard, including outside the site region (summarized in Table 1). Their use does not increase the hazard contributions of any source.

Proposed Turkey Point Units 6 and 7  
Docket Nos. 52-040 and 52-041  
FPL Revised Response to NRC RAI No. 02.05.02-6 (eRAI 5896)  
L-2014-282 Attachment 5 Page 2 of 3

Table 1. Evaluation of seismic sources used for the PSHA at the Turkey Point Site

| Source Model | Team | Sources Within Site Region | Sources Beyond Site Region | Final Sources Used for Rock Base Calc  |
|--------------|------|----------------------------|----------------------------|--|
| EPRI-SOG     | BEC  | BEC-BZ1                    | N/A                        | BEC-BZ1_A**<br>BEC-SUPP<br>DAM-20_A**<br>DAM-SUPP<br>LAW-126_A**<br>LAW-SUPP<br>RND-C01_A**<br>RND-51_A**<br>RND-SUPP<br>WCC-BG<br>WGC-107_A**<br>WGC-SUPP |
|              |      | BEC-SUPP                   |                            |  |
|              | DAM  | DAM-20                     | DAM-52                     |  |
|              |      | DAM-SUPP                   | DAM-53                     |  |
|              | LAW  | LAW-126                    | LAW-C09*                   |  |
|              |      | LAW-SUPP                   | LAW-C10*                   |  |
|              | RND  | RND-49-05 (C01)            | NA                         |  |
|              |      | RND-51                     |                            |  |
|              |      | RND-SUPP                   |                            |  |
|              | WCC  | WCC-BG-35                  | NA                         |  |
|              | WGC  | WGC-107                    | NA                         |  |
|              |      | WGC-SUPP                   |                            |  |
| Caribbean    | NA   | CUBA                       | --                         | CUBA   |
|              |      |                            | NO-HISP_EAST               | NO-HISP_EAST   |
|              |      |                            | NO-HISP_WEST               | NO-HISP_WEST   |
|              |      |                            | ORIENTE_EAST               | ORIENTE_EAST   |
|              |      |                            | ORIENTE_WEST               | ORIENTE_WEST   |
|              |      |                            | PLAN_GE                    | PLAN_GE  |
|              |      |                            | SEPTENTRIONAL              | SEPTENTRIONAL  |
|              |      |                            | SWAN_ISL_E                 | SWAN_ISL_E   |
|              |      |                            | SWAN_ISL_W                 | SWAN_ISL_W   |
|              |      |                            | WALT_DUA                   | WALT_DUA   |
| Charleston   | NA   | NA                         | C-A                        | C-A  |
|              |      |                            | C-B                        | C-B  |
|              |      |                            | C-BP                       | C-BP   |
|              |      |                            | C-C                        | C-C  |
|              |      |                            | C-A-EXP*                   |  |
|              |      |                            | C-B-EXP*                   |  |
|              |      |                            | C-BP-EXP*                  |  |
|              |      |                            | C-C-EXP*                   |  |
| New Madrid   | NA   | NA                         | BLYTHE*                    |  |
|              |      |                            | EASTP*                     |  |
|              |      |                            | REELFOOT*                  |  |

\* Sources determined to have low contribution to hazard were removed for the rock seismic hazard base calc.

\*\* Sources that include \_A at the end of their name indicate they are an EPRI SOG source that was augmented to include more degree cells to the east and west of Florida.

This response is PLANT SPECIFIC.

Proposed Turkey Point Units 6 and 7  
Docket Nos. 52-040 and 52-041  
FPL Revised Response to NRC RAI No. 02.05.02-6 (eRAI 5896)  
L-2014-282 Attachment 5 Page 3 of 3

**References:**

None

**ASSOCIATED COLA REVISIONS:**

No COLA changes have been identified as a result of this response.

**ASSOCIATED ENCLOSURES:**

None

**NRC RAI Letter No. PTN-RAI-LTR-037**

**SRP Section: 02.05.02 - Vibratory Ground Motion**

Question for Geosciences and Geotechnical Engineering Branch 1 (RGS1)

**NRC RAI Number: 02.05.02-7 (eRAI 5896)**

FSAR Subsection 2.5.2.3 discusses the correlation of seismicity with only the EPRI seismic source models. In accordance with NUREG-0800, Standard Review Plan, Chapter 2.5.2, "Vibratory Ground Motion," please provide a thorough, detailed, description in the FSAR that discusses the correlation of seismicity with all of the seismic sources used in the Turkey Point PSHA study.

**FPL RESPONSE:**

Seismic sources used in the Turkey Point Units 6 & 7 probabilistic seismic hazard analysis (PSHA) include updated EPRI seismic sources (FSAR Subsection 2.5.2.4.3.2), supplemental seismic sources (FSAR Subsection 2.5.2.4.4.1), Charleston, South Carolina seismic sources (FSAR Subsection 2.5.2.4.4.2), and Cuba and northern Caribbean seismic sources (FSAR Subsection 2.5.2.4.4.3). This RAI response includes descriptions of the correlation of earthquake epicenters with these seismic sources.

EPRI Seismic Sources

FSAR Figures 2.5.2-203 through 2.5.2-209 show the EPRI (FSAR Reference 2.5.2-243) seismic sources located within the site region and epicenters from the project Phase 1 earthquake catalog. Following are descriptions of the correlation of earthquakes with each EPRI seismic source.

- Bechtel BZ1 (Gulf Coast) – Seismicity within Bechtel source BZ1 is sparse and appears evenly distributed throughout (FSAR Figure 2.5.2-204). There is no clear association of seismicity with any known geologic structure within this source. The largest magnitude earthquake in this source from the Phase 1 earthquake catalog is Emb 5.90.
- Dames & Moore 20 (So. Coastal Margin) – Seismicity within Dames & Moore source 20 is sparse and appears evenly distributed throughout (FSAR Figure 2.5.2-205). There is no clear association of seismicity with any known geologic structure within this source. The largest magnitude earthquake in this source from the Phase 1 earthquake catalog is Emb 5.58.
- Law Engineering 126 (South Coastal Block) – Seismicity within Law Engineering source 126 is sparse and appears evenly distributed throughout (FSAR Figure 2.5.2-206). There is no clear association of seismicity with any known geologic structure within this source. The largest magnitude earthquake in this source from the Phase 1 earthquake catalog is Emb 4.96.
- Rondout Associates 51 (Gulf Coast to Bahamas Fracture Zone) – Seismicity within Rondout Associates source 51 is sparse and appears evenly distributed throughout (FSAR Figure 2.5.2-207). There is no clear association of seismicity with any known geologic structure within this source. The largest magnitude earthquake in this source from the Phase 1 earthquake catalog is Emb 5.90.

- Rondout Associates 49-05 (Appalachian Basement) – Seismicity within Rondout Associates source 49-05 is sparse and appears evenly distributed throughout (FSAR Figure 2.5.2-207). The largest magnitude earthquake in this source from the Phase 1 earthquake catalog is Emb 4.96.
- Weston Geophysical 107 (Gulf Coast Background) – Seismicity within Weston Geophysical source 107 is sparse and appears evenly distributed throughout (FSAR Figure 2.5.2-208). The largest magnitude earthquake in this source from the Phase 1 earthquake catalog is Emb 5.90.
- Woodward-Clyde BG-35 Turkey Point (Truncated) – Seismicity within truncated Woodward-Clyde source BG-35 is very sparse and appears evenly distributed throughout (FSAR Figure 2.5.2-209). The largest magnitude earthquake in this source from the Phase 1 earthquake catalog is Emb 4.09.

#### Supplemental Seismic Sources

FSAR Figures 2.5.2-204 through 2.5.2-208 show the supplemental seismic source zones and epicenters from the project Phase 1 earthquake catalog. These supplemental seismic source zones were developed by the Turkey Point Units 6 & 7 project to account for those portions of the site region not covered by EPRI source zones. As described in FSAR Subsection 2.5.2.4.4.1, there is one supplemental source zone for each EPRI team except Woodward-Clyde, for which no supplemental source is needed.

Seismicity within each of the supplemental sources is very sparse, with a total of just one or two earthquakes in each (FSAR Figures 2.5.2-204 through 2.5.2-208). The largest magnitude earthquake from the Phase 1 earthquake catalog in each supplemental source zone is Emb 4.09.

#### Charleston, South Carolina Seismic Sources

Alternate geometries representing the Charleston, South Carolina seismic source from the Updated Charleston Seismic Source (UCSS) characterization are shown in FSAR Figure 2.5.2-212. Revised FSAR Figure 2.5.2-212 (included herein in the Associated COLA Revisions section) shows these Charleston seismic sources along with epicenters from the project Phase 1 earthquake catalog. Following are descriptions of the correlation of earthquakes with each UCSS seismic source.

- Source A (Charleston) – Charleston Source A was developed in part to envelop the area of ongoing seismicity in the Middleton Place-Summerville area. The preponderance of these moderately abundant earthquakes is thought to be aftershocks of the historical 1886 Emb 6.75 event (FSAR References 2.5.2-272, 2.5.2-324, and 2.5.2-325). The largest magnitude earthquake from the Phase 1 earthquake catalog in Charleston Source A is the historical 1886 Emb 6.75 event.
- Source B (Coastal and Offshore Zone) – Charleston Source B is a coast-parallel source that includes all of Charleston Source A and extends farther to the northeast and southwest to capture more distant paleoliquefaction features, and to the southwest to include the offshore Helena Banks fault zone. Seismicity within Charleston Source B, outside of the area covered by Charleston Source A, is sparse. The largest magnitude

earthquake from the Phase 1 earthquake catalog in Charleston Source B is the historical 1886 Emb 6.75 event.

- Source B' (Coastal Zone) – Charleston Source B' also includes all of Charleston Source A and extends to the northeast and southwest to capture more distant paleoliquefaction features, but does not include the offshore Helena Banks fault zone. Seismicity within Charleston Source B', outside of the area covered by Charleston Source A, is sparse. The largest magnitude earthquake from the Phase 1 earthquake catalog in Charleston Source B' is the historical 1886 Emb 6.75 event.
- Source C (East Coast Fault System-South) – Charleston Source C represents the southern segment of Marple and Talwani's (FSAR Reference 2.5.2-278) East Coast Fault system. There is partial overlap between Charleston Sources A and C. Within the area of overlap, seismicity is moderately abundant and likely represents aftershocks of the 1886 earthquake. Outside the area of overlap, seismicity in Charleston Source C is very sparse. The largest magnitude earthquake from the Phase 1 earthquake catalog in Charleston Source C is the 1959 Emb 4.31 event. The location of the 1886 Emb 6.75 earthquake from the Phase 1 earthquake catalog plots just outside of Geometry C, but, given the uncertainty in the location of this earthquake, it is considered to have possibly occurred within Geometry C.

#### Cuba and Northern Caribbean Seismic Sources

Seismic sources for Cuba and the northern Caribbean region are shown in FSAR Figure 2.5.2-217. FSAR Figure 2.5.2-214 and Table 2.5.2-221 show significant earthquakes in this region. Revised FSAR Figure 2.5.2-217 (included herein in the Associated COLA Revisions section) shows the Cuba and northern Caribbean seismic sources along with epicenters from the project Phase 2 earthquake catalog. Following are descriptions of the correlation of earthquakes with each of the Cuba and northern Caribbean seismic sources.

- Cuba Areal Source – The Cuba areal source is associated with moderately abundant seismicity that is distributed throughout the source. There appears to be higher concentration of epicenters in the southeastern portion of the Cuba areal source, near the active plate boundary and the eastern and western Oriente fault sources. Also, there appears to be a higher concentration of epicenters distributed along the northern coast and near-shore portions of Cuba within the Cuba areal source. The largest earthquakes from the Phase 2 catalog associated with this source are the 1551  $M_w$  5.98 event in southeastern Cuba, the 1880  $M_w$  6.13 event in western Cuba, and the 1914  $M_w$  6.29 event offshore northeastern Cuba.
- Oriente Fault-Western – The Oriente Fault-Western source is associated with abundant seismicity along its length, with an apparent concentration of epicenters at its western end near the Cayman trough. Seismicity also appears concentrated near its eastern end near where the western and eastern segments of the Oriente fault form a transtensional step-over. The largest earthquakes from the Phase 2 catalog associated with this source are the 1917  $M_w$  7.20 and 1992  $M_w$  6.80 events.
- Oriente Fault-Eastern – The Oriente Fault-Eastern source is associated with abundant seismicity along its length, with an apparent concentration of epicenters along its west-central portion, just offshore of southernmost Cuba near the city of Santiago de Cuba.

The largest earthquake from the Phase 2 catalog associated with this source is the historical 1766  $M_w$  7.53 event.

- Septentrional Fault – The Septentrional Fault source is associated with abundant seismicity along its entire length. The largest earthquakes from the Phase 2 catalog associated with this source are the historical 1842  $M_w$  8.23 and 1887  $M_w$  7.93 events.
- Northern Hispaniola Fault-Western – The Northern Hispaniola Fault-Western source is associated with abundant seismicity along its entire length, with an especially high concentration of epicenters along its central and eastern portions. The largest earthquake from the Phase 2 catalog associated with this source is the 1953  $M_w$  6.93 event.
- Northern Hispaniola Fault-Eastern – The Northern Hispaniola Fault-Eastern source is associated with abundant seismicity along its entire length, much of which appears in map view to the south of the surface trace of this south-dipping fault. The largest earthquake from the Phase 2 catalog associated with this source is the 1946  $M_w$  7.90 event.
- Swan Islands Fault-Western – The Swan Islands Fault-Western source is associated with abundant seismicity along its entire length. The largest earthquake from the Phase 2 catalog associated with this source is the historical 1856  $M_w$  7.69 event.
- Swan Islands Fault-Eastern – The Swan Islands Fault-Eastern source is associated with abundant seismicity along its entire length, with an apparent concentration of epicenters located near its eastern end near the Cayman trough. No earthquakes from the Phase 2 catalog greater than or equal to  $M_w$  6.75 are associated with this source.
- Walton-Duanvale Fault – The Walton-Duanvale Fault source is associated with moderately abundant seismicity along its length, with an apparent concentration of epicenters located near its western end near the Cayman trough. Seismicity also appears concentrated at the eastern end of this source near Jamaica, where the left-lateral Walton-Duanvale and Enriquillo-Plantain Garden faults form a restraining bend. The largest earthquakes from the Phase 2 catalog associated with this source are the two approximately  $M_w$  6.6 events that occurred in 1907 and 1957.
- Enriquillo-Plantain Garden Fault – The Enriquillo-Plantain Garden Fault source is associated with abundant seismicity along its length, with apparent concentrations of epicenters at its western and eastern ends. Multiple large historical earthquakes have ruptured along the Enriquillo-Plantain Garden fault (FSAR Reference 2.5.2-282), including from the Phase 2 catalog the 1692  $M_w$  7.78 earthquake near Jamaica and the 1751  $M_w$  7.28 and 1770  $M_w$  7.53 earthquakes near Port-au-Prince, Haiti.

FSAR Subsection 2.5.2.4.6 provides a discussion of PSHA results.

This response is PLANT SPECIFIC.

**References:**

None

#### ASSOCIATED COLA REVISIONS:

The text in FSAR Subsection 2.5.2.3 will be revised as follows in a future update of the FSAR:

##### 2.5.2.3 Correlation of Seismicity with Geologic Structures and ~~EPRI~~ **Seismic** Sources

**Seismic sources used in the Turkey Point Units 6 & 7 PSHA include updated EPRI seismic sources (Subsection 2.5.2.4.3.2), supplemental seismic sources (Subsection 2.5.2.4.4.1), Charleston, South Carolina seismic sources (Subsection 2.5.2.4.4.2), and Cuba and northern Caribbean seismic sources (Subsection 2.5.2.4.4.3).** The EPRI earthquake catalog covers earthquakes in the CEUS through 1984, as described in Subsection 2.5.2.1. Figures 2.5.2-203 through 2.5.2-209 show the distribution of earthquake epicenters from both the EPRI (pre-1985) and Phase 1 update (through mid-February 2008) earthquake catalogs in comparison to the seismic sources identified by each of the EPRI ESTs. **Seismicity is sparse and appears evenly distributed throughout each EPRI source zone that is located within the site region. There is no clear association of seismicity with any known geologic structure in these sources.**

Comparison of the additional events of the updated **Phase 1** earthquake catalogs to the EPRI earthquake catalog shows:

- There are no new earthquakes within the site region that can be associated with a known geologic structure.
- There are no unique clusters of seismicity that suggest a new seismic source not captured by the EPRI seismic source model.
- The updated earthquake catalog does not show a pattern of seismicity that requires revision to the geometry of any of the EPRI seismic sources. ~~The updated catalog extends farther south than the original EPRI earthquake catalog to include seismicity in the Cuba area and the North America-Caribbean plate boundary region.~~
- ~~Subsection 2.5.2.4.4.3 describes the Cuba and northern Caribbean seismic source model.~~
- The updated **Phase 1** earthquake catalog does not imply a significant change in seismicity parameters (rate of activity, b-value) for any of the EPRI seismic sources.

The updated **Phase 1** earthquake catalog **does** indicate that Mmax updates are required for most of EPRI seismic sources located at least partially within the site region. Subsection 2.5.2.4.3 describes these Mmax updates.

**The correlation of seismicity from the Phase 1 earthquake catalog with supplemental seismic sources is described in Subsection 2.5.2.4.4.1. The correlation of seismicity from the Phase 1 earthquake catalog with the Charleston, South Carolina seismic source is described in Subsection 2.5.2.4.4.2. The correlation of seismicity from the Phase 2 earthquake catalog with Cuba and northern Caribbean seismic sources is described in Subsection 2.5.2.4.4.3.**

The following text will be inserted after the last bullet of the sixth paragraph of FSAR Subsection 2.5.2.4.4.1 in a future update of the FSAR:

- Assess Mmax distributions and weights for five new source zones based on the updated earthquake catalog. These five new source zones are largely devoid of historical seismicity (Table 2.5.2-211), thus Mmax distributions are based on Mmax estimates for their respective updated EPRI EST Gulf Coast zones (Table 2.5.2-207). Due to the similarity of the crust between the supplemental source zones and the original EPRI Gulf Coast source zones, the new zones reflect the same Mmax distributions as their updated Gulf Coast source zone counterpart for each EST.

**Figures 2.5.2-204 through 2.5.2-208 show the supplemental seismic source zones and epicenters from the Phase 1 earthquake catalog. Seismicity within each of the supplemental sources is very sparse, with a total of just one or two earthquakes in each (Figures 2.5.2-204 through 2.5.2-208). The largest magnitude earthquake from the Phase 1 earthquake catalog in each supplemental source zone is Emb 4.09.**

The following text will be inserted at the end of the third paragraph of FSAR Subsection 2.5.2.4.4.2.1 in a future update of the FSAR:

Geometry A also excludes outlying liquefaction features because liquefaction occurs as a result of strong ground shaking that may extend well beyond the areal extent of the tectonic source. Geometry A also envelops instrumentally located earthquakes spatially associated with the Middleton Place-Summerville Seismic Zone (MPSSZ), which is located in the meizoseismal zone of the 1886 Charleston earthquake (References 272, 324, and 325).

**The preponderance of these moderately abundant earthquakes is thought to be aftershocks of the historical 1886 Emb 6.75 event (References 272, 324, and 325). The largest magnitude earthquake from the Phase 1 earthquake catalog in Geometry A is the historical 1886 Emb 6.75 event.**

The text in the eighth paragraph of FSAR Subsection 2.5.2.4.4.2.1 will be revised as follows in a future update of the FSAR:

#### *Geometry B — Coastal and Offshore Zone*

Geometry B is a coast-parallel, approximately 260 x 100 kilometers source area that (a) incorporates all of Geometry A, (b) is elongated to the northeast and southwest to capture other, more distant liquefaction features in coastal South Carolina (References 207, 208, and 323), and (c) extends to the southeast to include the offshore Helena Banks fault zone (Reference 213) (Figure 2.5.2-212). **Seismicity within Geometry B, outside of the area of overlap with Geometry A, is sparse. The largest magnitude earthquake from the Phase 1 earthquake catalog in Geometry B is the historical 1886 Emb 6.75 event (Figure 2.5.2-212).** The elongation and orientation of Geometry B is roughly parallel to the regional structural grain as well as roughly parallel to the elongation of 1886 isoseismals. The mapped extent of paleoliquefaction features (References 207, 208, and 323) defines the northeastern and southwestern extents of Geometry B.

The following text will be added to the end of the twelfth paragraph of FSAR Subsection 2.5.2.4.4.2.1 in a future update of the FSAR:

#### Geometry B' — Coastal Zone

Geometry B' is a coast-parallel, approximately 260 x 50 kilometers source area that incorporates all of Geometry A, as well as the majority of reported paleoliquefaction features (References 207, 208, and 323). Unlike Geometry B, however, Geometry B' does not include the offshore Helena Banks fault zone (Figure 2.5.2-212). **Seismicity within Geometry B', outside of the area of overlap with Geometry A, is sparse. The largest magnitude earthquake from the Phase 1 earthquake catalog in Geometry B' is the historical 1886 Emb 6.75 event.**

The following text will be added to the end of the fifteenth paragraph of FSAR Subsection 2.5.2.4.4.2.1 in a future update of the FSAR:

#### Geometry C — East Coast Fault System-South

Geometry C is about 200 x 30 kilometers, north-northeast-oriented source area (Figure 2.5.2-212) enveloping the southern segment of the proposed East Coast fault system shown in Figure 3 of Reference 278. The area of Geometry C is defined to envelop the original depiction of the postulated East Coast Fault System-South by Marple and Talwani in Reference 278. **The largest magnitude earthquake from the Phase 1 earthquake catalog in Geometry C is Emb 4.31. The location of the 1886 Emb 6.75 earthquake from the Phase 1 earthquake catalog plots just outside of Geometry C, but, given the uncertainty in the location of this earthquake, it is considered to have possibly occurred within Geometry C. There is partial overlap between Geometries A and C. Within the area of overlap, seismicity in Geometry C is moderately abundant. To the north, outside the area of overlap, seismicity in Geometry C is very sparse.**

The following text will be inserted after the first paragraph of FSAR Subsection 2.5.2.4.4.3.2.1 in a future FSAR update:

#### 2.5.2.4.4.3.2.1 Cuba Areal Source Zone

The single areal source zone representing Cuba (Figure 2.5.2-217) encompasses the major tectonic elements on the island and the majority of the historical seismicity. Subsection 2.5.1.1.1.3.2.4 provides discussion of geologic, geophysical, and seismic data for Cuba. The northern and eastern boundary of the source zone is drawn near the base of the submarine escarpment that marks the location of the Nortecubana fault suture and the geologic boundary between the relatively undeformed North American crust of the Bahama Platform and the highly attenuated crust of the former leading edge of the plate boundary zone (Figures 2.5.1-210 and 2.5.1-202). To account for uncertainty in the position of the boundary, a buffer of 12.5 miles from the base of the escarpment toward the north and east

was added to the Cuba areal source zone. This buffer was added to account for poorly located earthquakes that probably occurred within the Cuba island arc region and/or a zone of fractured and faulted crust beyond the suture zone that formed during early Cenozoic subduction. The western boundary of the Cuba areal source zone is based on bathymetry and the locations and density of historical seismicity. This boundary approximately follows the boundary between the Yucatan Basin and the continental shelf surrounding Cuba. The southern boundary of the Cuba source zone coincides with the southern boundary of Cuba and the steep submarine escarpment that borders the Oriente fault. At closest approach, the Cuba areal source zone is located about 140 miles from the Units 6 & 7 site. **The Cuba areal source is associated with moderately abundant seismicity that is distributed throughout the source (Figure 2.5.2-217). There appears to be higher concentration of epicenters in the southeastern portion of the Cuba areal source, near the active plate boundary and the eastern and western Oriente fault sources. Also, there appears to be a higher concentration of epicenters distributed along the northern coast and near-shore portions of Cuba within the Cuba areal source. The largest earthquakes from the Phase 2 catalog associated with this source are the 1551  $M_w$  5.98 event in southeastern Cuba, the 1880  $M_w$  6.13 event in western Cuba, and 1914  $M_w$  6.29 event offshore northeastern Cuba.**

The first paragraph FSAR Subsection 2.5.2.4.4.3.2.2 will be divided into two paragraphs and the following text will be inserted as a new paragraph in-between in a future FSAR update:

#### 2.5.2.4.4.3.2.2 Oriente Fault — Western

At closest approach, the western Oriente fault source is located about 420 miles from the Units 6 & 7 site (Figure 2.5.2-217). Subsection 2.5.1.1.1.1.2 provides discussion of the geologic, geodetic, and seismic characteristics of the Oriente fault. Table 2.5.2-217 summarizes source parameters for this fault source.

**The western Oriente fault source is associated with abundant seismicity along its length, with an apparent concentration of epicenters at its western end near the Cayman trough (Figure 2.5.2-217). Seismicity also appears concentrated near its eastern end near where the western and eastern segments of the Oriente fault form a transtensional step-over (Figure 2.5.2-217). The largest earthquakes from the Phase 2 catalog associated with this source are the 1917  $M_w$  7.20 and 1992  $M_w$  6.80 events.**

The first paragraph of FSAR Subsection 2.5.2.4.4.3.2.3 will be divided into two paragraphs and the following text will be inserted as a new paragraph in-between in a future FSAR update:

#### 2.5.2.4.4.3.2.3 Oriente Fault — Eastern

At closest approach, the eastern Oriente fault source is located about 445 miles from the Units 6 & 7 site (Figure 2.5.2-217). Subsection 2.5.1.1.2.3.1.2 provides discussion of the

geologic, geodetic, and seismic characteristics of the Oriente fault. Table 2.5.2-217 summarizes source parameters for this fault source.

**The eastern Oriente fault source is associated with abundant seismicity along its length, with an apparent concentration of epicenters along its west-central portion, just offshore of southernmost Cuba near the city of Santiago de Cuba (Figure 2.5.2-217). The largest earthquake from the Phase 2 catalog associated with this source is the historical 1766  $M_w$  7.53 event.**

The first paragraph of FSAR Subsection 2.5.2.4.4.3.2.4 will be divided into two paragraphs and the following text will be inserted as a new paragraph in-between in a future FSAR update:

#### 2.5.2.4.4.3.2.4 Septentrional Fault

At closest approach, the Septentrional fault source is located about 545 miles from the Units 6 & 7 site (Figure 2.5.2-217). Subsection 2.5.1.1.2.3.2.1 provides discussion of the geologic, geodetic, and seismic characteristics of the Septentrional fault. Table 2.5.2-217 summarizes source parameters for this fault source.

**The Septentrional fault source is associated with abundant seismicity along its entire length (Figure 2.5.2-217). The largest earthquakes from the Phase 2 catalog associated with this source are the historical 1842  $M_w$  8.23 and 1887  $M_w$  7.93 events.**

The first paragraph of FSAR Subsection 2.5.2.4.4.3.2.5 will be divided into two paragraphs and the following text will be inserted as a new paragraph in-between in a future FSAR update:

#### 2.5.2.4.4.3.2.5 Northern Hispaniola Fault — Western

At closest approach, the western Northern Hispaniola fault source is located about 550 miles from the Units 6 & 7 site (Figure 2.5.2-217). Subsection 2.5.1.1.2.3.2.2 provides discussion of the geologic, geodetic, and seismic characteristics of the Northern Hispaniola fault. Table 2.5.2-217 summarizes source parameters for this fault source.

**The western Northern Hispaniola fault source is associated with abundant seismicity along its entire length, with an especially high concentration of epicenters along its central and eastern portions (Figure 2.5.2-217). The largest earthquake from the Phase 2 catalog associated with this source is the 1953  $M_w$  6.93 event.**

The first paragraph of FSAR Subsection 2.5.2.4.4.3.2.6 will be divided into two paragraphs and the following text will be inserted as a new paragraph in-between in a future FSAR update:

#### 2.5.2.4.4.3.2.6 Northern Hispaniola Fault — Eastern

At closest approach, the eastern Northern Hispaniola fault source is located about 760 miles from the Units 6 & 7 site (Figure 2.5.2-217). Subsection 2.5.1.1.2.3.2.2 provides discussion of the geologic, geodetic, and seismic characteristics of the Northern Hispaniola fault. Table 2.5.2-217 summarizes source parameters for this fault source.

**The eastern Northern Hispaniola fault source is associated with abundant seismicity along its entire length, much of which appears in map view to the south of the surface trace of this south-dipping fault (Figure 2.5.2-217). The largest earthquake from the Phase 2 catalog associated with this source is the 1946  $M_w$  7.90 event.**

The first paragraph of FSAR Subsection 2.5.2.4.4.3.2.7 will be divided into two paragraphs and the following text will be inserted as a new paragraph in-between in a future FSAR update:

#### 2.5.2.4.4.3.2.7 Swan Islands Fault — Western

At closest approach, the western Swan Islands fault source is located 620 miles from the Units 6 & 7 site (Figure 2.5.2-217). Subsection 2.5.1.1.2.3.1.1 provides discussion of the geologic, geodetic, and seismic characteristics of the Swan Islands fault. Table 2.5.2-217 summarizes source parameters for this fault source.

**The western Swan Islands fault source is associated with abundant seismicity along its entire length (Figure 2.5.2-217). The largest earthquake from the Phase 2 catalog associated with this source is the historical 1856  $M_w$  7.69 event.**

The first paragraph of FSAR Subsection 2.5.2.4.4.3.2.8 will be divided into two paragraphs and the following text will be inserted as a new paragraph in-between in a future FSAR update:

#### 2.5.2.4.4.3.2.8 Swan Islands Fault — Eastern

At closest approach, the eastern Swan Islands fault source is located 540 miles from the Units 6 & 7 site (Figure 2.5.2-217). Subsection 2.5.1.1.2.3.1.1 provides discussion of the geologic, geodetic, and seismic characteristics of the Swan Islands fault. Table 2.5.2-217 summarizes source parameters for this fault source.

**The eastern Swan Islands fault source is associated with abundant seismicity along its entire length, with an apparent concentration of epicenters located near its eastern end near the Cayman trough (Figure 2.5.2-217). No earthquakes from the Phase 2 catalog greater than or equal to  $M_w$  6.75 are associated with this source.**

The first paragraph of FSAR Subsection 2.5.2.4.4.3.2.9 will be divided into two paragraphs and the following text will be inserted as a new paragraph in-between in a future FSAR update:

#### 2.5.2.4.4.3.2.9 Walton-Duanvale Fault

At closest approach, the Walton-Duanvale fault source is located 490 miles from the Units 6 & 7 site (Figure 2.5.2-217). Subsection 2.5.1.1.2.3.2.3 provides discussion of the geologic, geodetic, and seismic characteristics of the Walton-Duanvale fault. Table 2.5.2-217 summarizes source parameters for this fault source.

**The Walton-Duanvale fault source is associated with moderately abundant seismicity along its length, with an apparent concentration of epicenters located near its western end near the Cayman trough (Figure 2.5.2-217). Seismicity also appears concentrated at the eastern end of this source near Jamaica, where the left-lateral Walton-Duanvale and Enriquillo-Plantain Garden faults form a restraining bend. The largest earthquakes from the Phase 2 catalog associated with this source are the two approximately  $M_w$  6.6 events that occurred in 1907 and 1957.**

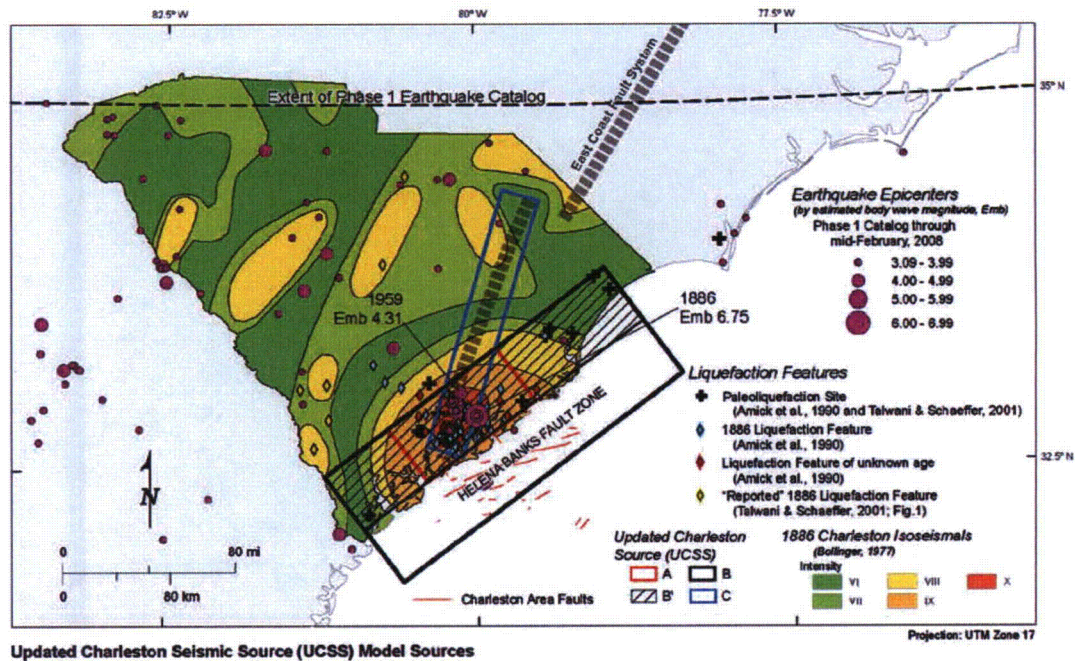
The first paragraph of FSAR Subsection 2.5.2.4.4.3.2.10 will be divided into two paragraphs and the following text will be inserted as a new paragraph in-between in a future FSAR update:

#### 2.5.2.4.4.3.2.10 Enriquillo-Plantain Garden Fault

At closest approach, the western Enriquillo-Plantain Garden fault source is located 560 miles from the Units 6 & 7 site (Figure 2.5.2-217). Subsection 2.5.1.1.2.3.2.3 provides discussion of the geologic, geodetic, and seismic characteristics of the Enriquillo-Plantain Garden fault. Table 2.5.2-217 summarizes source parameters for this fault source.

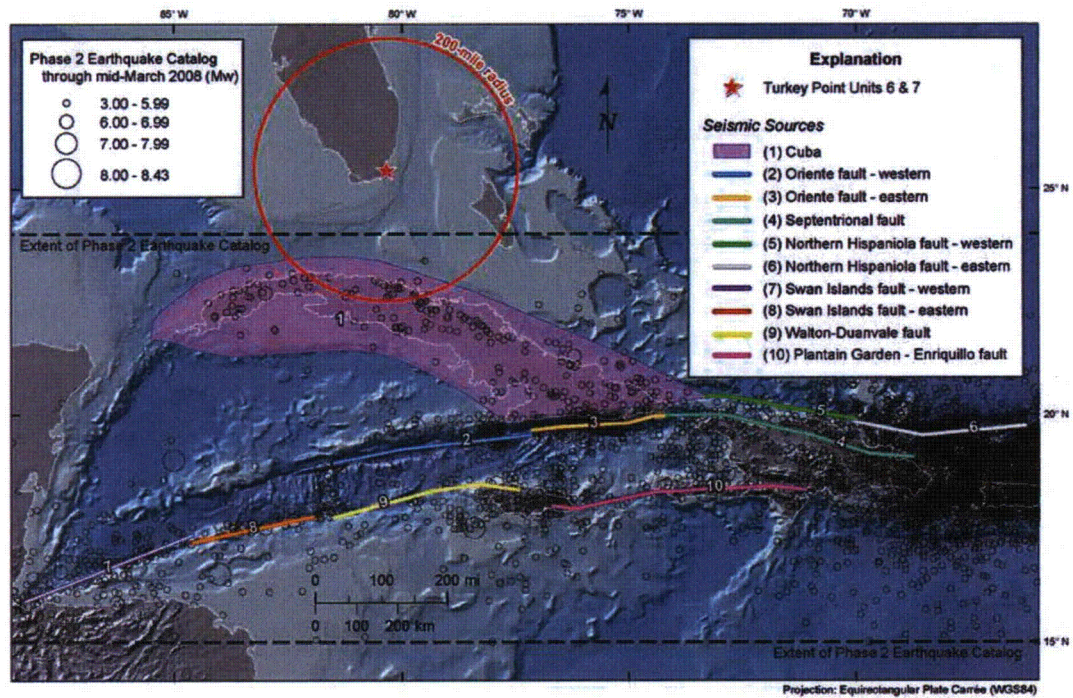
**The Enriquillo-Plantain Garden fault source is associated with abundant seismicity along its length, with apparent concentrations of epicenters at its western and eastern ends (Figure 2.5.2-217). Multiple large historical earthquakes have ruptured along the Enriquillo-Plantain Garden fault (FSAR Reference 2.5.2-282), including from the Phase 2 catalog the 1692  $M_w$  7.78 earthquake near Jamaica and the 1751  $M_w$  7.28 and 1770  $M_w$  7.53 earthquakes near Port-au-Prince, Haiti.**

Figure 2.5.2-212 will be replaced with the following revised figure in a future FSAR update:



Sources of liquefaction features: References 207, 208, and 323  
Source of the 1886 Charleston isoseismals: Reference 216

Figure 2.5.2-217 will be replaced with the following revised figure in a future FSAR update:



**ASSOCIATED ENCLOSURES:**

None

**NRC RAI Letter No. PTN-RAI-LTR-037**

**SRP Section: 02.05.02 - Vibratory Ground Motion**

Question for Geosciences and Geotechnical Engineering Branch 1 (RGS1)

**NRC RAI Number: 02.05.02-8 (eRAI 5896)**

FSAR Subsection 2.5.2.4.6 lists the Cuba areal source as one of the major contributing seismic sources to the total hazard. However, the deaggregation results shown in FSAR Figure 2.5.2-226 indicate only a minor contribution from the distance range of the Cuba areal source. In accordance with NUREG-0800, Standard Review Plan, Chapter 2.5.2, "Vibratory Ground Motion," and Regulatory Guide (RG) 1.208, "A Performance-Based Approach to Define the Site-Specific Earthquake Ground Motion", please explain this apparent discrepancy. What is the percentage of the Cuba areal source's hazard contribution (at  $10E-04$  and  $10E-05$  levels) to the total site hazard at all seven frequencies defined by the EPRI 2004 and 2006 GMPEs? Are these consistent with the deaggregation results?

**FPL RESPONSE:**

FSAR section 2.5.2.4.6 states that distant sources have the major contribution to low frequency rock hazard and these sources include the Cuba areal source, Caribbean faults, and Charleston source. Table 1 shows the rock hazard from the Cuba areal source alone for the overall  $10^{-4}$  and  $10^{-5}$  amplitudes and also shows the percent contribution to the total  $10^{-4}$  and  $10^{-5}$  rock hazard. These percentages are consistent with the deaggregation plots (FSAR Figures 2.5.2-226 through 2.5.2-229). Note, for example, that at  $10^{-4}$ , contributions from the Cuba areal source at 1 Hz and 2.5 Hz are 14.6% and 29.7% respectively, which average to approximately 22%. This contribution in FSAR Figure 2.5.2-226 (for 1 Hz and 2.5 Hz) is spread over about 25 magnitude-distance bins with magnitudes ranging from 6.0 to 7.5 and distances ranging from 210 km to about 480 km. This example illustrates that the percent contributions in Table 1 are consistent with the deaggregation plots (FSAR Figures 2.5.2-226 through 2.5.2-229).

Table 1. Percent contribution of total mean rock hazard from the Cuba areal source.

| Frequency (Hz) | % Contribution at 10 <sup>-4</sup> |                | % Contribution at 10 <sup>-5</sup>    |                |
|----------------|------------------------------------|----------------|---------------------------------------|----------------|
|                | Mean Hazard<br>(Cuba Areal Source) | % Contribution | Mean Hazard<br>(Cuba Areal<br>Source) | % Contribution |
| 0.5            | 6.13E-06                           | 6.1            | 4.33E-07                              | 4.3            |
| 1              | 1.46E-05                           | 14.6           | 1.21E-06                              | 12.1           |
| 2.5            | 2.97E-05                           | 29.7           | 1.45E-06                              | 14.5           |
| 5              | 3.10E-05                           | 31.0           | 5.82E-07                              | 5.8            |
| 10             | 2.08E-05                           | 20.8           | 1.52E-07                              | 1.5            |
| 25             | 4.50E-06                           | 4.5            | 6.97E-09                              | 0.1            |
| 100 (PGA)      | 1.25E-05                           | 12.5           | 4.49E-08                              | 0.4            |

This response is PLANT SPECIFIC.

**References:**

None

**ASSOCIATED COLA REVISIONS:**

None

**ASSOCIATED ENCLOSURES:**

None

**NRC RAI Letter No. PTN-RAI-LTR-037**

**SRP Section: 02.05.02 - Vibratory Ground Motion**

Question for Geosciences and Geotechnical Engineering Branch 1 (RGS1)

**NRC RAI Number: 02.05.02-9 (eRAI 5896)**

FSAR Subsection 2.5.2.5.1 states that P-wave velocities from eight deep wells were used to develop the deeper (>636 ft) sections of the site response model. The wells that provide the P-wave velocity information are approximately 100 km to 180 km away from the site. In accordance with Regulatory Guide (RG) 1.208, "A Performance-Based Approach to Define the Site-Specific Earthquake Ground Motion", please provide:

- a. additional information on the applicability of seismic velocity information obtained at such great distances to the Turkey Point site. How was the variation in geology considered in these projections?
- b. individual velocity profiles for each of the eight wells used in estimating the average profile shown in FSAR Figure 2.5.4-211
- c. further details on how larger uncertainties in deeper layers' thicknesses/depths are taken into account in the randomization of the site profile

**FPL RESPONSE:**

**Background**

Sonic logs 0001, 0002, 0005, 0007, 0008 and 0010 (files purchased from the Florida Geological Survey Division of Oil and Gas) were derived from wells located approximately 66 miles (approximately 106.2 kilometers), 62 miles (approximately 100.0 kilometers), 81 miles (approximately 130.4 kilometers), 110 miles (approximately 177.0 kilometers), 82 miles (approximately 132.0 kilometers), and 71 miles (approximately 114.3 kilometers) from the FPL Turkey Point site, respectively (FSAR Figure 2.5.4-210). The measurements recorded by the probe at these locations were depth, expressed in feet below the drill rig's Kelly bushing, and the interval travel time (Delta T ( $DT_p$ )) expressed in microseconds ( $10^{-6}$  seconds) per foot. The logs were initiated at an upper depth of 3,610 to 4,100 feet (El. -3,555 to -4,059 feet NAVD 88) below each drill rig's Kelly bushing and terminated at a lower depth of 11,600 to 11,920 feet (El. -11,564 to -11,879 feet NAVD 88) below Kelly bushing.

Because these six sonic logs do not possess  $DT_p$  data for depths above 3,610 (El. -3,555 feet NAVD88), a gap in the compression wave velocity data existed between the depths of 620 and 3,610 feet (El. -600 and -3,555 feet NAVD 88). To fill much of this data gap, two sonic logs, LAB-TW and PBF-12, obtained from U.S. Geological Survey (Reference 1) were manually digitized over ten- foot intervals.

Sonic logs LAB-TW and PBF-12 (Reference 1) were derived from wells located approximately 115 miles (approximately 185.1 kilometers) and 64 miles (approximately 103.0 kilometers) from the Turkey Point site, respectively (FSAR Figure 2.5.4-210). The measurements recorded by the probe at these locations were depth, expressed in feet

below land surface, and  $DT_p$ , expressed in microseconds ( $10^{-6}$  seconds) per foot. The logs were initiated at an upper depth of 500 to 900 feet (El. -482 to -834 feet NAVD88) below land surface and terminated at a lower depth of 1,900 to 2,350 feet (El. -1882 to -2334 feet NAVD88) below land surface.

The wells noted in the preceding two paragraphs are the closest wells to the Turkey Point Units 6 & 7 site with available subsurface seismic velocity data. This response is structured to respond to parts a, b, and c of the RAI.

- a) The well locations with the sonic logs used for this analysis are shown on FSAR Figure 2.5.4-210. FSAR Figure 2.5.1-232 shows a north-south regional geologic cross section (Section E-F) through the Upper Mesozoic and Lower Cenozoic rocks in southern Florida. Point 39 on the cross section (and on the Inset Map on FSAR Figure 2.5.1-232) is the closest location on the regional geologic cross section to the majority of the sonic log locations on FSAR Figure 2.5.4-210. The distance from Point 39 to the Turkey Point site is about 80 miles (128.7 kilometers). Based on the review of publications (FSAR Subsection 2.5.1 References 374, 377, 378, and 397), regional geologic cross sections (FSAR Figures 2.5.1-232, 233, 235, and 236) and the sonic logs (0001, 0002, 0005, 0007, 0008, 0010, LAB-TW and PBF-12), there appears to be relatively little variation, on a regional scale, in the stratigraphy of the upper 6,000 ft between the Point 39 area and the Turkey Point site. Based upon this review the stratigraphic units generally show less variation with increasing depth. Therefore, it is reasonable to assume that the lack of stratigraphic variation on the scale shown in FSAR Figure 2.5.1-232 continues below 6,000 feet. The stratigraphic information and shear wave velocity data, which is calculated from Poisson's ratio and interval travel time derived from the sonic logs, were migrated down the gentle regional dip from the locations of the wells shown on FSAR Figure 2.5.4-210 to the Turkey Point Units 6 & 7 site. Geologic variations, where they exist, are most likely due to facies changes within the gross stratigraphic units. This regional geology-based approach is a reasonable means for developing a stratigraphic and shear wave velocity column for the stratigraphic units below the deepest site borings. This approach provides a technical basis for the development of the deep portion of the site response model. Variations in both unit thickness and material properties, that might be the result of facies changes within stratigraphic units, are accounted for by the randomization process described in part c of this RAI response.
- b) The compression and shear wave velocity profiles for each of the 8 wells are shown in Figures 1 through 8.

- c) The uncertainties in the dynamic properties of the deeper layers were taken into account by the following two steps.
1. The calculated logarithmic standard deviation for each of the converted shear-wave velocity ( $V_s$ ) values was increased to account for uncertainty in Poisson's ratio and to account for the number of profiles used to construct the deep portion of the base case profile.
  2. The layer thicknesses of each synthetic profile were obtained using a randomization approach where the rate of layer boundary changes at a given depth (which is closely related to the probability of having a layer boundary at that depth) is the sum of a smooth continuous function and a non-smooth function that takes non-zero values where the base case profiles have discontinuities in  $V_s$ . The value of the latter function is proportional to the relative change in  $V_s$  and inversely proportional to the logarithmic standard deviation of  $V_s$ . Because the size of the steps in the base case  $V_s$  profile is relatively small compared to the logarithmic standard deviation of  $V_s$ , these discontinuities tend to occur at different depths in different synthetic profiles, as can be verified in FSAR Figure 2.5.2-239. This implies that the layer thicknesses are strongly randomized in the lower portion of the profile.

Figure 1. Shear Wave ( $V_s$ ) and Compression Wave ( $V_p$ ) Velocity Profiles for Sonic Log 0001

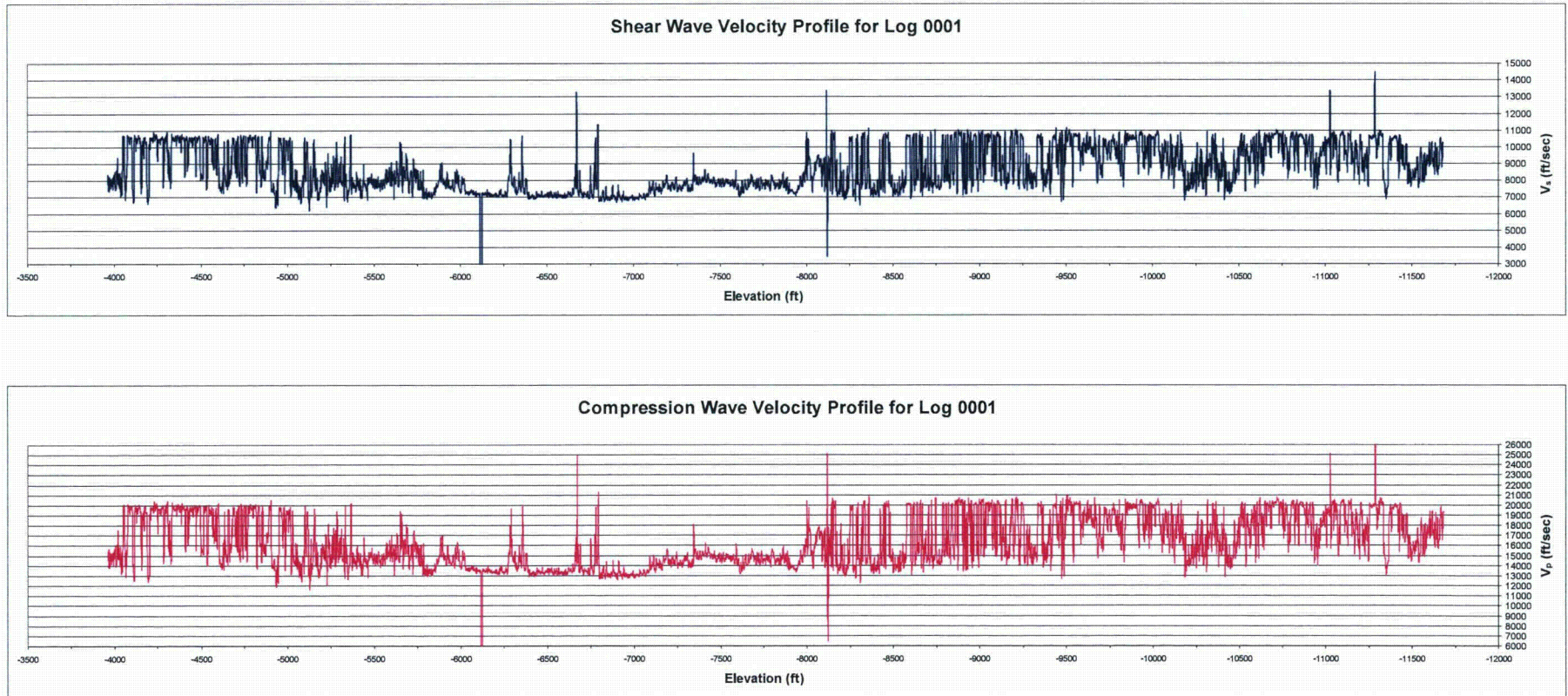


Figure 2. Shear Wave ( $V_s$ ) and Compression Wave ( $V_p$ ) Velocity Profiles for Sonic Log 0002

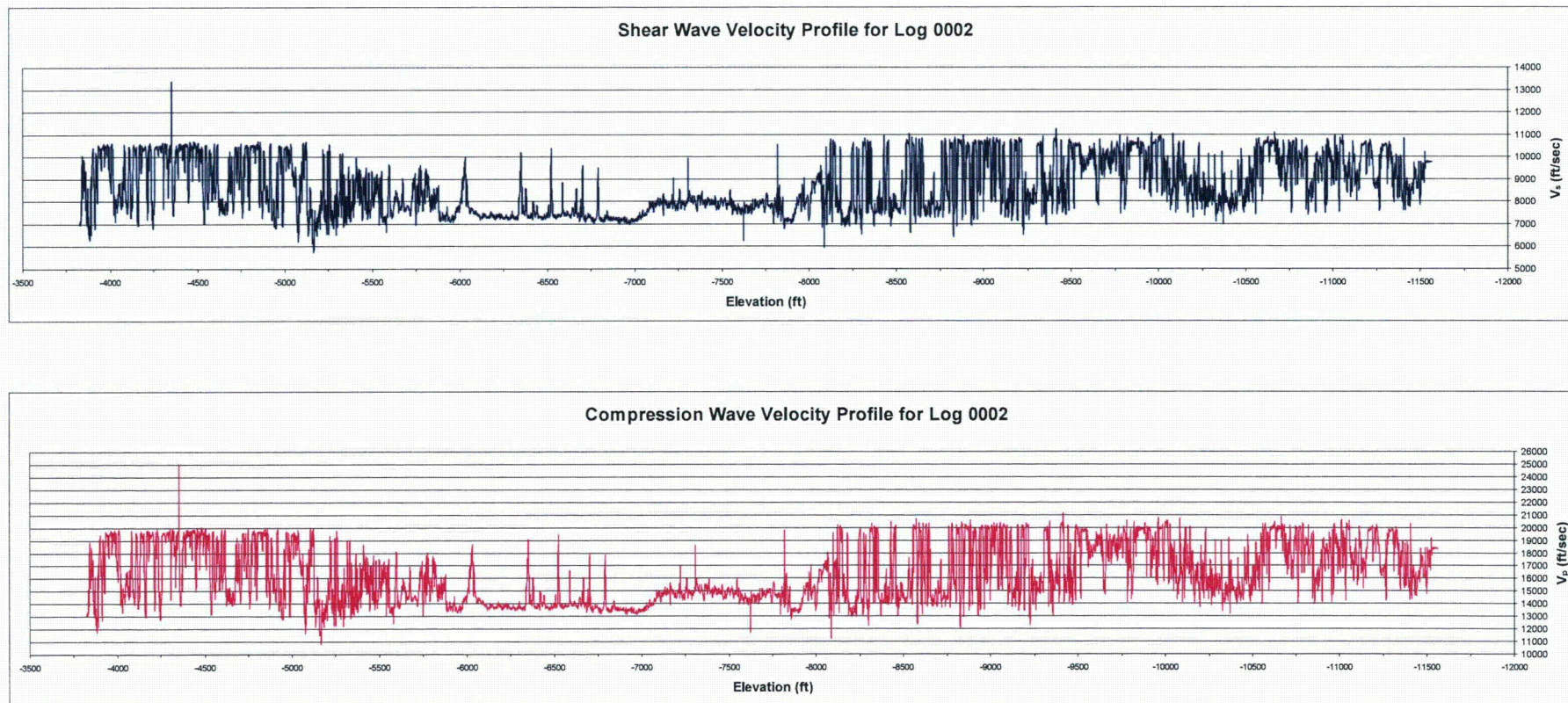


Figure 3. Shear Wave ( $V_s$ ) and Compression Wave ( $V_p$ ) Velocity Profiles for Sonic Log 0005

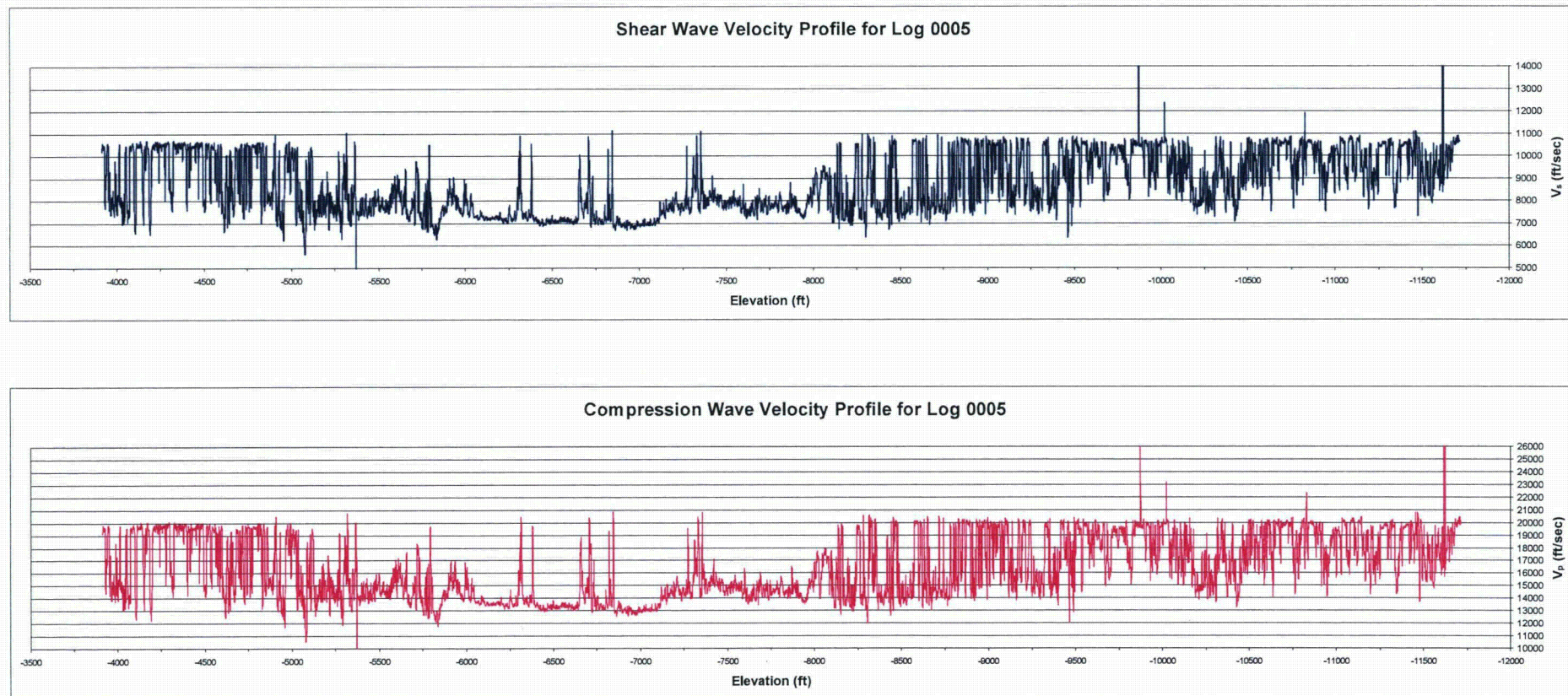


Figure 4. Shear Wave ( $V_s$ ) and Compression Wave ( $V_p$ ) Velocity Profiles for Sonic Log 0007

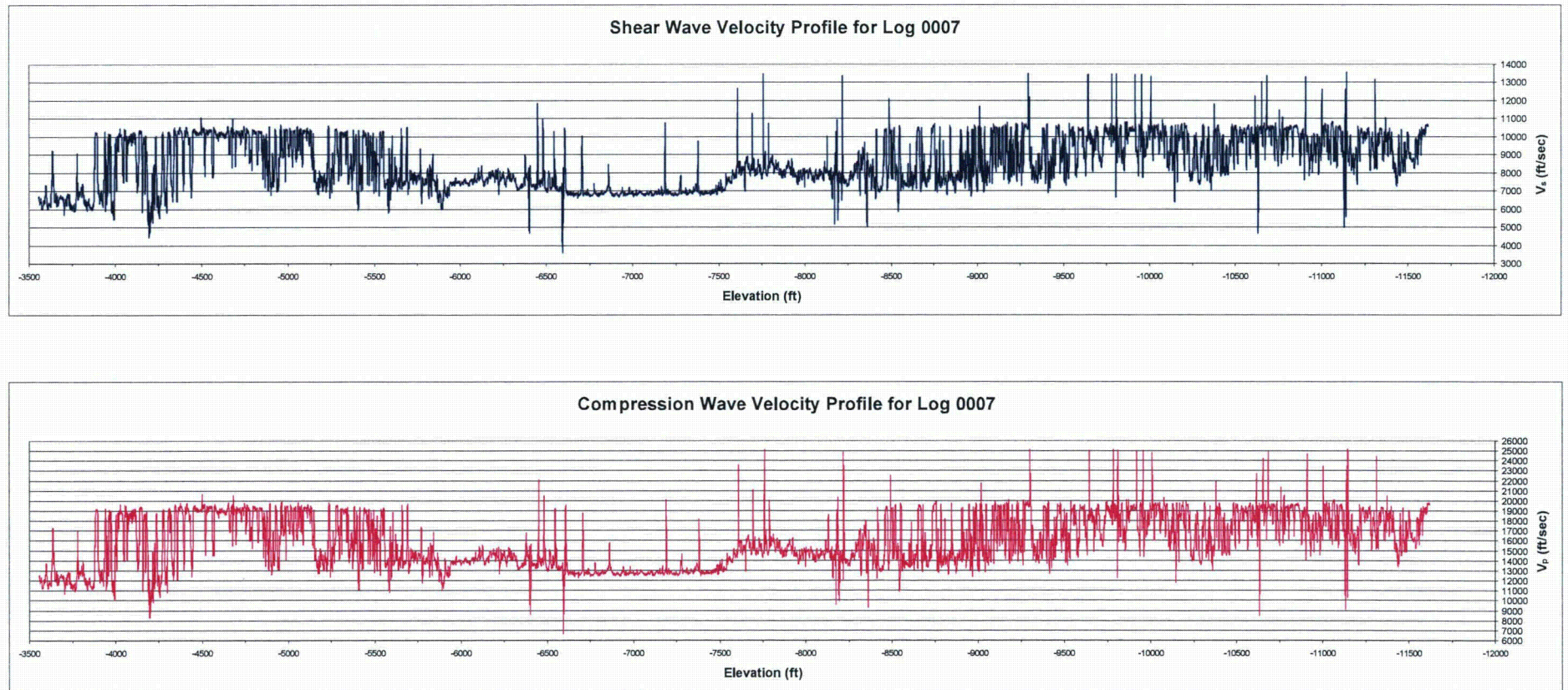


Figure 5. Shear Wave ( $V_s$ ) and Compression Wave ( $V_p$ ) Velocity Profiles for Sonic Log 0008

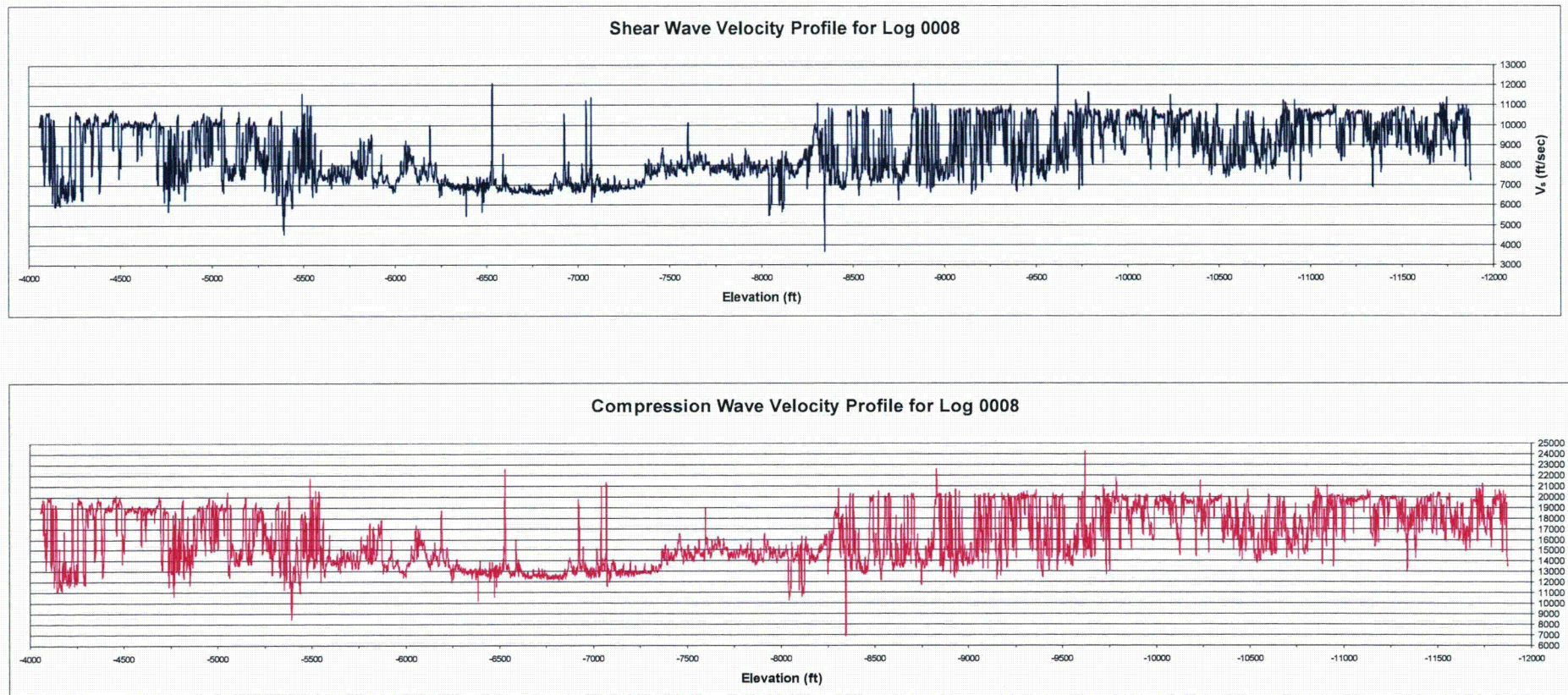


Figure 6. Shear Wave ( $V_s$ ) and Compression Wave ( $V_p$ ) Velocity Profiles for Sonic Log 0010

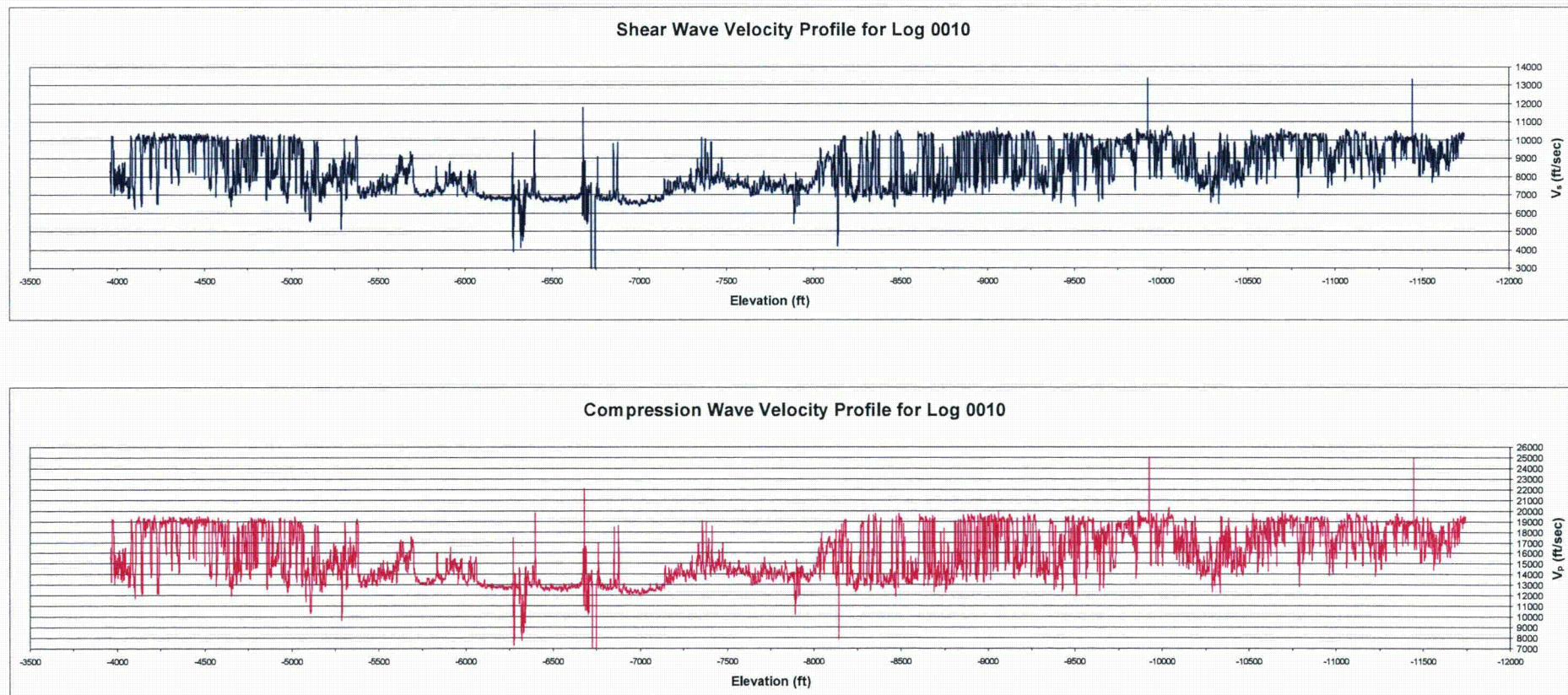


Figure 7. Shear Wave ( $V_s$ ) and Compression Wave ( $V_p$ ) Velocity Profiles for Sonic Log LAB-TW

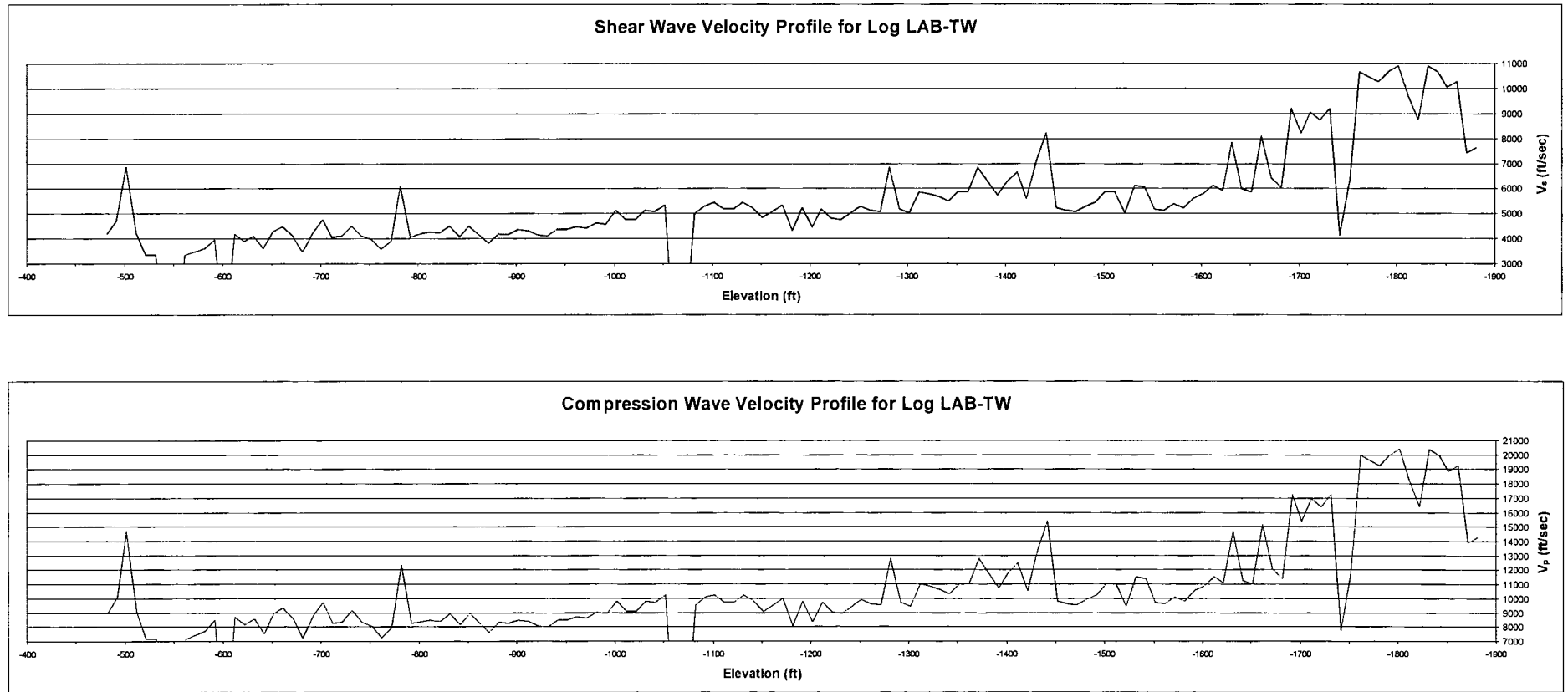
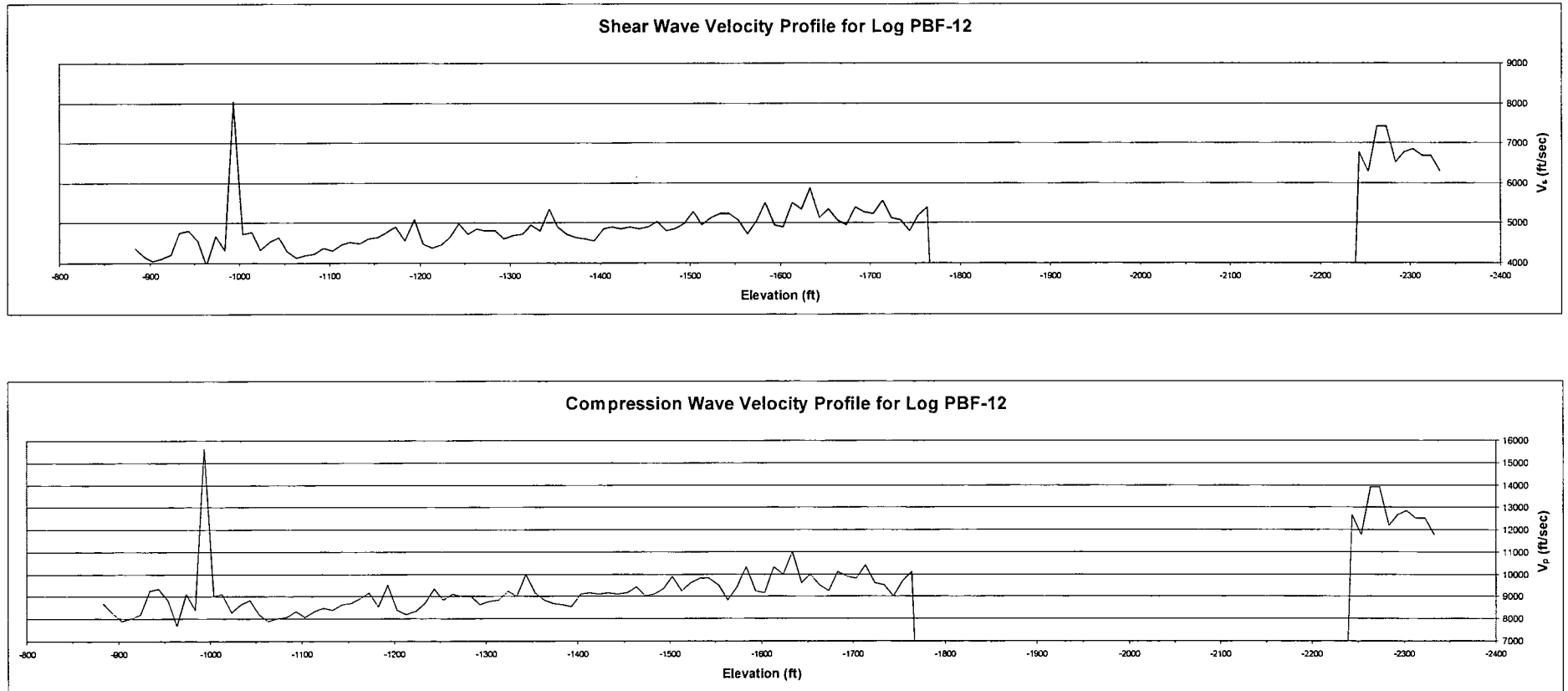


Figure 8. Shear Wave ( $V_s$ ) and Compression Wave ( $V_p$ ) Velocity Profiles for Sonic Log PBF-12



This response is PLANT SPECIFIC.

Proposed Turkey Point Units 6 and 7  
Docket Nos. 52-040 and 52-041  
FPL Revised Response to NRC RAI No. 02.05.02-9 (eRAI 5896)  
L-2014-282 Attachment 8 Page 12 of 12

**References:**

1. Reese, R.S. and Richardson, E., Synthesis of the Hydrogeologic Framework of the Floridan Aquifer System and Delineation of a Major Avon Park Permeable Zone in Central and Southern Florida, Scientific Investigations Report 2007-5207, U.S. Geological Survey, 2008.

**ASSOCIATED COLA REVISIONS:**

None

**ASSOCIATED ENCLOSURES:**

None

**NRC RAI Letter No. PTN-RAI-LTR-037**

**SRP Section: 02.05.02 - Vibratory Ground Motion**

Question for Geosciences and Geotechnical Engineering Branch 1 (RGS1)

**NRC RAI Number: 02.05.02-10 (eRAI 5896)**

FSAR Subsection 2.5.2.1.2 describes the updated Phase 1 and Phase earthquake catalogs. Of the 34 source earthquake catalogs listed on pages 2.5.2-3 through 2.5.2-5 for Phase 1 updates, 15 cite Reference 307, which is the USGS NEIC "Earthquake Search" website. A similar situation exists for the Phase 2 catalog update. In accordance with Regulatory Guide (RG) 1.208, "A Performance-Based Approach to Define the Site-Specific Earthquake Ground Motion", please clarify the relationship between Reference 307 and the corresponding 15 source catalogs used in the Phase 1 seismicity update. Specifically, how is the contribution from each sub-catalog identified?

**FPL RESPONSE:**

Reference 307 is cited as the source for several catalogs used for both the Phase 1 and Phase 2 earthquake catalogs, discussed in FSAR Sections 2.5.2.1.2 and 2.5.2.1.3, respectively. The reference listed in FSAR 2.5.2.7 References as Reference 307 is incorrect. The correct Reference 307 should be given as:

307. National Geophysical Data Center [NGDC]. The Seismicity Catalog CD-ROM Collection: Volume 1: North America, 1492-1996 A.D., Volume 2: Global and Regional, 2150 B.C. - 1996 A.D., National Oceanic and Atmospheric Administration / National Geophysical Data Center, World Data Center-A Solid Earth Geophysics, 325 Broadway, E/GC1, Boulder, Colorado, 2 volume CD-ROM, 1996. The CD-ROM data are available on-line at <http://www.ngdc.noaa.gov/hazard/fliers/se-0208.shtml>.

The earthquake data from this 1996 CD-ROM collection, used for the FSAR evaluations, are now available on the NGDC web site: <http://www.ngdc.noaa.gov/hazard/fliers/se-0208.shtml>. The web site describes the compilation as follows:

*A two-CDROM compilation of seismicity catalogs from NOAA's National Geophysical Data Center and U.S. Geological Survey's National Earthquake Information Center is available online. The two-volume CD-ROM collection contains data on over four million earthquakes dating from 2100 B.C. to 1995 A.D. The data include information on epicentral time of origin, location, magnitudes, depth and other earthquake-related parameters.*

*Three types of catalogs are included on the CDs: **local** (containing data from single stations or local networks); **regional** (containing data from regional networks, such as CALNET in central California) and **teleseismic** (containing data from around the world). Records have been contributed from various worldwide industrial, academic, governmental, and private sources. The CDs also contain auxiliary data bases (such as world stress, tsunami, volcanic, fault parameters, etc.) which aid in earthquake investigations.*

[Note: while otherwise accurate in its description of the CD-ROM data, the web site quotation above has a typo in the date range of "2100 B.C. to 1995 A.D." As given in the reference citation, the correct date range of the seismicity data is 2150 B.C. - 1996 A.D.].

The identification of the contribution from each sub-catalog is indicated in the **Catalog Reference** column in Tables 2.5.2-201 [Phase 1] and 2.5.2-203 [Phase 2] either by reference to the parenthetical symbolic name indicated in the bulleted lists of the catalogs in FSAR Sections 2.5.2.1.2 and 2.5.2.1.3 or by footnotes to the FSAR Tables 2.5.2-201 and 2.5.2-203.

This response is PLANT SPECIFIC.

#### References:

None

#### ASSOCIATED COLA REVISIONS:

The text in Revision 2 of FSAR subsection 2.5.2.1.2, Updated Seismicity Data in the Phase 1 Investigation Region, 18<sup>th</sup> bullet below the second paragraph on existing page 2.5.2-4, will be revised as follows in a future update of the FSAR.

- National Geophysical Data Center **USGS "PDE" Catalog** (Reference 307)

The text in Revision 2 of FSAR subsection 2.5.2.1.3, Caribbean Seismicity Data in the Phase 2 Investigation Region, 10<sup>th</sup> bullet below the seventh paragraph on existing page 2.5.2-9, will be revised as follows in a future update of the FSAR.

- National Geophysical Data Center **USGS "PDE" Catalog** (Reference 307)

Reference 307 in Revision 2 of FSAR Subsection 2.5.2.7, References, on existing page 2.5.2-98, will be revised as follows in a future update of the FSAR.

~~307. Rinehart, W., Ganse, R., and Teik, P., National Geophysical Data Center (NGDC); Arnold, E., and Stover, C., U.S. Geological Survey (USGS), and Smith, R.H., (CIRES), National Earthquake Information Center (NEIC), Seismicity of Middle America, National Geophysical Data Center and National Earthquake Information Service, U.S. Geological Survey, 1982. Available at [http://neic.usgs.gov/neis/epic/code\\_catalog.html](http://neic.usgs.gov/neis/epic/code_catalog.html), accessed February 15, 2008.~~

**307. National Geophysical Data Center. The Seismicity Catalog CD-ROM Collection: Volume 1: North America, 1492-1996 A.D., Volume 2: Global and Regional, 2150 B.C.-1996 A.D., National Oceanic and Atmospheric Administration/National Geophysical Data Center, World Data Center-A Solid Earth Geophysics, 325 Broadway, E/GC1, Boulder, Colorado, 2 volume CD-ROM, 1996. Available at <http://www.ngdc.noaa.gov/hazard/fliers/se-0208.shtml>.**

Proposed Turkey Point Units 6 and 7  
Docket Nos. 52-040 and 52-041  
FPL Revised Response to NRC RAI No. 02.05.02-10 (eRAI 5896)  
L-2014-282 Attachment 9 Page 3 of 3

Footnote (a) of Tables 2.5.2-201 and 2.5.2-203 in Revision 2 of FSAR Subsection 2.5.2, Vibratory Ground Motion, on existing pages 2.5.2-127 and 2.5.2-137, will be revised as follows in a future update of the FSAR.

Footnote to Table 2.5.2-201

- (a) "EPRIm" are the "MAIN" events from the EPRI catalog.  
"\*\*\*c" are constituent catalogs from IPGH catalog  
"\*\*\*wy" are constituent catalogs from Wyession et al. catalog (Reference 338)  
"\*\*\*me" are constituent catalogs from the Mexico Composite Catalog  
"\*\*\*np" are constituent catalogs from National Geophysical Data Center **USGS "PDE"** catalog

Footnote to Table 2.5.2-203

- (a) "\*\*\*c" are constituent catalogs from IPGH catalog  
"\*\*\*np" are constituent catalogs from National Geophysical Data Center **USGS "PDE"** catalog

**ASSOCIATED ENCLOSURES:**

None

Proposed Turkey Point Units 6 and 7  
Docket Nos. 52-040 and 52-041  
FPL Revised Response to NRC RAI No. 02.05.02-11 (eRAI 5896)  
L-2014-282 Attachment 10 Page 1 of 1

**NRC RAI Letter No. PTN-RAI-LTR-037**

**SRP Section: 02.05.02 - Vibratory Ground Motion**

Question for Geosciences and Geotechnical Engineering Branch 1 (RGS1)

**NRC RAI Number: 02.05.02-11 (eRAI 5896)**

FSAR Subsection 2.5.2.4.4.1 describes the supplemental source zones which are developed to extend the original EPRI zones to cover the entire site region. The FSAR discusses that updated *a* and *b* values are borrowed from peninsular Florida for the supplemental zones, but the parameters are not provided. In accordance with NUREG-0800, Standard Review Plan, Chapter 2.5.2, "Vibratory Ground Motion," and Regulatory Guide (RG) 1.208, "A Performance-Based Approach to Define the Site-Specific Earthquake Ground Motion" please provide the *a* and *b* parameters for each supplemental zone.

**FPL RESPONSE:**

An average rate (*a*-value) and *b*-value for the 15 degree-cells comprising the Florida peninsula were calculated using the updated earthquake catalog, because this is the most up-to-date information available. The average values for the 15 degree-cells are  $a = -2.28$  and  $b = 1.03$ . The *a*-value is the base 10 logarithm of the annual rate of earthquakes with body-wave magnitude (*m<sub>b</sub>*) between 3.3 and 3.9, per equatorial square degree. The *a*-value and *b*-value were used for each supplemental source by converting them into a total rate for each supplemental source, using the area of each supplemental source given in FSAR Table 2.5.2-211.

This response is PLANT SPECIFIC.

**References:**

None

**ASSOCIATED COLA REVISIONS:**

No COLA changes have been identified as a result of this response.

**ASSOCIATED ENCLOSURES:**

None

**NRC RAI Letter No. PTN-RAI-LTR-037**

**SRP Section: 02.05.02 - Vibratory Ground Motion**

Question for Geosciences and Geotechnical Engineering Branch 1 (RGS1)

**NRC RAI Number: 02.05.02-12 (eRAI 5896)**

FSAR Subsection 2.5.2.4.4.3.2 discusses the existence of several large, but very distant seismic sources. Regarding these sources the FSAR states that: "... these tectonic features would not significantly contribute" to the hazard at TPNPP. In accordance with NUREG-0800, Standard Review Plan, Chapter 2.5.2, "Vibratory Ground Motion," and Regulatory Guide (RG) 1.208, "A Performance-Based Approach to Define the Site-Specific Earthquake Ground Motion," please explain whether this assessment is based on preliminary sensitivity calculations showing very small hazard contributions from these sources or simply on best judgment. If best judgment, please further elaborate on the rationale used.

**FPL RESPONSE:**

Distant seismic sources were excluded in the source model, based on a combination of judgment and preliminary sensitivity studies that demonstrated the New Madrid seismic source was an insignificant contributor to the site hazard. Comparing the contributions of individual sources from PSHA deaggregated results also supports this rationale. The specific tectonic features that were excluded from the source model described in FSAR Subsection 2.5.2.4.4.3.2 are the Muertos Trough, Mona Passage extensional zone, eastern portion of the Puerto Rico Trench, and Beata Ridge.

As shown on FSAR Figures 2.5.1-202 and Figure 1 (Map of Cuba and Caribbean Seismic Sources and Other Distant Tectonic Features Not Included in the Seismic Source Model) of this response, the Muertos Trough, Mona Passage extensional zone (MPEZ), Puerto Rico Trench, and Beata Ridge are elements of the Northern Caribbean-North America plate boundary and are located more than 760 miles from the Turkey Point Units 6 & 7 site. More detailed descriptions of these tectonic features are included in FSAR Subsection 2.5.1.1.2.3. The western portion of the Puerto Rico Trench is included in the seismic source model as the North Hispaniola fault – Eastern fault source (FSAR Figure 2.5.2-217 and Figure 1). However, more distant portions of the Puerto Rico Trench were not included in the seismic source model.

The rationale to exclude these tectonic features (partially or entirely) from the seismic source model is based on: (1) their great distance from the site; (2) the insignificant hazard contribution from the distant New Madrid source; (3) the presence of high slip rate plate boundary structures capable of generating large to great earthquakes much closer to the site; and (4) the very small hazard contribution from the North Hispaniola fault – Eastern, which lies closer to the site than the subject tectonic features that were excluded.

As stated in FSAR Subsection 2.5.2.4.6, sensitivity runs demonstrated that the New Madrid seismic source contributed less than 0.1% of the mean hazard from other sources for 1 Hz spectral acceleration. The New Madrid source, which is approximately 900 miles from the Turkey Point Units 6 & 7 site, has a return period on the order of 500 years for Mmax earthquakes (Exelon, 2006).

Comparing the contribution of individual sources to the mean total hazard also supports the initial decision to exclude the Beata Ridge, Muertos Trough, and Mona Passage extension zone, and eastern portion of the Puerto Rico Trench from the seismic source model. The most distant Caribbean seismic source included in the model is the Northern Hispaniola fault – Eastern fault source. At its nearest point, this source is approximately 760 miles from the site.

For a 1 Hz spectral acceleration of 0.03g (which corresponds to a mean total hazard of  $1.59 \times 10^{-4}$ ), the contribution of the most distant source, the Northern Hispaniola fault – Eastern, is only 0.3% of the total mean hazard. At higher spectral accelerations, the contribution of this source is less. Therefore, any source with the same magnitude and slip rate as the Northern Hispaniola fault – Eastern, but at greater distance to the site, would contribute less than 0.3% of the total mean hazard at 0.03g spectral acceleration, and would contribute even less at higher amplitudes.

The Northern Hispaniola fault – Eastern is assigned a maximum magnitude range of Mw 8.0 to 8.6 and a slip rate of 4 to 8 mm/yr (Table 2.5.2-217) and it is unlikely that the subject seismic sources excluded from the model can be modeled with both magnitudes and slip rates greater than these values. This is supported in that the Beata Ridge is not a major plate boundary element and visually exhibits a lower rate of earthquakes (revised Figure 2.5.2-217 that accompanies RAI 02.05.02-7), the Muertos Trough exhibits lower slip rates (FSAR Reference 2.5.1-577) and some researchers do not consider it an active feature (Reference 2.5.1-589), the Mona Passage extension zone cannot produce great earthquakes with its much smaller dimensions (Figure 2.5.1-322), and the plate interface along the eastern portion of the Puerto Rico Trench is largely decoupled (FSAR References 2.5.1-577 and 2.5.1-643). Since these distant potential sources are located at similar or greater distances to the site than the Northern Hispaniola fault – Eastern (Figure 1), they would not be significant contributors to the mean total hazard at spectral accelerations of interest (those with annual frequencies of exceedence of  $1 \times 10^{-4}$  and less). Spectral frequencies higher than 1 Hz would be even less affected by distant sources. Based on our judgment and the rationale presented above, these distant sources were excluded from hazard calculations.

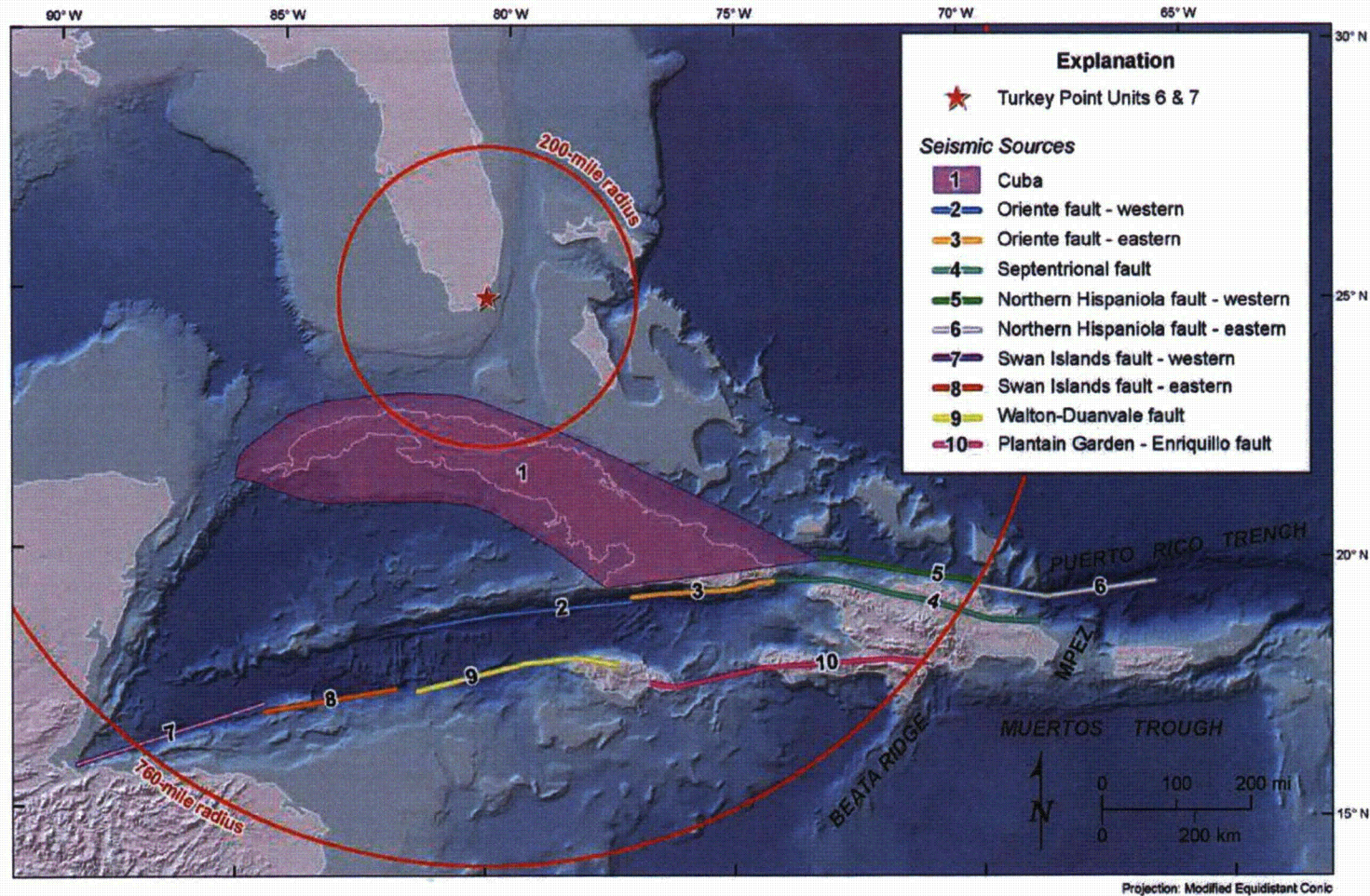


Figure 1 - Map of Cuba and Caribbean Seismic Sources and Other Distant Tectonic Features Not Included in the Seismic Source Model

Proposed Turkey Point Units 6 and 7  
Docket Nos. 52-040 and 52-041  
FPL Revised Response to NRC RAI No. 02.05.02-12 (eRAI 5896)  
L-2014-282 Attachment 11 Page 4 of 4

This response is PLANT SPECIFIC.

**References:**

Exelon Generation Company, LLC, *Site Safety Analysis Report for the Clinton ESP Site*, Rev. 4, April 2006.

**ASSOCIATED COLA REVISIONS:**

The text in the second paragraph of FSAR Subsection 2.5.2.4.4.3.2 will be revised in a future update of the FSAR:

These ten seismic sources are based on geologic, geophysical, and seismic data described in Subsections 2.5.1.1.1.3.2.4 (Cuba) and 2.5.1.1.2.3 (Active Tectonic Structures of the Northern Caribbean Plate). Subsection 2.5.1.1.2.3 also describes tectonic features that are too distant from the Units 6 & 7 site to contribute to the ground motion hazard, even from the largest earthquakes that could occur in them. These distant tectonic features are not included in the seismic source characterization, and include the Muertos Trough, Mona Passage extensional zone, **eastern portion of the** Puerto Rico Trench, and the Beata Ridge (Figure 2.5.1-202). The decision to exclude these tectonic features from this seismic source characterization is based on the assessment that these tectonic features would not significantly contribute to ground motion hazard at the Units 6 & 7 site. Specifically, this assessment is based on the great site-to-source distances for these tectonic features.

**ASSOCIATED ENCLOSURES:**

None

**NRC RAI Letter No. PTN-RAI-LTR-037**

**SRP Section: 02.05.02 - Vibratory Ground Motion**

Question for Geosciences and Geotechnical Engineering Branch 1 (RGS1)

**NRC RAI Number: 02.05.02-13 (eRAI 5896)**

The FSAR does not list the USGS national seismic hazard map project as a potential source for EPRI seismic source model updates. The USGS regularly updates its own national seismic hazard maps using the most recent data and information. Within the last decade, the USGS published two comprehensive national seismic hazard reports in 2002 and 2008. RG 1.208 indicates that existing seismic source models should be evaluated in light of more recent data and evolving knowledge. Please discuss why the USGS national seismic hazard maps and model parameters are not discussed as potential studies to be considered in updating the existing EPRI seismic source geometries and/or model parameters.

**FPL RESPONSE:**

A new discussion of the USGS National Seismic Hazard Mapping Project (NSHMP) will be added to the FSAR. The USGS NSHMP (FSAR Reference 300) characterizes seismic sources throughout the continental United States using multiple classes of earthquake source models. The general approach used by the USGS for modeling distributed seismicity in the Central and Eastern United States (CEUS) is based on gridded, spatially smoothed seismicity in large background zones. Seismic sources within the CEUS most relevant to the Turkey Point Units 6 & 7 site are modeled with: (1) a regional uniform background source model dividing the Extended Margin of the CEUS from the Craton; (2) special zones accounting for variability in catalog completeness, seismicity, maximum magnitude, and b-value, such as the uniform source zones for the Eastern Tennessee and New Madrid seismic zones; and (3) finite fault sources, such as those included for the New Madrid and Charleston seismic sources.

The 2008 NSHMP earthquake sources are depicted in Figure 1. Significant changes from the 2002 NSHMP (FSAR Reference 251) model of seismic hazard in the CEUS include: (1) uncertainty in the maximum magnitude ( $M_{max}$ ) assigned to  $M_{max}$  zones (e.g., Extended Margin); (2) revised geometry of the Charleston seismic source zones; and (3) revised magnitudes, rates, and geometry for the New Madrid seismic source. As a result of these updates, the 2008 NSHMP characterizes  $M_{max}$  for the Extended Margin and Craton as weighted distributions ranging between  $M7.1 - 7.7$  and  $M6.6 - 7.2$ , respectively. The two areal zones defining the Charleston source are both assigned  $M_{max}$  distributions of  $M6.8 - 7.5$  with a recurrence interval of 550 years, unchanged from the 2002 NSHMP (FSAR Reference 251). The Charleston seismic source updates from the NSHMP (FSAR Reference 300) are discussed in Subsections 2.5.2.4.4.2.2 and 2.5.2.4.4.2.3.

The NSHMP model only covers a small portion of the site region (Figure 1) and does not include seismically active areas in the southern part of the site region and beyond, such as Cuba and the North America-Caribbean plate boundary that contribute to the seismic hazard in southern Florida. Therefore, a direct comparison between the NSHMP SSC model and the FSAR SSC model is not presented in the FSAR.

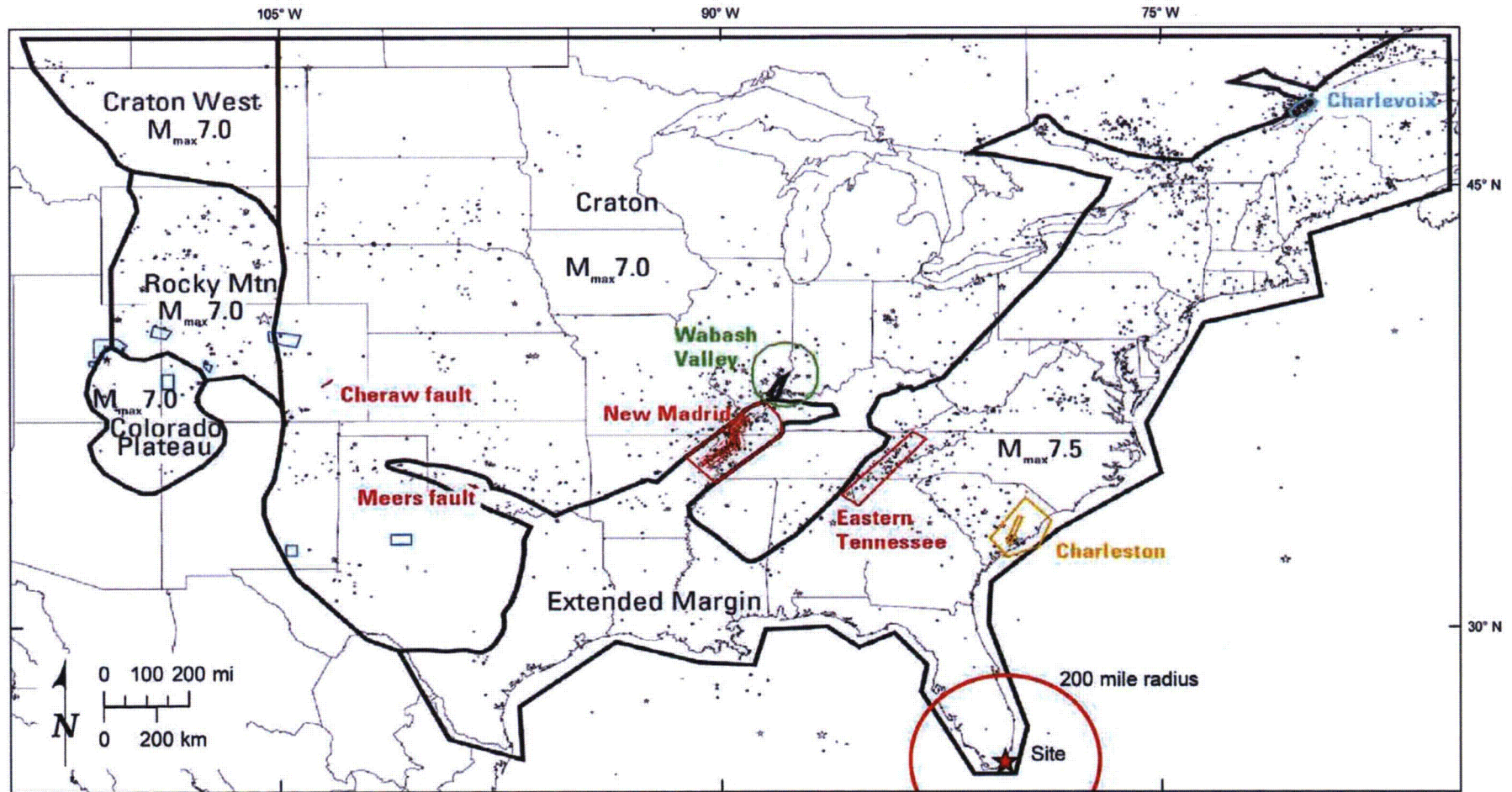


Figure 1. Seismic Sources from the U.S. Geological Survey's 2008 National Seismic Hazard Mapping Project  
(Petersen et al. 2008 FSAR Reference 300)

This response is PLANT SPECIFIC.

**References:**

None

**ASSOCIATED COLA REVISIONS:**

FSAR Subsection 2.5.2.4.4 will be revised in a future COLA revision as follows:

**2.5.2.4.4 New Seismic Source Characterizations**

To complement the updated EPRI seismic source model described above, three new seismic source characterizations are included for analysis. These three new source characterizations are:

- Supplemental seismic source zones that fill the area of the site region beyond the area covered by the original EPRI source model (Subsection 2.5.2.4.4.1).
- New, post-EPRI characterization of the Charleston seismic source (Subsection 2.5.2.4.4.2).
- New, post-EPRI characterization of seismic sources located in the Cuba area and the North America-Caribbean plate boundary region (Subsection 2.5.2.4.4.3).

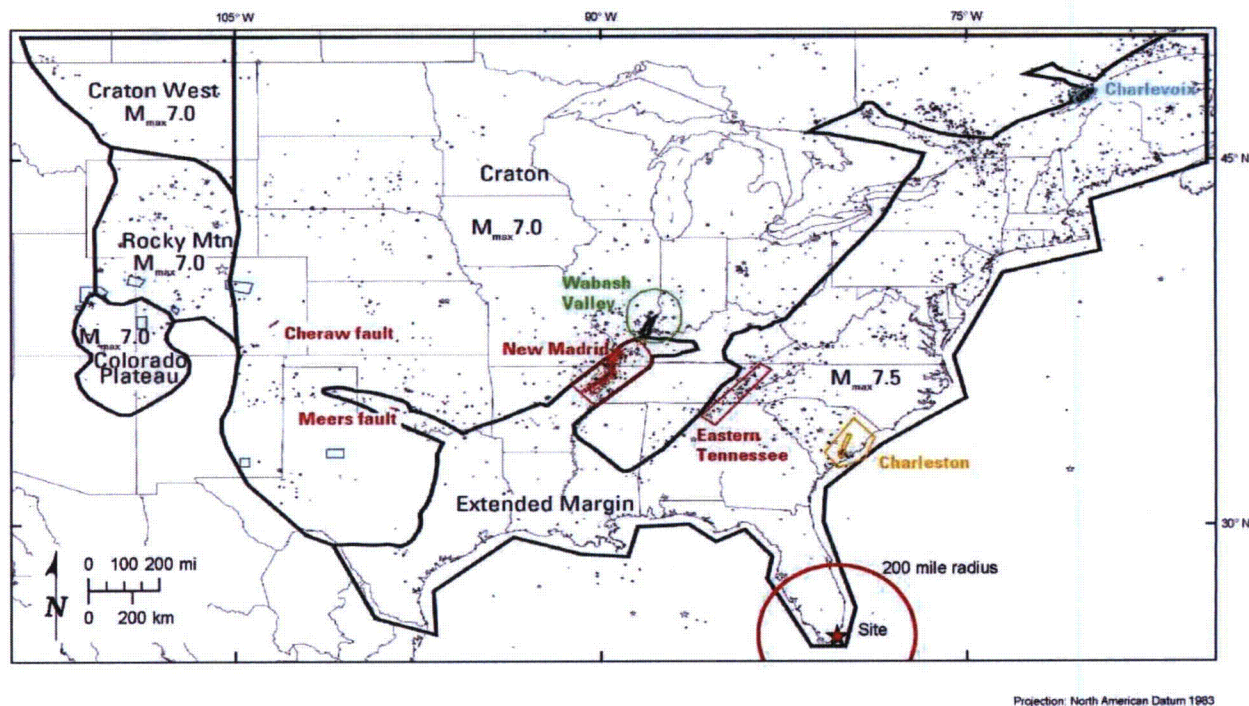
**An additional post-EPRI model is the USGS National Seismic Hazard Mapping Project (NSHMP) (Reference 300), which characterizes seismic sources throughout the continental United States using multiple classes of earthquake source models. While the NSHMP source model is described below, source parameters from this model are not included in the updated PSHA for the Turkey Point Units 6 & 7 site. The general approach used by the USGS for modeling distributed seismicity in the CEUS is based on gridded, spatially smoothed seismicity in large background zones. Seismic sources within the CEUS most relevant to the Turkey Point Units 6 & 7 site are modeled with: (1) a regional uniform background source model dividing the Extended Margin of the CEUS from the Craton; (2) special zones accounting for variability in catalog completeness, seismicity, maximum magnitude, and b-value, such as the uniform source zones for the Eastern Tennessee and New Madrid seismic zones; and (3) finite fault sources, such as those included for the New Madrid and Charleston seismic sources.**

**The 2008 NSHMP earthquake sources are depicted in Figure 2.5.2-276. Significant changes from the 2002 NSHMP model of seismic hazard in the CEUS (Reference 251) include: (1) uncertainty in the maximum magnitude ( $M_{max}$ ) assigned to  $M_{max}$  zones (e.g., extended margin); (2) revised geometry of the Charleston seismic source zones; and (3) revised magnitudes, rates, and geometry for the New Madrid seismic source. As a result of these updates, the 2008 NSHMP characterizes  $M_{max}$  for the Extended Margin and Craton as weighted distributions ranging between  $M7.1-7.7$  and  $M6.6-7.2$ , respectively. The two areal zones defining the Charleston source are both assigned  $M_{max}$  distributions of  $M6.8-7.5$  with a recurrence interval of 550 years, unchanged from the 2002 NSHMP. The USGS NSHMP Charleston seismic source update is discussed in Subsections 2.5.2.4.4.2.2 and 2.5.2.4.4.2.3.**

#### 2.5.2.4.4.1 Supplemental Source Zones

The following new figure will be included in a future COLA revision.

**Figure 2.5.2-276 Seismic Sources from the U.S. Geological Survey's 2008 National Seismic Hazard Mapping Project**



**Source: Reference 300**

#### ASSOCIATED ENCLOSURES:

None